


12-2016

Discord and Global Discord in Systems of Coupled Quantum Dots in Driven Cavities with Dissipation, and a Method for the Calculation of Global Discord

Willa Danielle Rawlinson
University of Arkansas, Fayetteville

Follow this and additional works at: <http://scholarworks.uark.edu/etd>

 Part of the [Optics Commons](#), and the [Quantum Physics Commons](#)

Recommended Citation

Rawlinson, Willa Danielle, "Discord and Global Discord in Systems of Coupled Quantum Dots in Driven Cavities with Dissipation, and a Method for the Calculation of Global Discord" (2016). *Theses and Dissertations*. 1815.
<http://scholarworks.uark.edu/etd/1815>

This Dissertation is brought to you for free and open access by ScholarWorks@UARK. It has been accepted for inclusion in Theses and Dissertations by an authorized administrator of ScholarWorks@UARK. For more information, please contact scholar@uark.edu, ccmiddle@uark.edu.

Discord and Global Discord in Systems of Coupled Quantum Dots in Driven Cavities with
Dissipation, and a Method for the Calculation of Global Discord

A dissertation submitted in partial fulfillment
of the requirements for the degree of
Doctor of Philosophy in Physics

by

Willa Rawlinson
Hendrix College
Bachelor of Art in Physics, 2009
University of Arkansas
Master of Science in Physics, 2015

December 2016
University of Arkansas

This dissertation is approved for recommendation to the Graduate Council.

Dr Reeta Vyas
Dissertation Director

Dr Mark Arnold
Committee Member

Dr Julio Gea-Banacloche
Committee Member

Dr Surendra Singh
Committee Member

Dr Laurent Bellaïche
Committee Member

This research is supported by the Arkansas High Performance Computing Center which is funded through multiple National Science Foundation grants and the Arkansas Economic Development Commission.

Abstract

In the field of quantum information, which is subdivided into quantum computing and quantum cryptography, quantum correlations are essential for a performance or security boost not achievable with classical means. Various quantum correlation measures exist for evaluating a state's potential to be a qubit (quantum bit). Entanglement, or nonseparability of quantum states, is the older, better known class of measures. However, for a mixed state, quantum entanglement is an incomplete measure of quantumness. Quantum discord, and its multibody extension global discord, encompass all quantum correlations. We study systems of coupled quantum dots using these measures.

We study the discord of two quantum dots in the steady state with dissipation and detuning. The entanglement of the system was previously studied by Mitra and Vyas [1]. We compare quantum discord to entanglement, finding high discord in an unentangled region, namely the upper branch of the bistability curve, where the driving field is high. By adjusting the detuning between the dots and the driving field, we can optimize the quantum discord and entanglement.

We present an efficient numerical method for calculating global discord and analyze its speed and scaling. We verify that the method works for two, three, and four qubits and run speed tests. We present further simplifications that greatly enhance the scaling of the method with system size provided that the bodies are identical, but which also improve the speed otherwise.

We compare our system of two quantum dots to an otherwise identical system with three quantum dots. We observe tristability in the cavity field as a function of driving field. The high field limit of global discord is a larger portion of the maximum than the discord in the same limit for the system of two quantum dots. The improvement in correlations due to detuning is still present but diminished compared to that in our two quantum dot system. The decreased effectiveness of detuning is, however, offset by the increased effect of high dot coupling, whereby the peak found in said limit with no detuning may exceed the asymptotic value without the aid of detuning.

Acknowledgements

I am not sure that anyone who enters a doctoral program has the slightest idea at the beginning how to compose their dissertation. That knowledge is passed on from professors who in the past were themselves beginning graduate students at some juncture, having learned what skills they know from still previous professors who also began without knowing what they were doing. The question of how the first generations of graduate students managed is left as an exercise for the reader. I am fortunate to have entered the process centuries since that time and to benefit from the wisdom of various professors over the years.

I first would like to thank my advisor, Dr Reeta Vyas, for extensive guidance in regard to both research and navigating the logistics of conference presentations and the academic publication process. I walked into the University of Arkansas an utter beginner in those areas and now at the least am not such any longer. With her help and encouragement, I gained the skills I needed to make this dissertation possible today instead of becoming completely weighed down with new information which I would not have processed well on my own. I would also like to thank my committee members, Dr Surendra Singh, Dr Mark Arnold, Dr Laurent Bellaiche, and Dr Julio Gea-Banacloche, for helpful input and advice regarding my ongoing works. I would additionally like to thank my undergraduate advisor, Dr Anne Wright, and my undergraduate quantum professor Dr Todd Tinsley, for their help in my early career. I also thank various other physics faculty and staff.

In the years I've been in the physics program at the University of Arkansas, I've faced a number of barriers. I am grateful to a number of my friends for encouraging me in this journey, especially Santoshi, Grey, Laura, Justine, Lily, Hollis, Tobi, Justin, Jillian, Mars, Katie, Stephanie, Shannon, Royal, Tina, Aisling, Viviana, Lola, and Gershwin. Thank you everyone for your kindness.

Dedication

To Santoshi, for helping me make major life transitions during my time in the physics program.

To Hollis, for her warm support.

To Katie, for many years of friendship.

And to Mars, for helping me to see this through to the end.

Contents

1	Introduction	1
1.1	Research Objective	1
1.2	History	1
1.3	Organization of the Work	4
2	Discord of Two Coupled Quantum Dots in a Driven Cavity with Dissipation	6
2.1	Discord	7
2.1.1	History and Significance of Quantum Discord	7
2.1.2	Algorithms and Experiments Utilizing Discord	8
2.1.3	Geometric Discord as an Alternate Measure	9
2.1.4	Calculation of Discord	10
2.2	Entanglement	14
2.2.1	Some Important Measures	15
2.2.2	Relationship to Discord	17
2.3	Quantum Dots as a source of Quantum Correlations	18
2.4	System of Two Quantum Dots in a Driven Cavity with Dissipation	20
2.4.1	The Phenomenon of Bistability	20
2.4.2	Model	21
2.4.3	Correlations in the Bistable Regime	24
2.4.4	Non Bistable Regime and Effect of Detuning	28
2.5	Conclusion	35
3	Method of Calculating Global Discord of Multiple Qubits	36
3.1	Global Discord as an Extension of Quantum Discord	36
3.1.1	Formal Definition	36
3.1.2	Limited Known Cases	38
3.2	A Brief Overview of Some Applications Involving Asymmetric Sets of Qubits	40
3.3	Outline of Numerical Method	41
3.3.1	Search Method	41
3.3.2	Matrix Method and Preliminary simplifications	45
3.3.3	Use of Vectors to Greatly Diminish Computational Time	50
3.3.4	Verification of Density Matrices with Known Global Discord	52
3.4	Speed Comparison for Matrix and Vector Methods	54
3.4.1	Generation of Random Density Matrices	55
3.4.2	Two Qubits	56
3.4.3	Three Qubits	57
3.4.4	Four Qubits	58
3.4.5	Tabulated Speedtest Results	59
3.5	Conclusion	59
4	Examining Global Discord of Three Quantum Dots in a Driven Cavity with Dissipation	61
4.1	Multibody Entanglement	61

4.2	Model	66
4.3	Results	70
4.3.1	Low Interdot Coupling Range	70
4.3.2	High Interdot Coupling and the Effects of Detuning	75
4.4	Conclusion	77
5	Conclusion	79
5.1	Future Work	80
A	Probability Amplitudes of $\Phi(\rho)$ for Two, Three, and Four Qubits	87
A.1	Two Qubits	87
A.2	Three Qubits: Asymmetric Case	88
A.3	Three Qubits: Symmetric Case	89
A.4	Four Qubits: Asymmetric Case	90
A.5	Four Qubits: Symmetric Case	95
B	Equations of Motion—Three Quantum Dots	101
B.1	Summary of Operator Effects	101
B.2	Field Parameter α Equation	102
B.3	Dot variable parameters: Repeatable simplifications	102
B.4	x , y , and z Equations	103
B.5	p , q , and r Equations	104
B.6	s , u , and v Equations	105
B.7	Summary of Equations of motion	106
C	Steady State Solutions of the Equations of Motion for Three Quantum Dots	107
C.1	Preparation	107
C.2	Solve Eqn C.1 for p , Solve Eqn C.8 for s , and Solve Eqn C.9 for u	108
C.3	Solve Eqn C.10 for v	110
C.4	Solve Eqn C.5 for r	111
C.5	Solve Eqn C.7 for q	112
C.6	Solve Eqn C.2 for y	113
C.7	Solve Eqn C.3 for x	116
C.8	Solve Eqn C.4 for z	120
C.9	Cleanup prior to last equation	121
C.10	Summary of abstractions:	122
D	Equations of Motion for Four Quantum Dots	124
D.1	Summary of Operator Effects and Repeatable Simplifications	125
D.2	Field Parameter α Equation	126
D.3	x , y , z , and Ω Equations	127
D.4	p , q , and r Equations	128
D.5	s , u , and v Equations	129
D.6	Γ , Θ , ϖ , and ϑ Equations	130
D.7	Summary of all equations	131

List of Figures

2.1	Illustration of mutual information without measurement	12
2.2	Relationship of Discord and Entanglement via Venn Diagram	18
2.3	Illustration of Two Different Ways to Graph a Bistability Curve	21
2.4	Example of Bistability in System of Two Coupled Quantum Dots	26
2.5	Non-Bistable System with $W = 0.1$ and No Detuning	29
2.6	Non-Bistable System with $W = 1$ and No Detuning	29
2.7	Non-Bistable System with $W = 5$ and No Detuning	30
2.8	Non-Bistable System with $W = 30$ and No Detuning	30
2.9	Effect of Dot Detuning on a System with $W = 10$	31
2.10	Effect of Dot Detuning on a System with $W = 20$	31
2.11	Discord and Entanglement of formation vs Dot Detuning and Driving Field, $W = 10$	32
2.12	Discord and Entanglement of formation vs Dot Detuning and Driving Field, $W = 15$	33
2.13	Discord and Entanglement of formation vs Dot Detuning and Driving Field, $W = 30$	34
3.1	One Dimensional Cross Section of a Randomly Chosen Asymmetric Tripartite Density Matrix	42
3.2	The Same State as Fig 3.1, with All Parameters Except θ_1 Optimized	42
3.3	Illustration of Process Used to Find Optimum Point in a Sinusoid of arbitrary Phase, Amplitude, and Frequency	43
3.4	Illustration of Mesh Search for Global Discord	44
3.5	Global Discord for a Bipartite Werner-GHZ State	53
3.6	Global Discord of a Tripartite Werner-GHZ State	53
3.7	Global Discord of a Quadpartite Werner-GHZ State	54
3.8	Global Discord of a Tripartite W-GHZ State	54
4.1	Illustration of a $2 \times 2 \times 2$ Hypermatrix for Use in Caley's Second Hyperdeterminant	63
4.2	Hypermatrix for Calculation of 3-Tangle	63
4.3	Global Discord of a Three-Body System: Asymptote and the Peak in Upper Branch	71
4.4	Example of Bistability in Cavity Field Amplitude for Three Qubits	71
4.5	Bistability in the Probability Overlaps of Maximally Entangled Three-Body States .	72
4.6	An Example of Tristability for Three Qubits	73
4.7	Tristability in the Probabilities of Maximally Entangled States for Three Bodies . .	74
4.8	Approximate Linearity of Cavity Field in the Case of Strongly Coupled Quantum Dots	75
4.9	Global Discord in a Non-Multistable Range with No Detuning	76
4.10	Entangled State Probabilities for the State in Fig 4.9	76
4.11	Effect of Detuning on Global Discord in the Case of Three Strongly Coupled Dots .	77
4.12	Entangled State Probabilities for the State from Fig 4.11	77

Notation and Conventions

Given in chronological order.

- $\sigma_{x,y,z}$ —The pauli spin matrices
- $a^{(\dagger)}$ —Ladder operators for a field of light.
- J, J_{\pm}, J_z —Quasispin operators.
- γ, κ —Decay constants for the quantum dots and the cavity field, respectively. As a simple, if grammatically and linguistically questionable, mnemonic: κ is for cavity.
- x, y, z —Diagonal parameters in the density matrix for three quantum dots with dissipation (in the case of two, there is no z)
- p, q, r, s, u, v —Complex off-diagonal parameters of density matrix for three quantum dots. In the case of two quantum dots, there will not be s, u, v
- Δ_d, Δ_c —Detuning parameters. Δ_d is the detuning between dots and driving field. Δ_c is the detuning between cavity field and driving field.
- ω —Generally used as frequency.
- W, g —Coupling constants. The first refers to interdot coupling. The second refers to coupling between dots and surrounding field.
- n_s —Photon saturation number.
- $D(\rho)$ —The quantum discord or global discord, depending on chapter, of a density matrix for a system consisting solely of qubits.
- E_f —A measurement of entanglement known as the entanglement of formation
- $h(x) = -x \log_2 x - (1 - x) \log_2 (1 - x)$ —A common function of use in bipartite information theory.
- $C(\rho)$ —An entanglement measure known as the concurrence. Related to E_f
- $S(\rho)$ —The Von Neumann entropy of a system.
- $\tilde{\rho}$ —This is the matrix $\sigma_y^{\otimes 2} \rho^* \sigma_y^{\otimes 2}$
- $I(\rho)$ —The mutual information of a system without measurement
- $J(\rho)$ —The mutual information of a system after measuring. Typically used in cases of quantum discord, in which the measurement is performed on just one subsystem, rather than global discord, where all subsystems are measured. For global discord, one may transform the density matrix and just use the unmeasured mutual information with the post-measurement density matrix as an argument, effectively treating the post-measurement state as a fresh system.

- \otimes —The tensor product operator.
- $A^{\otimes p}$ —Refers to the tensor exponential, raising an arbitrary operator A to the arbitrary power p .
- ρ —A matrix representing the density of states for a quantum system. More simply, a density matrix. Such a matrix having N parameters will generally be a $2^N \times 2^N$ element matrix having Hermitian, normalized form. If the bodies are identical, the system state may instead be written as an $N \times N$ matrix.
- Absence of \hbar —In this work, we choose units such that \hbar is unity to simplify the notation.
- I —Identity operator
- N —This will generally refer to the total number of bodies in a system of qubits unless expressly stated otherwise.
- n —Generally in reference to the n^{th} qubit in a system of N qubits.
- ϕ_n —A parameter used in the complex exponential portion of the n^{th} qubit's measurement projector.
- θ_n —A parameter similar to ϕ_n but as an argument in the sinusoidal functions.
- $\{L_i\}$ —A set of variables L_i for all valid index i . For example, $\{\theta_n\}$ in the case of three qubits is $\theta_1, \theta_2, \theta_3$. This is useful in notating functions of all N of θ_n and ϕ_n . $f(\{\theta_n\})$ in the above example is a function f which is solely dependent on the parameters $\theta_1, \theta_2, \theta_3$
- Π_j —A projector consisting of a tensor product of N different 2×2 projectors, each chosen out of two orthogonal possibilities, producing an outcome denoted by index j , where j runs from 1 to 2^N . Used for calculation in global discord.
- $\Phi(\rho)$ —The resulting state of the N qubit system after the measurement is performed on all N subsystems. Used in calculation of global discord.
- $|\psi_i\rangle$ —The i^{th} eigenvector of a density matrix.
- $|\psi_{i'}\rangle$ —Element i' of i^{th} eigenvector
- $|\overset{\prime}{i}\rangle$ —A scaled eigenvector for a potentially asymmetric system, with the eigenvalue absorbed.
- $|\overset{''}{i}\rangle$ —A further scaling of $|\overset{\prime}{i}\rangle$ in the special case of a symmetric system, absorbing normalization factors.
- q_i —Specifically when used in the context of $|\psi_i\rangle$, an eigenvalue corresponding thereto.
- p_j —The probability that the entire system of N qubits will have outcome j post measurement

- $|B_j\rangle$ —The ket portion of the projector $\Pi_j = |B_j\rangle\langle B_j|$
- $|b_{n,\pm}\rangle$ —Individual measurement vectors for n^{th} qubit.
- $|b_{n,0}\rangle, |b_{n,1}\rangle$ —Alternate form of $|b_{n,\pm}\rangle$ to make the relationship to the binary sequence more obvious.
- $b_{n,\pm}$ (or $b_{n,0}, b_{n,1}$)—Probabilities corresponding to one of two possible outcomes in the specific n^{th} qubit subspace post measurement.
- $\{\theta_n\}, \{\phi_n\}$ —A shorthand to refer to the entire set of θ_n or ϕ_n at once. For example, if $N = 3$, $\{\theta_n\} = \theta_1, \theta_2, \theta_3$.
- $C(\{\theta_n\})$ —Placeholder function used to indicate which portion of expression for $\langle B_j|\psi_{i,i'}\rangle$ may be precalculated based entirely on θ_n if asymmetric
- $C'(\{\phi_n\})$ —See also $C(\{\theta_n\})$
- $F(\{\theta_n\}, \{\phi_n\})$ —Similar to C and C' but for symmetric case. While the separation of $\{\theta_n\}$ and $\{\phi_n\}$ is lost, carefully planned precalculation is more efficient in this case.

Glossary

Given in chronological order.

- Quantum dot—Artificial object in solid state that exhibits similar properties in some ways to an atom.
- Mixed state—A quantum state which is a statistical mixture of pure state vectors.
$$\rho = \sum q_i |\psi_i\rangle \langle \psi_i|.$$
- Optical bistability—Having two physically stable solutions for one value of driving field.
- Unstable solution—A mathematically valid solution to the density matrix of a system, found in between stable solutions, but one into which the system will never physically settle. Purely an artifact.
- Entanglement—Non-separability of a state. Useful in quantum information.
- Factorized state—A quantum state which can be written as a tensor product of states on individual qubits. Also known as a separable state.
- Qubits—A subsystem of a quantum system which is used as a quantum analogue to a bit as defined in computer science. A classical bit is a binary unit of information which is either on or off, or in the common parlance a one or a zero.
- Determinant in relation to entanglement—Separable states will have zero determinant.
- Entanglement of formation, concurrence—Quantitative measures of entanglement. Can be written in the form of a determinant
- Bell state—A maximally entangled two quantum dot state.
- Bell diagonal state—A system which, if cast in the basis of all four possible Bell states, is a diagonal matrix. Has useful properties.
- Optically isolated—Usage: This state (or states) is optically isolated from that state (or those states). The phenomenon of being unable to migrate between types of states using the hamiltonian. In our work, the symmetric and antisymmetric states of our systems of coupled quantum dots are optically isolated from one another. A symmetric initial state will never become antisymmetric. (See chapters 2 and 4).
- Symmetric in exchange of bodies—The property that the designation of systems as A,B,C, etc. cannot change the resulting value of a quantity. If the bodies are identical, as in the systems in chapters 2 and 4, all quantities whatsoever will be symmetric in exchange of bodies.
- Quantum correlations—Statistical correlations between two or more subsystems which cannot be attributed to classical effects.
- Mutual information—A statistical measure of correlations

- Mutual information with and without measurement—A distinction in the formalism which makes no numerical difference in classical systems but does produce a discrepancy in the case of quantum systems. This is due to the collapsing of the wave function.
- Quantum discord—A measure of quantum correlations which encompasses the types of quantum correlations that entanglement leaves out, as well as entanglement itself. Not necessarily numerically higher. It is possible to have non-zero discord without any entanglement but not the reverse. This quantity is also not symmetric in exchange of bodies. Two parameter optimization required.
- Master equation—Time differential equation in operators by which one may numerically obtain the density matrix of a system.
- Equations of motion—Derived from the master equation, these will give the time derivatives of various system parameters which are related to ρ .
- The asymptotic limit—In the context of our findings in chapters 2 and 4 of this work, the limit of discord or global discord as the driving field amplitude grows arbitrarily large.
- Bipartite, tripartite, etc.—A reference to the number of bodies in the system of concern.
- Greenberger-Horne-Zeilinger, or GHZ, state—An extension of the Bell state for multiple bodies
- W state—A state of three qubits comprised of an equal superposition of all possible single exciton states.
- Flipped W, or \tilde{W} , state—The state that results if all excited qubit states in the W state are made to be ground states and vice versa. An equal superposition of double exciton states.
- GHZ-type and W-type entanglements—Tripartite entanglement can be divided into two types, named for the states which exhibit those types of entanglement. A GHZ state is three mutually entangled bodies, while a W state or flipped W state relies on bipartite entanglement amongst all bodies.
- Quantum global discord—A recently proposed extension of the quantum discord into arbitrary number of bodies. This measure is symmetric in exchange of qubit designation, at the price of more parameters than its predecessor. The global discord of two qubits is a four parameter problem.
- Post-measurement density matrix $\Phi(\rho)$ —A density matrix which has been modified such that the non-measurement mutual information function may be used with the post-measurement state as an input.
- Matrix Method—A numerical method of calculating the global discord of N qubits without the need to produce $\phi(\rho)$ or take partial traces thereof, forming the projectors Π_j expressly and then finding the diagonal terms of the product $\Pi_j \rho$.

- Vector method—An improvement upon the matrix method, allowing further simplifications by working with $|B_j\rangle$ instead of Π_j , reducing computational time.
- AMD FX8350—A high end desktop central processing unit, utilizing AM3 architecture by AMD. Unit has eight cores, no hyperthreading within the core, and is clocked at 4.0 GHz.
- Hypermatrix—An extension of matrices to higher dimensions, similar to the use of the word hypercube or hypersphere.
- Hyperdeterminant—A higher dimensional analogue of the determinant.
- Tristability, multistability—Extension of bistability beyond two stable solutions.
- Three-tangle—A common measure of three body entanglement employing the use of a $2 \times 2 \times 2$ hypermatrix in the pure state form. Based in hyperdeterminants.

1 Introduction

1.1 Research Objective

In recent years, the quantity known as quantum discord has been developed as a measure of bipartite quantum correlations which are not necessarily limited to entanglement. These quantum correlations provide significant changes to the field as a more robust and easier to produce source of quantum computational advantage. In a similar time frame, coupled quantum dots subject to a field of light in a cavity have been studied as a potential way to generate usable qubits for quantum informational tasks.

Discord is a fairly young quantity. Its multipartite extension, global discord, is all the more so, and is considered computationally difficult to calculate. Building on prior study of entanglement in coupled quantum dots in a cavity with a field of light, we study the problem of the discord of two dots and the quantum global discord of three dots, with each system consisting of identical quantum dots in a driven cavity with dissipation in the steady state. We compare these results to entanglement.

To produce the global discord of three dots we were left with little choice but to devise a computationally efficient manner in which to calculate the global discord. We have achieved a level of efficiency which produces quite rapid computations even on a high end home desktop. We present this numerical method for two, three, and four quantum dots and show that it is accurate. Preliminary work on the problem of four quantum dots in a driven cavity with dissipation is presented as well, in one of the appendices.

1.2 History

Entanglement is a form of correlation between two or more subsystems that is exclusively found in quantum mechanics. Simply put, if a system cannot be written as a factorized state, or a

statistical mixture thereof in the case of a mixed state, then it must necessarily have correlations that can only be accounted for via quantum mechanics. In effect, then, entanglement can be thought of as non-separability. Entanglement was first brought to light in the famous paper by Einstein, Podolski, and Rosen [2], in which the potential consequences of entanglement, namely the effect of measuring one system on another system regardless of distance from one another, were cited as reason to believe that there must be an underlying determinism as the phenomenon of entanglement was considered absurd. However, Bell later showed that all hidden variable theories would require an inequality, later termed Bell's inequality, to be upheld, even though some systems do not obey this inequality [3], and experimental tests were later proposed as well [4]. A number of measures for the entanglement of two bodies have been proposed, such as the entanglement of formation and concurrence [5]. Additionally, the quantity has been extended to multiple bodies, as seen in the N-concurrence and the three-tangle [6, 7].

A key application of entangled quantum states is their role in allowing for more efficient computations and more secure communication than classical bits, which hold a much more limited amount of information in comparison to quantum bits or qubits, can allow [8]. A number of computational schemes have been developed that take advantage of quantum entanglement over the years [9, 10]. Additionally, the use of entangled states has the potential to create key exchange communications which cannot be eavesdropped upon without alerting the people legitimately participating in the communication [11]. However, a key disadvantage of the use of entanglement is the sheer difficulty in maintaining it once it is generated as entangled systems are quite vulnerable to the environment, necessitating overly expensive and unwieldy cooling systems, creating an obstacle in producing less cumbersome quantum computers [12].

Among the proposed means of producing useable qubits, the use of light to produce quantum entanglement in identical coupled quantum dots in a cavity has garnered considerable interest recently. For example, Quiroga and Johnson [13] studied systems of two and three coupled quantum dots interacting with classical light in a lossless cavity. In the above, they used the probabilities of finding the system in two orthogonal Bell states as makeshift measures of

entanglement as a function of time. This work was later expanded upon by Reina et al [14]. Mitra et al [15] later studied a system of two quantum dots interacting with a quantized field of light in a coherent state, using the concurrence as a measure of entanglement rather than probability overlaps. Mitra and Vyas [1]. would later study the steady state concurrence of a system of two quantum dots in a driven cavity with dissipation, showing that the system exhibits bistability and that there is no entanglement in the high field limit. The entanglement of the system studied by Mitra and Vyas was later studied in the time dependent regime by Shiau et al [16]. Rawlinson et al [17] studied a system that was identical to the system studied in Ref. [1] except with a squeezed state of light, on the intuition that the use of a squeezed state, where the photons are invariably even in number [18], might increase the correlations between the dots over the use of a coherent state.

Though entanglement has been largely assumed through the decades to be a necessary component of any quantum information task, recent experiments cast doubt on this assumption [12], such as the room temperature performance of Shor's Algorithm by Vandersypen et al [19] using seven qubits and nuclear magnetic resonance, or NMR. The results in question were initially regarded as doubtful as entanglement cannot survive at room temperature [12]. However, shortly thereafter it was shown mathematically that a separable mixed state can have correlations that are not attributable to classical physics [20], which was thought to be impossible as, by definition, these states are unentangled. Since this revelation, various algorithms have been proposed and in some cases tested, that utilize the discord. For example, DQC1 (deterministic quantum computing with one qubit) [21, 22, 23] is a method which uses a single pure qubit which is correlated with a number of unentangled qubits to produce the normalized trace of a unitary matrix. In DQC1 methods, all the qubits except one are in maximally mixed states and therefore not entangled with any other body. However, there is a speedup, and one which is not attainable with classical systems. This shows the utility of quantum correlations beyond entanglement. The most well known measurement of these quantum correlations is quantum discord [12, 20]. This quantity is calculated by taking all correlations whatsoever and removing the classical correlations, logically

leaving only the quantum correlations. However, other quantities measuring quantum correlations have been proposed such as the geometric quantum discord, which works by finding the minimum distance between a quantum state and the nearest state having zero discord [24]. There exists an analytical solution to the geometric discord in the case of two qubit bodies [24].

Recently, Rulli and Sarandy [25] have created an extension of quantum discord to multiple bodies. Their extension is known as global discord. It uses an extension of the mutual information with and without measurement to produce an analogous quantity. Unlike quantum discord, global discord is an intrinsically symmetric quantity under exchange of bodies, due to measurements on all subspaces rather than just one. However, our methods for calculation of global discord will work better with systems whose states are also symmetric in exchange of bodies, due to a decreased need for calculation steps in the program. Some limited cases have been analyzed analytically or numerically [25, 26]. Global discord, unlike quantum discord, is not normalized to unity, but instead has a maximum dependent on the number of bodies, namely $\log_2 N$ [27]. The quantity is considered difficult to compute.

Due to the aforementioned interesting characteristics of quantum discord and global discord, we have begun to study these quantities in systems of quantum dots interacting with a field of light in a cavity [28, 29, 30]. The case of three quantum dots necessitated the development of an efficient way to calculate the global discord of three identical dots. We have extended our method to other numbers of bodies and to non-identical bodies, making it an efficient general purpose method for the problem at hand. We expect that this method will make the study of the global discord of multipartite systems considerably more practical than it is presently.

1.3 Organization of the Work

In Chapter 2, we discuss the quantity known as quantum discord and use it to explore a system of two identical coupled quantum dots in a driven cavity in the steady state, accounting for the dissipation and detuning but not for noise terms. We compare these results to the entanglement in

this system. In Chapter 3, we introduce a numerical method to efficiently and accurately compute the global discord of three identical quantum dots and we expand this method, showing results for two, three, and four bodies, both identical and non identical. We use both analytically known density matrices and randomly generated ones as test cases. In Chapter 4, we apply the above numerical method to a system of three identical coupled equidistant quantum dots, once again choosing the steady state regime and accounting for losses and detuning but not for noise.

2 Discord of Two Coupled Quantum Dots in a Driven Cavity with Dissipation

This chapter will give an introduction to the measure of quantum correlations known as quantum discord, its history, and how it is calculated. It will additionally give an overview of some entanglement measures and how they relate to discord. We then use these measures of correlations to study a system of two quantum dots in a driven cavity with dissipation in the steady state. The dots are identical and coupled with both each other and in the internal field of the cavity. The cavity field of the system exhibits bistability with respect to the driving field [1]. This is to say that there are at times two stable solutions for the cavity field amplitude which correspond to a single value of the driving field amplitude. We find that the system exhibits a high level of quantum discord in a high field regime and that in that same region there is no entanglement whatsoever. This is the highest level of discord in the case that the dots are weakly coupled with each other. With strong coupling, we see a peak in the discord and an increased amount of entanglement. This is still not as high as the asymptotic limit unless the detuning between the dots and the driving field is adjusted in the negative direction until an optimum value is reached. In this case, the quantum discord is higher than the asymptotic limit and the highest possible entanglement is reached [28].

In section **2.1** we discuss the quantum discord, beginning with its history and importance in **2.1.1**, then how to calculate it, both numerically and in limited analytical cases, in **2.1.2**. We briefly outline alternative measures in **2.1.3**. In section **2.2** we move on to the subject of entanglement.

2.1 Discord

2.1.1 History and Significance of Quantum Discord

For the majority of the existence of the field of quantum information it was thought that the sole way to get a quantum advantage in computational or communicational tasks was to have entangled states. However, it has been known for nearly two decades now that entanglement is not needed to create a quantum computational advantage, provided that the state is mixed rather than pure [12, 20]. Measures have been proposed for this phenomenon by applying information theory to quantum systems, the most prominent of which measures is known as quantum discord [20].

The existence of quantum correlations beyond entanglement was first noticed after Vandersypen et al [19] performed Shor's algorithm with a seven qubit configuration at room temperature and gained a nonclassical advantage, despite the fact that entanglement could not survive in appreciable amounts under those conditions [12]. These results were called into question due to the lack of entanglement, but it was shown later that some statistical mixtures of separable states can hold correlations that cannot be attributed to classical phenomena alone [20].

Because of the difficulty in maintaining entanglement compared to discord and due to the applications mentioned above, discord is considered much more resilient than entanglement [12]. The measure quantum discord specifically refers to the quantum correlations between two bodies. For multiple bodies, extensions such as global discord are needed [25]. Said extension is of key importance in chapters 3 and 4. Due to the need to maximize classical correlations over the various measurement bases possible, discord is considered computationally intensive for a two parameter problem. The problem is asymmetric in exchange of dots if the bodies are nonidentical [20]. Other measures have been proposed such as geometric discord [24] and a second version of geometric discord defined via a different norm [31]. In addition, the concept of geometric discord has been extended to arbitrary number of bodies [32]

Quantum discord has been used in other applications such as deterministic quantum

computing with one qubit (or DQC1) algorithms, such as calculating the normalized trace of a unitary matrix [21, 22, 23]. This method utilizes n bodies in the n^{th} dimensional normalized identity state, which are coupled to a pure qubit.

We use quantum discord to more fully study the useful quantum correlations which may be generated by the system of two quantum dots in a driven cavity with dissipation in the steady state, a system whose entanglement was studied earlier by Mitra and Vyas [1] via the entanglement measure concurrence, which measure is discussed in a later section.

2.1.2 Algorithms and Experiments Utilizing Discord

Knowing that entanglement is not needed for quantum correlations certainly makes quantum discord and similar quantities more complete measures of quantum correlations than entanglement alone. However, this quality by itself is useless unless one can use discord for quantum information tasks in situations where entanglement is completely absent. In this section, we will first overview the experiment of Vandersypen et al [19] mentioned in the previous section, then we will outline the DQC1 algorithm for the trace of a unitary matrix [21, 22, 23].

Vandersypen et al [19] performed an experimental realization of the prime factorization of 15 using Shor's algorithm [10]. Their system consisted of seven qubits in a room temperature nuclear magnetic resonance, NMR, setup. The results were questioned initially due to the room temperature conditions, which are not hospitable for entanglement, but because discord does not require entanglement, this did not ultimately prove to be a problem [12].

The method for calculating the trace of a unitary matrix proposed by Knill and Laflamme [21] and studied by Datta et al [22, 23] requires a single pure qubit prepared in the state $\rho_1 = \frac{1}{2}(I + \alpha Z)$, where I is the identity operator for a single qubit, α is a polarization constant, and Z is a Pauli operator. This qubit is sent through a Hadamard gate and the set of n other qubits, which are initially in a state of $I_n/2^n$, are sent through a controlled unitary gate whose unitary matrix corresponds to the matrix which one desires to measure, after which the prepared

qubit is exposed to the others. This process is repeated over and over with measurements taken in order to gain expectation values for the Pauli operators σ_x and σ_y . The expectation values then give the real and imaginary parts of the desired trace within normalization constants. This can be seen in the expression derived for the density matrix of the combined system by Datta et al [22]

$$\rho_{n+1} = \frac{1}{2^{n+1}} \begin{pmatrix} I_n & \alpha U_n^\dagger \\ \alpha U_n & I_n \end{pmatrix}$$

where U_n is the $n \times n$ unitary matrix of concern.

2.1.3 Geometric Discord as an Alternate Measure

One of the measures of quantum correlations that has received much attention as an alternative to quantum discord is quantum geometric discord [24, 31, 33, 34, 35, 36, 37, 38]. Originally proposed by Dakic et al [24], geometric discord is defined below.

$$D_A^{(2)}(\rho) = \min_{\chi \in \Omega_0} \|\rho - \chi\|^2$$

where Ω_0 is the entire set of states having zero discord and $\|A\|^2 = \text{Tr}(A^\dagger A)$. The geometric discord measure can be modified to use other norms as well [31]. When the quantity geometric discord was first proposed, the two qubit case was analyzed in detail and an analytic solution was found by Dakic et al [24]. They found that if one rewrites the two qubit state in Bloch form

$$\rho_{\text{Bloch}} = \frac{1}{4} \left(I \otimes I + \sum_{i=1}^3 x_i \sigma_i \otimes I + \sum_{i=1}^3 y_i I \otimes \sigma_i + \sum_{i=1}^3 \sum_{j=1}^3 T_{ij} \sigma_i \otimes \sigma_j \right)$$

where I is the identity, $x_i = \text{Tr} \rho(\sigma_i \otimes I)$, $y_i = \text{Tr} \rho(I \otimes \sigma_i)$, and $T_{ij} = \text{Tr} \rho(\sigma_i \otimes \sigma_j)$, and σ_i are the Pauli matrices, the minimum distance to the set of zero-discord states may be found as follows.

$$D_A^{(2)}(\rho) = \frac{1}{4} (\|\mathbf{x}\|^2 + \|T\|^2 - k_{\max}) \quad (2.1)$$

where k_{\max} is the greatest eigenvalue of $K = \mathbf{x}\mathbf{x}^T + TT^T$ and \mathbf{x} is a vector composed of the elements x_i . In the special case of Bell diagonal states, that is to say states of the form

$$\rho_{Bell-diag} = \frac{1}{4} \begin{pmatrix} 1 + c_3 & 0 & 0 & c_1 - c_2 \\ 0 & 1 - c_3 & c_1 + c_2 & 0 \\ 0 & c_1 + c_2 & 1 - c_3 & 0 \\ c_1 - c_2 & 0 & 0 & 1 + c_3 \end{pmatrix}$$

then the geometric discord can be calculated with a considerably simpler mathematical prescription, shown below [35].

$$D_A^{(2)}(\rho_{Bell-diag}) = \frac{1}{4} (c_1^2 + c_2^2 + c_3^2 - \max\{c_1^2, c_2^2, c_3^2\}) \quad (2.2)$$

The author is not aware of any proposals to directly measure quantum discord as such, but there is a proposed method by Passante et al [33] by which one can experimentally measure the related quantity geometric quantum discord. The method uses the DQC1 algorithm for the trace of a unitary matrix (see also [22, 23]). Passante et al use the trace result of the algorithm and the initial conditions of the experiment to gain enough information to calculate the global discord of an experimentally produced state. They are able to experimentally reproduce their proposed algorithm via an NMR implementation of the DQC1 algorithm for the trace of a unitary [33].

However, in contrast to the advantage of using the simpler geometric discord over the quantum discord, there is some evidence that geometric discord may be an inferior quantity. It can change even under some operations that should not affect the quantum correlations of a system, due to these operations being both local and reversable [34].

2.1.4 Calculation of Discord

First proposed by Oliver et al [20], quantum discord is a measure of how much of the correlations in a system must be attributed to quantum effects at minimum. The discord is based in a measure of statistical correlations known as mutual information. There are two ways to define the mutual

information. The first is mutual information without any measurement having been taken. It is defined as follows [39]

$$I(A : B) = S(\rho_{AB}) - S(\rho_A) - S(\rho_B) \quad (2.3)$$

where $S(\rho) = -\text{Tr} \rho \log_2 \rho$ is the entropy of a state ρ , the state of the two dots is defined as ρ_{AB} , and ρ_A and ρ_B are the reduced density matrices of the A and B subsystems, respectively. The second is the mutual information post measurement, defined in equation (2.4) [39].

$$J(A : B) = S(\rho_A) - S(\rho_A|j) \quad (2.4)$$

In this case, one must use the conditional entropy $S(\rho_A|j)$. Conditional entropy is the statistically weighted average of all the entropies of states which the A system may take on after a measurement in the other subsystem is performed with outcome j .

The two measures will produce identical values in a completely classical system as measurement does not change the state of such a system. In the case of a quantum system, however, the two definitions can have different resulting values. The mutual information after measurement may be less than or equal to the mutual information before measurement.

$$I(A : B) \geq J(A : B) \quad (2.5)$$

With this in mind, we can determine how much of the correlation must be due to quantum effects so long as we minimize the discrepancy over possible measurement bases. In other words, Oliver et al define the quantum discord as follows:

$$D(A : B) = \min_{\Pi_B} (I(A : B) - J(A : B)) \quad (2.6)$$

This optimization is taken over the possible projectors in the system B space. Because the optimization involves choosing an optimum measurement projector, it is considered a

computationally intensive problem [12, 20]. The mutual information of two bodies without measurement is illustrated in the following venn diagram [40].

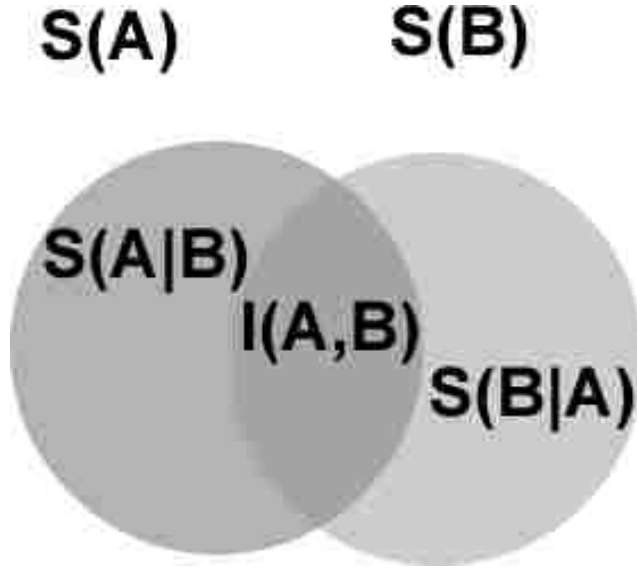


Figure 2.1: Illustration of mutual information without measurement

The connection between entropy and information can be readily seen. Consider a set of sixteen bits. There are 2^{16} possible configurations for the set of bits, which is to say that the multiplicity is 2^{16} . The number of bits then can clearly be seen as the base two logarithm of the multiplicity, whereas the von Neumann entropy of a system is $S(\rho) = -Tr \rho \log_2 \rho$. Therefore the entropy S of a system is connected to the informational content of the system via a logarithmic function. While any base may be used, base two is most convenient for us due to the use of binary information storage in computers. The quantum discord is a two parameter problem and both parameters are periodic [41].

Some methods have been developed for analytical calculation of discord in limited sets of states, such as Bell diagonal states (states diagonal in the Bell state basis) [42] or X-states (which have only diagonal and anti-diagonal terms) [43]. We will use the former method by Luo to find the discord in a limiting case later in this work. The formula derived by Luo [42] is as follows

$$D = 2 + \sum_{i=1}^4 \lambda_i \log_2 \lambda_i - \left(\frac{1-r}{2} \right) \log_2 (1-r) - \left(\frac{1+r}{2} \right) \log_2 (1+r) \quad (2.7)$$

where $r = \max(|r_i|)$ and r_i are coefficients in the Bell diagonal state $\rho = \frac{1}{4} (I + \sum_i r_i \sigma_i^{\otimes 2})$ [44] and λ_i are the eigenvalues of ρ_{BellD} . which may be written as

$$\begin{aligned}\lambda_1 &= (1 - r_1 - r_2 - r_3) / 4 \\ \lambda_2 &= (1 - r_1 + r_2 + r_3) / 4 \\ \lambda_3 &= (1 + r_1 + r_2 + r_3) / 4 \\ \lambda_4 &= (1 + r_1 + r_2 - r_3) / 4\end{aligned}\tag{2.8}$$

The projectors in the single dot subspace may be parameterized as $|b_{n\pm}\rangle\langle b_{n\pm}| = \frac{I \pm \mathbf{a} \cdot \boldsymbol{\sigma}}{2}$, which is the parameterization employed by Datta et al [41] in numerically calculating quantum discord. We employ this parameterization in our own study of the quantum discord of two identical coupled quantum dots in a driven cavity.

Girolami and Adesso [45] found that the quantum discord of a general state can be simplified analytically by first transforming the matrix into bloch normal form

$$\rho = \frac{1}{4} \left(I_4 + \sum a_i \sigma_i \otimes I_2 + \sum b_i I_2 \otimes \sigma_i + \sum c_i \sigma_i \otimes \sigma_i \right)\tag{2.9}$$

where I_ℓ is the ℓ dimensional identity, and then showing that the best eigenvalues post measurement may be found by numerically solving the following system of transcendental equations.

$$\begin{aligned}\lambda_0^- &= \frac{\left(\frac{\lambda_1^+}{\lambda_1^-}\right)^{\frac{\alpha}{\beta}}}{1 + \left(\frac{\lambda_1^+}{\lambda_1^-}\right)^{\frac{\alpha}{\beta}}} \\ \lambda_1^- &= \lambda_0^- \left(\frac{\lambda_0^+}{\lambda_0^-}\right)^{\frac{\alpha+\beta+\gamma}{2\alpha}}\end{aligned}\tag{2.10}$$

where the constants α, β, γ are defined as follows.

$$\begin{aligned}
\alpha &= \det \begin{pmatrix} \frac{\partial p}{\partial \theta} & \frac{\partial p}{\partial \phi} \\ \frac{\partial r_+}{\partial \theta} & \frac{\partial r_+}{\partial \phi} \end{pmatrix} \\
\beta &= \det \begin{pmatrix} \frac{\partial p}{\partial \theta} & \frac{\partial p}{\partial \phi} \\ \frac{\partial r_-}{\partial \theta} & \frac{\partial r_-}{\partial \phi} \end{pmatrix} \\
\gamma &= \det \begin{pmatrix} \frac{\partial r_+}{\partial \theta} & \frac{\partial r_+}{\partial \phi} \\ \frac{\partial r_-}{\partial \theta} & \frac{\partial r_-}{\partial \phi} \end{pmatrix}
\end{aligned} \tag{2.11}$$

where

$$\begin{aligned}
p &= \mathbf{b} \cdot \mathbf{X}, & r_{\pm} &= |\mathbf{m}_{\pm}| \\
\mathbf{X} &= \{x, y, z\}, & \mathbf{m}_{\pm} &= \{a_i \pm c_i X_i\}
\end{aligned} \tag{2.12}$$

However, we find that the method developed by Datta et al to be sufficient. The discord is considered numerically intensive. However, for our purposes, it is enough to simply use the parameterization of the projectors detailed by Datta, whereupon the optimum is easily found by built-in numerical solvers in mathematica and even by uniform search of the two parameter space without any real difficulty.

Recently, this quantity has been extended to multiple bodies via a measure known as global discord [25]. This measure is applicable for N bodies, is a $2N$ parameter problem, and is intrinsically symmetric in exchange of bodies. This quantity will be discussed in depth in chapter 3, where we develop a numerical method for calculation of global discord. We use the above numerical method in the study of the system of three quantum dots detailed in chapter 4. This correlation measure is based in an extension of the mutual information to N bodies.

2.2 Entanglement

Prior to the discovery of quantum discord, entanglement was considered by default to be the only way to produce useful quantum computational advantage. The concept was first discussed in the Einstein–Podolsky–Rosen, or EPR, paper [2] as a direct consequence of the nondeterminate

nature of quantum mechanics. The authors of the EPR paper had believed the odd nature of entanglement was evidence that there must exist hidden variables. However, hidden variable theories as a whole were later disproven [3]. Entanglement allows one to glean information about one subsystem from information regarding the other. The classic example of a maximally entangled state is the Bell States shown below.

$$\Psi_{\pm} = \frac{|00\rangle \pm |11\rangle}{\sqrt{2}}, \quad \Phi_{\pm} = \frac{|10\rangle \pm |01\rangle}{2}$$

If a quantum state may be written as a superposition of Bell state projectors, which is to say the matrix is diagonal in the Bell states basis, it is said to be Bell diagonal and has the form shown below [44]. Bell diagonal states are not necessarily entangled [46]. The special properties of this class of states, described by the matrix [44]

$$\rho_{Bell\ Diagonal} = \begin{pmatrix} p_I + p_z & 0 & 0 & p_I - p_z \\ 0 & p_x + p_y & p_x - p_y & 0 \\ 0 & p_x - p_y & p_x + p_y & 0 \\ p_I - p_z & 0 & 0 & p_I + p_z \end{pmatrix} \quad (2.13)$$

where $p_{I,x,y,z}$ are real numbers, can prove useful in the various areas of quantum information methods [46, 47, 48, 49, 50].

Such states need not be entangled themselves as there may be an unentangled decomposition of the state. However, they are simpler to work with and their properties lend themselves to the derivation of exact expressions for quantum discord of Bell diagonal state [42].

2.2.1 Some Important Measures

The entanglement of formation is defined as the minimum entanglement, as measured by entropy, required to create a state [5]. It can be defined in terms of the concurrence (discussed

later) in the following way, as set forth by W.K. Wootters et al [5].

$$E(C) = h\left(\frac{1 + \sqrt{1 - C^2}}{2}\right) \quad (2.14)$$

where $h(x) = -x \log_2 x - (1 - x) \log_2 (1 - x)$. It is worth noting that while the entanglement of formation is more easily calculated from concurrence, conceptually concurrence may be better understood from entanglement of formation [5].

Wootters defined the concurrence of a state vector $|\psi\rangle$ as $\langle\psi|\sigma_y \otimes \sigma_y|\psi^*\rangle$ where σ_y is a Pauli spin matrix. The pure state definition fails to work in a mixed state due both an ambiguity in which state vector a system is and an ambiguity in how a mixed state is decomposed into projectors in the first place [51]. While it is standard to decompose it into eigenvector projectors $\rho = \sum_i p_i |\psi_i\rangle \langle\psi_i|$, one can define other decompositions that are just as valid. Therefore, one must find the minimum weighted average of the pure state concurrence ($C(\rho) = \min_\phi \sum_i p_i C(|\phi_i\rangle)$). There exists a simple analytical solution to this optimization [5].

$$C = \max[0, \lambda_1 - \lambda_2 - \lambda_3 - \lambda_4] \quad (2.15)$$

In the above λ_i are the square roots of the eigenvalues of the matrix $\rho\tilde{\rho}$, with $\tilde{\rho}$ defined as $(\sigma_y \otimes \sigma_y) \rho^* (\sigma_y \otimes \sigma_y)$ and $\lambda_{i+1} > \lambda_i$.

The pure state form can also be written as

$$C_{pure} = \det \begin{pmatrix} \psi_{00} & \psi_{01} \\ \psi_{10} & \psi_{11} \end{pmatrix} \quad (2.16)$$

where ψ_{ij} are components of the vector $|\psi\rangle$ [51]. It can be shown that if you substitute an arbitrary separable state, the determinant will be zero, giving a connection between determinants and separability.

$$\psi_{sep} = (a|0\rangle + b|1\rangle) \otimes (c|0\rangle + d|1\rangle) \Rightarrow \det \begin{pmatrix} \psi_{00} & \psi_{01} \\ \psi_{10} & \psi_{11} \end{pmatrix} = acbd - adbc = 0$$

While it is tempting to think this quantity would be easily extendable to all N , it turns out that for odd N the measure will always go to zero, making it meaningless in those cases [6]. For even N , it can be defined as follows for a pure state [6].

$$C_N = \langle \psi | \sigma_y^{\otimes N} | \psi^* \rangle \quad (2.17)$$

The analytical solution for mixed states can also be extended to even numbers of bodies.

$$C_N = \max[0, \lambda_1 - \sum_{i=2}^{2^N} \lambda_i] \quad (2.18)$$

Here, λ_i are the square roots of the eigenvalues of the matrix $\rho \tilde{\rho}$, with $\tilde{\rho}$ defined as $(\sigma_y^{\otimes N}) \rho^* (\sigma_y^{\otimes N})$ and $\lambda_{i+1} > \lambda_i$ and N is the number of bodies in the system. For odd numbers of bodies, alternate measures are needed, such as the three tangle, which was first proposed by Coffman, Kundu, and Wootters [7].

2.2.2 Relationship to Discord

While both quantum discord and the various measures of quantum entanglement are indicators of quantum correlations, quantum discord is decidedly not a measure of entanglement per se. Quantum discord, by definition, is a measure of all quantum correlations. But there are separable states, states which by definition have no entanglement, that nonetheless have nonzero quantum discord [52]. These states only exist in the case of mixed state regimes, states that are statistical mixtures of separable states [52]. For a pure state all discord is due to entanglement, and for a mixed state, you can have discord without entanglement but not the reverse [53].

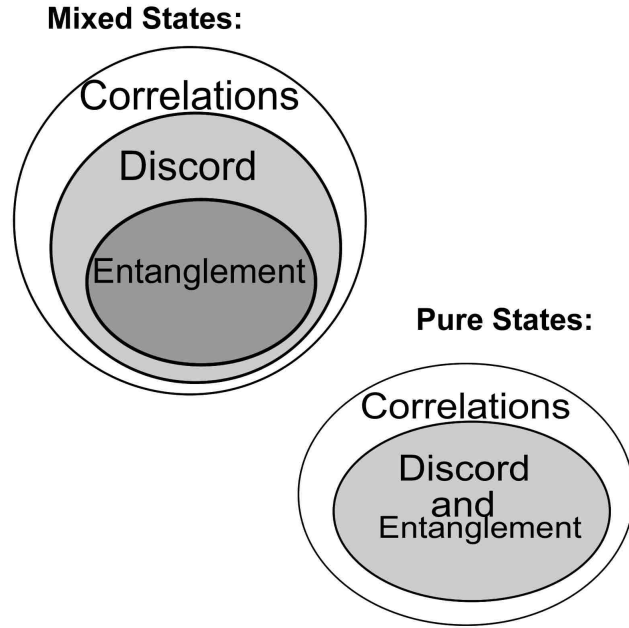


Figure 2.2: Relationship of Discord and Entanglement via Venn Diagram

It is worth noting, in particular, that for a pure state, the entanglement of formation and the quantum discord are numerically equal [54]. Note, however, that despite this equality, discord may be numerically less than entanglement of formation, not just greater or equal. The behavior of these two quantities in a pure state enables one to immediately notice a region of a graph in which the state is relatively pure simply by comparing the two curves.

2.3 Quantum Dots as a source of Quantum Correlations

There has been much interest in the recent past in the use of light to generate quantum entanglement in a set of coupled quantum dots for eventual use in quantum information applications [1, 13, 15, 16]. In early works, while the dots were treated quantumly, the field of light in the cavity was classical, as seen in the case of Quroga, who studied systems of two and three quantum dots in a cavity without losses and with a field of light, using the overlap of

maximally entangled states with system state as a measure of quantum entanglement in the time dependent regime [13]. Mitra et al [15] would later examine the time variation of quantum entanglement of two quantum dots (via the concurrence measure) in a cavity with a quantized field of light, which allowed for a more exact system model and a more reliable way of finding the entanglement than previously, as they showed it was possible for an unentangled state to have non-zero overlaps, and additionally showed that the magnitude of the difference between the maximally entangled state probabilities would be a better measure than the probabilities alone. Mitra et al found that unlike in the case of Quiroga and Johnson, their system was not able to reach maximal entanglement under any circumstance. Mitra and Vyas later examined a system of two quantum dots in a cavity with dissipation and a driving field in the steady state regime [1]. The internal cavity field was treated as quantized. They showed that with high driving field, the entanglement would cut to zero and that the system showed bistability. This system was also examined by Shiao et al in the time dependent regime [16]. The system studied by Mitra and Vyas was examined once more by Rawlinson and Vyas with regard to the quantum discord of the system, which had not been previously analyzed [28]. It was found that the system exhibited high quantum discord where the entanglement was zero, that the system was mostly pure for low cavity field amplitude, and that in the high inter-dot coupling regime the discord would show a peak whose height could be adjusted via changes in the dot detuning. Those results are detailed in this chapter.

As seen in the aforementioned case of the DQC1 algorithms, entanglement is not actually necessary for quantum computations. It is of interest, therefore, to reexamine the system of two identical coupled quantum dots in a driven cavity with dissipation in the steady state and calculate the behavior of the quantum discord in various regions of the parameter space to seek out new interesting results that were not apparent when examining entanglement alone. This system was explored by Rawlinson and Vyas [28] and will be the focus of the remainder of this chapter.

2.4 System of Two Quantum Dots in a Driven Cavity with Dissipation

2.4.1 The Phenomenon of Bistability

An optical cavity system is said to be bistable if for some range of values of the driving field the internal cavity field may take on two different physically possible strengths for the same driving field [55]. The system of two identical coupled quantum quantum dots in a driven field studied by Mitra and Vyas, Shiau et al, Freed et al, and Rawlinson and Vyas exhibited optical bistability [1, 16, 29, 28]. The aforementioned system is the subject of this chapter. In our work and that of Mitra and Vyas [1] the graphs of bistable systems include three mathematically possible solutions, but only two are stable.

Optical bistability has been investigated quite extensively both theoretically [56, 57] and experimentally [58, 59, 60, 61, 62, 63]. Additionally, it is possible for a system to exhibit multistability, which is to say that there are three or more stable solutions for the cavity field amplitude for some values of amplitude [64, 65]. The appearance of optical bistability is known to be affected in part by a quantity known as the cooperativity parameter defined below [66].

$$C = \frac{g^2}{\gamma\kappa} \quad (2.19)$$

There are two common ways to illustrate a bistability curve. One can include the middle solution, which is a mere mathematical artifact and has no physical meaning, as seen in Mitra and Vyas' study of the system [1], or one can draw the upper and lower branch and connect the two of them with vertical lines at the points where the field is forced to jump if the driving field is adjusted past the point at which its current branch runs out [62]. The two methods of graphing a bistability curve are exhibited below.

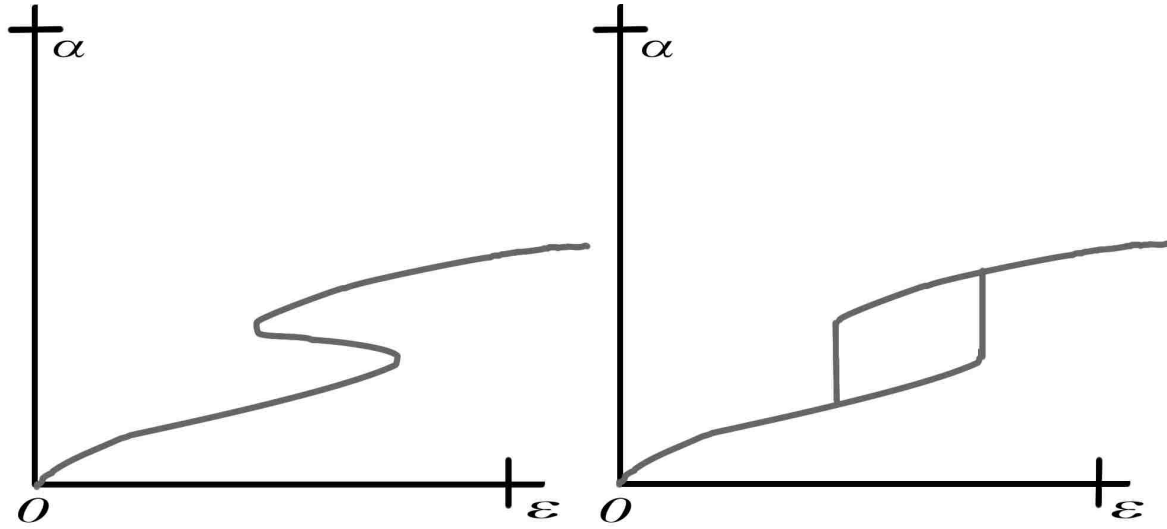


Figure 2.3: Two different ways to graph a bistable system's cavity field amplitude ε as a function of driving field amplitude α . This figure is presented for illustration purposes only. No actual data is used.

2.4.2 Model

The system consists of two identical quantum dots in a cavity. There is a driving field and the dots are both coupled with each other and with the cavity field. We account for detuning between the dots and the driving field and detuning between the cavity and driving fields. We account for decay rates on both the the dots and the cavity. The entanglement of this system was previously studied by Mitra and Vyas [1]. The system is symmetric in exchange of dots and it was shown that only the triplet states $|\psi_0\rangle \equiv |00\rangle$, $|\psi_1\rangle \equiv \frac{|01\rangle+|10\rangle}{\sqrt{2}}$, $|\psi_2\rangle \equiv |11\rangle$ are optically active.

This system was studied by obtaining a Fokker Planck equation from the Hamiltonian and then getting equations of motion [1, 67, 68, 69, 70]. The master equation is

$$\begin{aligned}
\dot{\rho} = & -i\Delta_c[a^\dagger a, \rho] - i\Delta_d[J_z, \rho] + g[aJ_- - aJ_+, \rho] \\
& + \epsilon[a^\dagger - a, \rho] - iw[T, \rho] + \frac{\gamma}{2}[2J_- \rho J_+ - J_+ J_- \rho - \rho J_+ J_-] \\
& + \kappa[2a\rho a^\dagger - a^\dagger a \rho - \rho a^\dagger a]
\end{aligned} \tag{2.20}$$

where w is the inter-dot coupling strength, g is the coupling strength of the dots and the cavity field, $a^{(\dagger)}$ is the cavity field annihilation(creation) ladder operator, ω_o is the field frequency, ω_d is the dot excitation energy, ω_c is the cavity field frequency, γ is the decay rate of the dots, κ is the cavity decay rate, $\Delta_d = \omega_d - \omega_o$ is the detuning between the dots and the driving field, $\Delta_c = \omega_c - \omega_o$ is the detuning between the cavity and driving fields, ϵ is the driving field amplitude. This definition applies to any number of eqidistant identical dots [1, 15]. In the case of two dots, the operators J_{\pm}, J_z are quasispinors in the dot space and are given by

$$\begin{aligned}
J_{\pm} &= \frac{1}{\sqrt{2}} \sum_{n=1}^2 e_n^{(\dagger)} h_n^{(\dagger)} \\
J_z &= \frac{1}{2} \sum_{n=1}^2 (e_n^{\dagger} e_n + h_n^{\dagger} h_n) \\
J_{i\pm} &= e_i^{(\dagger)} h_i^{(\dagger)}
\end{aligned} \tag{2.21}$$

In this definition, $e_n^{(\dagger)}$ and $h_n^{(\dagger)}$ are the fermion annihilation(creation) operators for the electron and hole of dot n . The operator T is defined in the following fashion. $T = J_{1+} J_{2-} + J_{1-} J_{2+} + I$, where I is the identity operator. In all cases we are using units such that $\hbar = 1$ for convenience. We can parameterize the system's reduced density matrix in the dot space in the following way using the basis of $|00\rangle, |10\rangle, |01\rangle, |11\rangle$ [1].

$$\Lambda = \begin{pmatrix} \frac{1}{3} + x & \frac{p}{\sqrt{2}} & \frac{p}{\sqrt{2}} & q \\ \frac{p^*}{\sqrt{2}} & \frac{\frac{1}{3} - x - y}{2} & \frac{\frac{1}{3} - x - y}{2} & \frac{r}{\sqrt{2}} \\ \frac{p^*}{\sqrt{2}} & \frac{\frac{1}{3} - x - y}{2} & \frac{\frac{1}{3} - x - y}{2} & \frac{r}{\sqrt{2}} \\ q^* & \frac{r^*}{\sqrt{2}} & \frac{r^*}{\sqrt{2}} & \frac{1}{3} + y \end{pmatrix} \tag{2.22}$$

The density matrix may also be cast into the basis $\{|k\rangle\}, k \in \{0, 1, 2\}$ just as easily; however, the 4×4 density matrix is useful for calculations of quantum entanglement measures, such as the concurrence and entanglement of formation, and of quantum discord.

In Mitra and Vyas' study of this system [1], the equations of motion were originally found using a Fokker-Planck equation, which also contains information about noise terms and higher order averages. However, for calculating equations of motion for operator averages, we can also use $\langle \dot{A} \rangle = Tr A \dot{\rho}$ and substituting the master equation (eq 2.7). Both of these methods result in the equations of motion shown below, but the latter method is a simpler approach and is the most feasible way to extend this methodology to multiple dots (see also chapter 4) [67, 68, 69].

$$\begin{aligned}
\langle \dot{\alpha} \rangle &= \varepsilon - (\kappa + i\Delta_c) \langle \alpha \rangle + g (\langle p_* \rangle + \langle r_* \rangle) \\
\langle \dot{x} \rangle &= -\gamma \left(\langle x \rangle + \langle y \rangle - \frac{1}{3} \right) + g (\langle \alpha p \rangle + g \langle \alpha_* p_* \rangle) \\
\langle \dot{y} \rangle &= -\gamma \left(\langle y \rangle + \frac{1}{3} \right) - g (\langle \alpha r \rangle + \langle \alpha_* r_* \rangle) \\
\langle \dot{p} \rangle &= -\gamma \left(\frac{\langle p \rangle}{2} - \langle r \rangle \right) - g (2 \langle \alpha_* x \rangle + \langle \alpha_* y \rangle) + g \langle \alpha q \rangle + i (w + \Delta_d) \langle p \rangle \\
\langle \dot{q} \rangle &= -\gamma \frac{\langle q \rangle}{2} - g (\langle \alpha_* p \rangle - \langle \alpha_* r \rangle) + 2i\Delta_d \langle q \rangle \\
\langle \dot{r} \rangle &= \gamma \langle r \rangle + g (\langle \alpha_* x \rangle + 2 \langle \alpha_* y \rangle) - g \langle \alpha q \rangle - i (w - \Delta_d) \langle r \rangle
\end{aligned} \tag{2.23}$$

The original work by Mitra contained more equations of motion for α^*, p^*, q^*, r^* , which are not necessarily complex conjugates of each other; however, . Mitra and Vyas chose to transform the system parameters as unitless quantities in the following way.

$$W = 2w/\gamma, \quad \delta_d = 4\Delta_d/\gamma, \quad \delta_c = \Delta_d/\gamma \tag{2.24}$$

It can also be seen either by numerical verification or by examining the steady state solutions below that α, α_* must be complex conjugates of one another. It is not possible to find α analytically after the other variables are solved in terms of it, but it is readily found as a two parameter numerical problem. The system of equations of motion was solved by Mitra et al by assuming low noise and thereby using the approximation that $\langle AB \rangle = \langle A \rangle \langle B \rangle$ [1]. Without such an approximation, the averaged products must be found through a new set of equations of motion in higher order terms using $\langle AB \rangle = Tr AB \dot{\rho}$, similarly to how the original set of equations of motion were produced. This new set of equations of motion for averaged products will themselves contain order three terms, requiring further equations of motion that generate higher

terms, ad infinitum. At most, we can only truncate the series of equations of motion at some point, and we choose to truncate at the first order. It was found by Mitra [72] that this neglect of noise matters most near the transitional region from lower to upper branch in the bistability curve. It is possible that in the future this system could again be studied with a higher order truncation of equations of motion. The expressions found for x, y in the steady state are of the most interest to us and are reproduced below.

$$x = \frac{2(1 + \delta_d^2) \left(1 + W^2 + \frac{\alpha\alpha_*}{4n_s} + \delta_d W + \frac{\delta_d^2}{4} \right)}{3K(\alpha, \alpha_*)} \quad (2.25)$$

$$y = -\frac{2(1 + \delta_d^2) \left(1 + W^2 + \frac{\alpha\alpha_*}{n_s} + \delta_d W + \frac{\delta_d^2}{4} \right)}{3K(\alpha, \alpha_*)} \quad (2.26)$$

where the cavity photon saturation is given by n_s and

$$K \equiv \frac{3}{4} \frac{\alpha^2 \alpha_*^2}{n_s^2} + \left[\frac{\alpha\alpha_*}{n_s} + 1 + \left(W + \frac{\delta_d}{2} \right)^2 \right] (1 + \delta_d^2) \quad (2.27)$$

For a given value of the driving field it is possible for there to be as many as three mathematical solutions, but only two of them will be stable. These will be the solutions having highest and lowest $|\alpha|^2$. The solution in the middle is unstable, which was also seen when the time dependent entanglement was studied for this system [16].

2.4.3 Correlations in the Bistable Regime

Mitra and Vyas [1] found that this system only has entanglement in the lower branch of the bistability curve. The measure used for entanglement was the concurrence. Due to the increased ease of comparing discord to entanglement of formation we primarily concern ourselves with that measure, but the concurrence is included for completeness. The highest concurrence that Mitra et al were able to find was 0.43 which is equivalent to 0.28 when converted to entanglement of

formation. This was found by increasing the dot-dot coupling relative to other parameters.

Both the cavity field and the quantum discord exhibit bistability for certain parameters as exhibited below. Note that the discord approaches a value of $1/3$ asymptotically as the driving field grows higher, yet there is no entanglement in this region.

The dot system density matrix has been shown [1] to approach the following form for high fields.

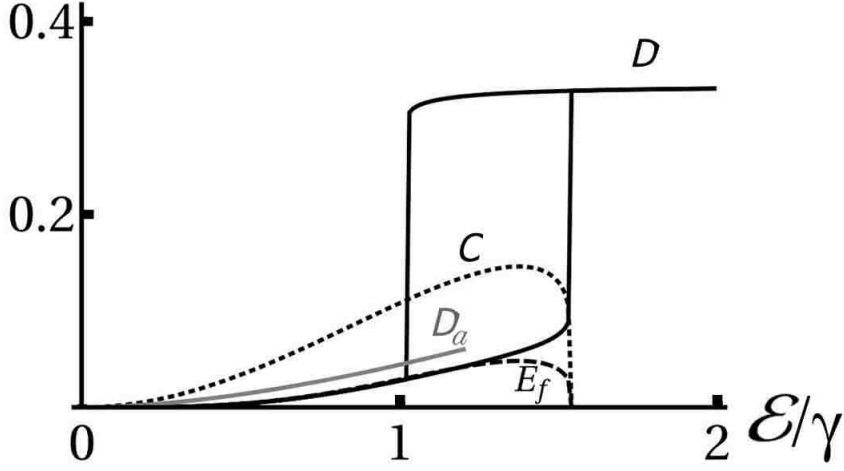
$$\Lambda_{high\ field} \rightarrow \frac{1}{3} \begin{pmatrix} 1 & 0 & 0 & 0 \\ 0 & \frac{1}{2} & \frac{1}{2} & 0 \\ 0 & \frac{1}{2} & \frac{1}{2} & 0 \\ 0 & 0 & 0 & 1 \end{pmatrix} \quad (2.28)$$

In the 3×3 basis this state would simply be a normalization of the three-dimensional identity. Therefore, this is a statistical mixture of separable states, meaning it has no entanglement. This matrix can also be written as a Bell Diagonal state, which is to say it has the following form [44].

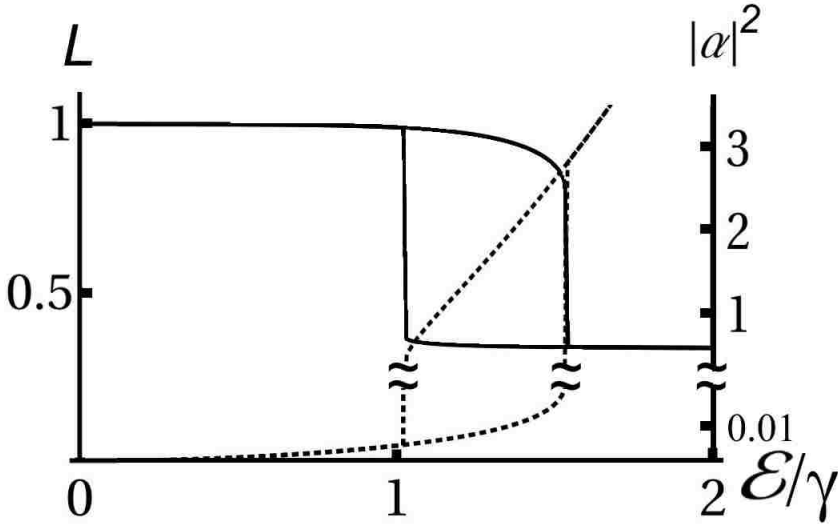
$$\Lambda = \frac{1}{4} \left(I + \sum_{j=1}^3 c_j \sigma_j \otimes \sigma_j \right) \quad (2.29)$$

In our particular case, $c_j = \frac{1}{3} \forall j$. Based on this we can use the analytical method for discord of Bell Diagonal states as set forth by Luo et al [42]. Here, too, we find a value of $\frac{1}{3}$ for quantum discord in the high field limit.

We can see that the entanglement of formation is virtually equal to the quantum discord in the low field range. It is tempting, therefore, to think that the state in this region needs to be correspondingly close to purity. The purity of the state is shown in the following figure. We can see that the purity is initially nearly one but will fall off to $1/3$ in the upper branch as the state loses the majority of its purity, becoming more of a mixed state. The purity is mathematically defined as $L(\rho) = Tr \rho^2$, making it essentially a measure of how close the state is to idempotency.



(a)



(b)

Figure 2.4: (a) Bistable behavior of Discord (D), entanglement of formation (E_f), and concurrence (C) as a function of scaled driving field ε/γ . Discord D_a for pure state given by Eq. 2.28 is also shown. (b) Shows bistability in purity (L) and cavity field intensity $|\alpha|^2$ with a gap in the bistability gap for visual clarity, as it would otherwise be impossible to see both the shape of the upper branch and the shape of the lower branch at the same time. Parameters for (a) and (b) are $g/\gamma = 2.8$, $W = 0.2$, $\delta_d = 0$, $\delta_c = 0$, $\kappa/\gamma = 0.8$.

Since the high purity occurs in the lower branch, a sensible way to understand this interesting phenomenon is to examine the limit $|\alpha|^2/n_s \ll 1$, where the saturation photon number is defined as $n_s = \gamma^2/8g^2$. If we use Eqs (14)-(17) derived by Mitra and Vyas [1] and neglect dot variable

terms that are higher order than $|\alpha|^2/n_s$ in the expansion, and choose zero detuning as a simplification, we find that $|q|, |r| \ll |p|$ and that the system may be described may be approximated as follows.

$$\begin{aligned} x &\rightarrow \left(\frac{2}{3} - |p|^2\right), & y &\rightarrow -\frac{1}{3} \\ p &\rightarrow \frac{|\alpha|}{\sqrt{2n_s}\sqrt{1+W^2}} e^{i\phi_p}, & \phi_p &= \tan^{-1}\left(\frac{W}{1+2C}\right) \\ |\alpha| &\rightarrow \frac{\varepsilon}{\kappa} \frac{(1+W^2)}{[(1+W^2+2C)^2+(2CW)^2]^{1/2}} \end{aligned}$$

In the above, the cooperativity parameter C is defined as $C = g^2/\gamma\kappa$, $W = 2w/\gamma$. By substituting these into the parameterization of Λ we get a density matrix which is a projector given by the following state vector.

$$|\psi\rangle \approx \sqrt{(1-|p|^2)} |\psi_0\rangle + |p| e^{i\phi_p} |\psi_1\rangle \quad (2.30)$$

where $|\psi_0\rangle = |00\rangle$ and $|\psi_1\rangle = \frac{|10\rangle+|01\rangle}{\sqrt{2}}$. In other words, the state in this limit is a superposition of ground and single exciton states. Because it is a pure state, the expressions for the discord and entanglement of formation of this state are identical and can be analytically derived.

$$D_a = -2|p|\log_2|p| - (1-|p|^2)\log_2(1-|p|^2) \quad (2.31)$$

It can be shown that the quantum discord of this system will always be nonzero unless either the driving field or the cavity-dot coupling is zero, which are both trivial cases. To show this, we use the method employed by Huang et al [73] and partition the density matrix Λ into four corners having dimensions 2×2 in each case, calling the corners $\Lambda^{(i,j)}$ with $i, j \in \{1, 2\}$.

$$\Lambda = \begin{pmatrix} \Lambda^{(1,1)} & \Lambda^{(1,2)} \\ \Lambda^{(2,1)} & \Lambda^{(2,2)} \end{pmatrix} \quad (2.32)$$

According to Huang et al, with such a partition, all the corner matrices will commute with one another, that is $[\Lambda^{(i,j)}, \Lambda^{(k,l)}] = 0 \forall i, j, k, l$, if and only if the discord of that matrix is zero. To

prove the discord is nonzero, therefore, requires only one counterexample. Consider the upper left and lower right partitions. Taking this commutator, one finds

$$\begin{aligned}
[\Lambda^{(1,1)}, \Lambda^{(2,2)}] &= \left[\left(\begin{array}{cc} \frac{1}{3} + x & \frac{p}{\sqrt{2}} \\ \frac{p^*}{\sqrt{2}} & \frac{1}{3} - x - y \end{array} \right), \left(\begin{array}{cc} \frac{1}{3} - x - y & \frac{r}{\sqrt{2}} \\ \frac{r^*}{\sqrt{2}} & \frac{1}{3} + y \end{array} \right) \right] \\
&= \left(\begin{array}{cc} \frac{pr^*}{2} - \frac{rp^*}{2} & -\frac{1}{3} - x - 3y \frac{p}{2^{3/2}} - r \frac{-\frac{1}{3} - 3x - y}{2^{3/2}} \\ p^* \frac{-\frac{1}{3} - 3x - y}{2^{3/2}} + \frac{-\frac{1}{3} - x - 3y}{2^{3/2}} r^* & \frac{p^*r}{2} - \frac{r^*p}{2} \end{array} \right)
\end{aligned} \tag{2.33}$$

This commutator is nonzero in all cases except the trivial case of no cavity field; therefore, the discord must be nonzero for all states wherein $\alpha \neq 0$

2.4.4 Non Bistable Regime and Effect of Detuning

In the case that we increase the dot-dot coupling and keep the detunings at zero, we find that a peak appears in the quantum discord curve. This peak does not go above the asymptotic value of $1/3$ regardless of how much W is increased. At the same time, as previously shown, the concurrence and correspondingly the entanglement of formation increase with high W up to a point, at which point the concurrence reaches the value of 0.43 which was thought previously [1] to be the highest it could be. Figures 2.5—2.8 illustrate the way in which varying W changes the discord as a function of ε .

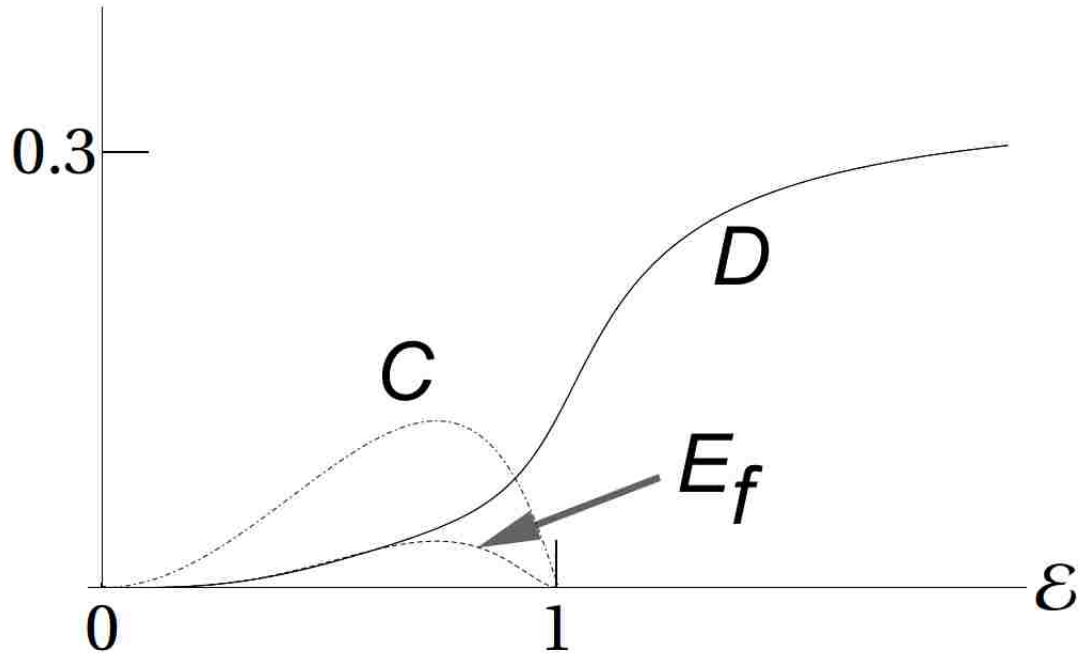


Figure 2.5: Comparison of concurrence (C), discord (D), and entanglement of formation (E_f), for a system of the parameters $\kappa = 1, \gamma = 1, g = 1, \delta_d = 0, \delta_c = 0, W = 0.1$

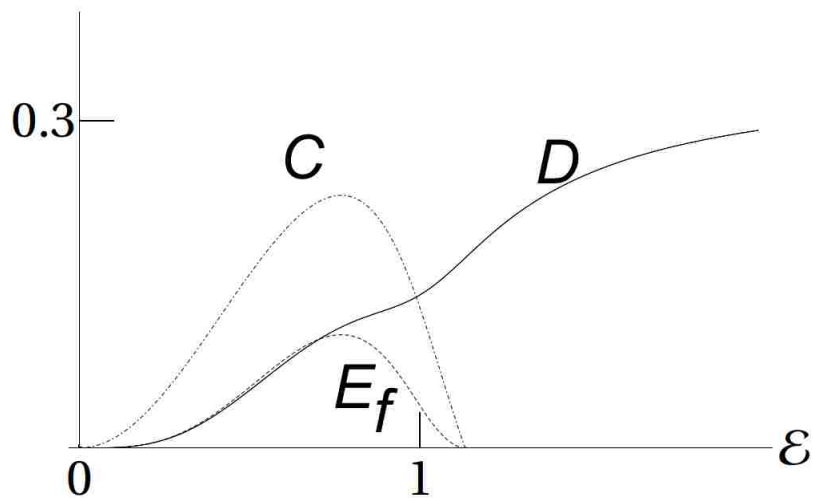


Figure 2.6: Comparison of concurrence (C), discord (D), and entanglement of formation (E_f), for a system of the parameters $\kappa = 1, \gamma = 1, g = 1, \delta_d = 0, \delta_c = 0, W = 1$

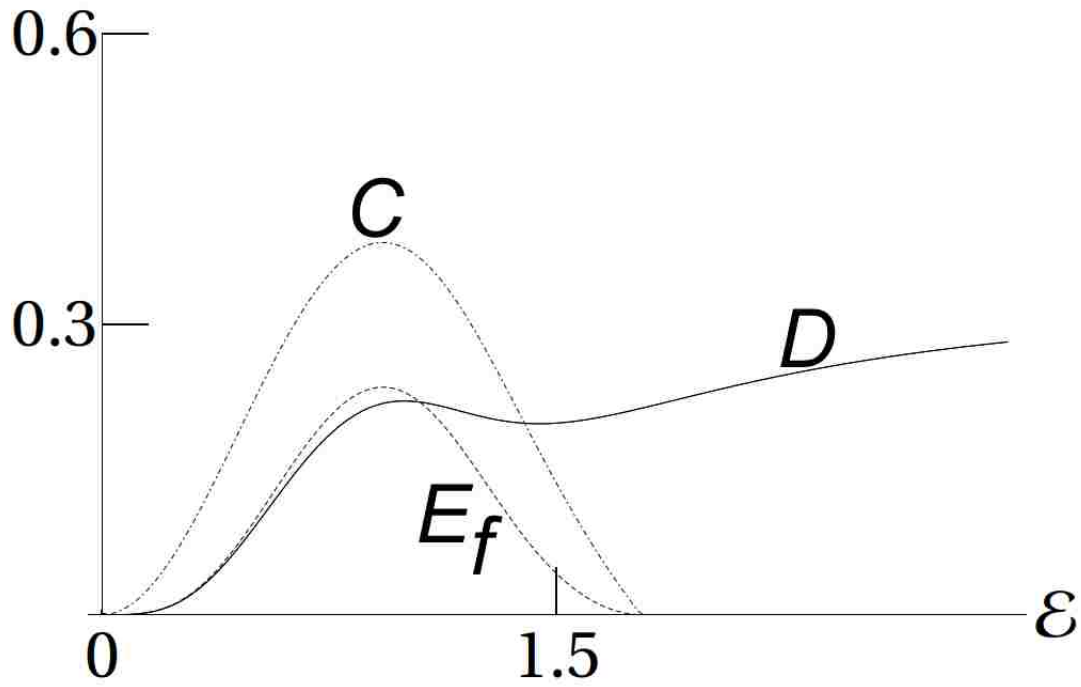


Figure 2.7: Comparison of concurrence (C), discord (D), and entanglement of formation (E_f), for a system of the parameters $\kappa = 1, \gamma = 1, g = 1, \delta_d = 0, \delta_c = 0, W = 5$

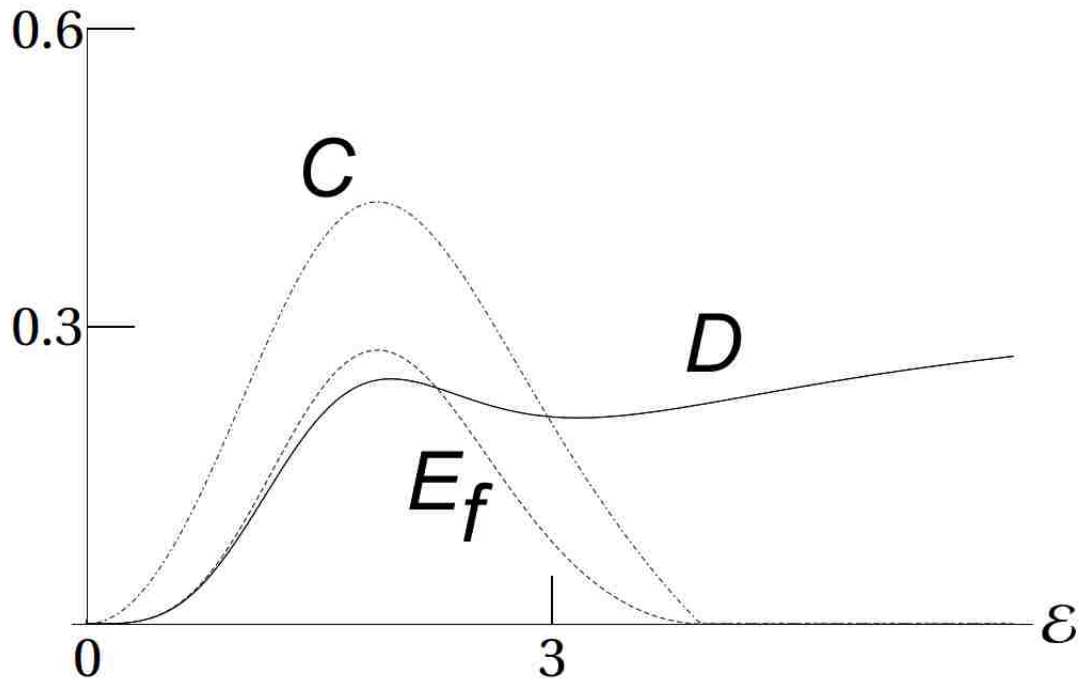


Figure 2.8: Comparison of concurrence (C), discord (D), and entanglement of formation (E_f), for a system of the parameters $\kappa = 1, \gamma = 1, g = 1, \delta_d = 0, \delta_c = 0, W = 30$

Given the fact that in a low W regime all correlations decrease quickly with adjustments in detuning, one might think that this would be the case in a high dot-dot coupling regime as well, and indeed this was previously assumed to be the case [1]. For δ_c that remains the case, but we see that proper adjustment of δ_d can result in higher values of discord, concurrence, and entanglement of formation. Note that as the magnitude of the dot detuning increases for negative δ_d , the position of the peak will first move to the right and then later to the left.

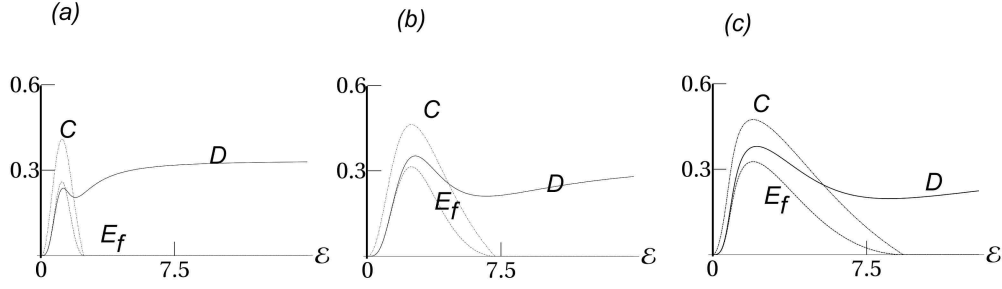


Figure 2.9: Comparison of concurrence (C), discord (D), and entanglement of formation (E_f), for a system of the parameters $W = 10$. (a) $\delta_d = 0$, (b) $\delta_d = -10$, (c) $\delta_d = -17$

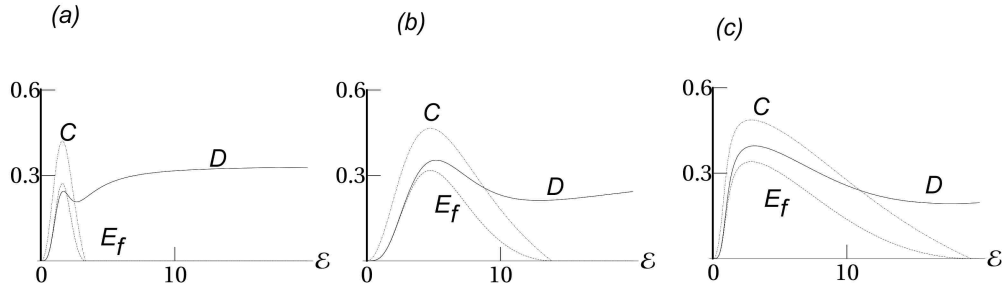


Figure 2.10: Comparison of concurrence (C), discord (D), and entanglement of formation (E_f), for a system of the parameters $W=20$. (a): $\delta_d = 0$, (b) $\delta_d = -19$, (c), $\delta_d = -37$

We find that adjusting the dot detuning in the positive direction decreases the correlations, but adjusting it in the negative direction increases the correlations up to a point before decreasing again. The trend is further illustrated below in 3D plots, once again using the parameters $\kappa = 1, \gamma = 1, g = 1, \delta_c = 0$.

As with the purity of states in the low field regime, we can examine this interesting behavior

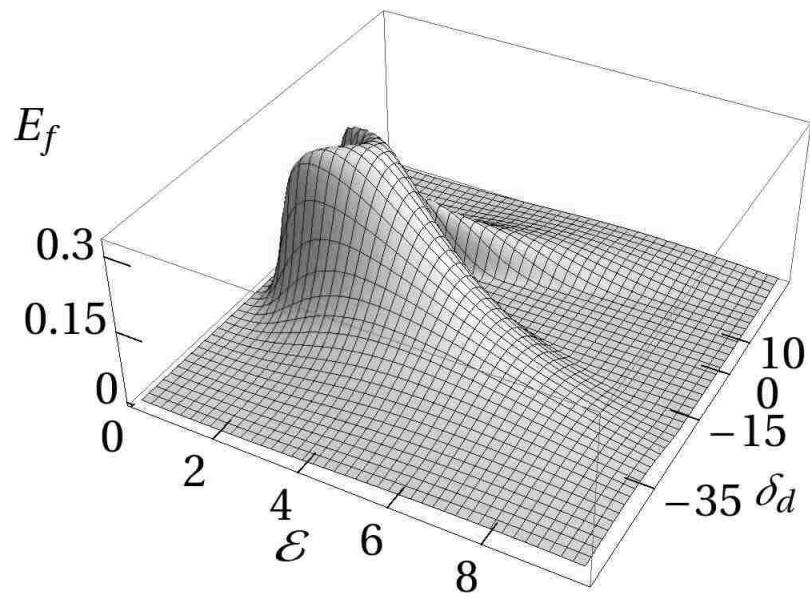
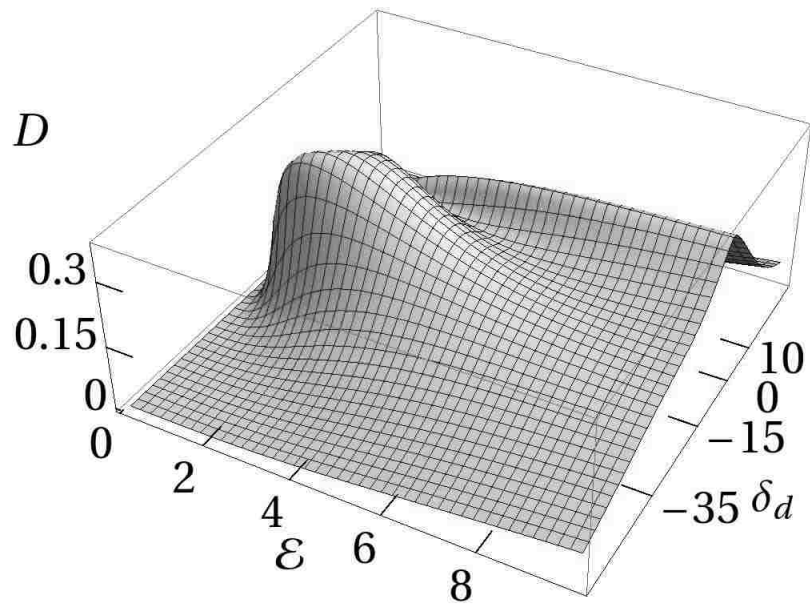


Figure 2.11: Discord and entanglement of formation as functions of dot detuning and driving field amplitude. $W = 10$, $\gamma = g = \kappa = 1$, $\delta_c = 0$

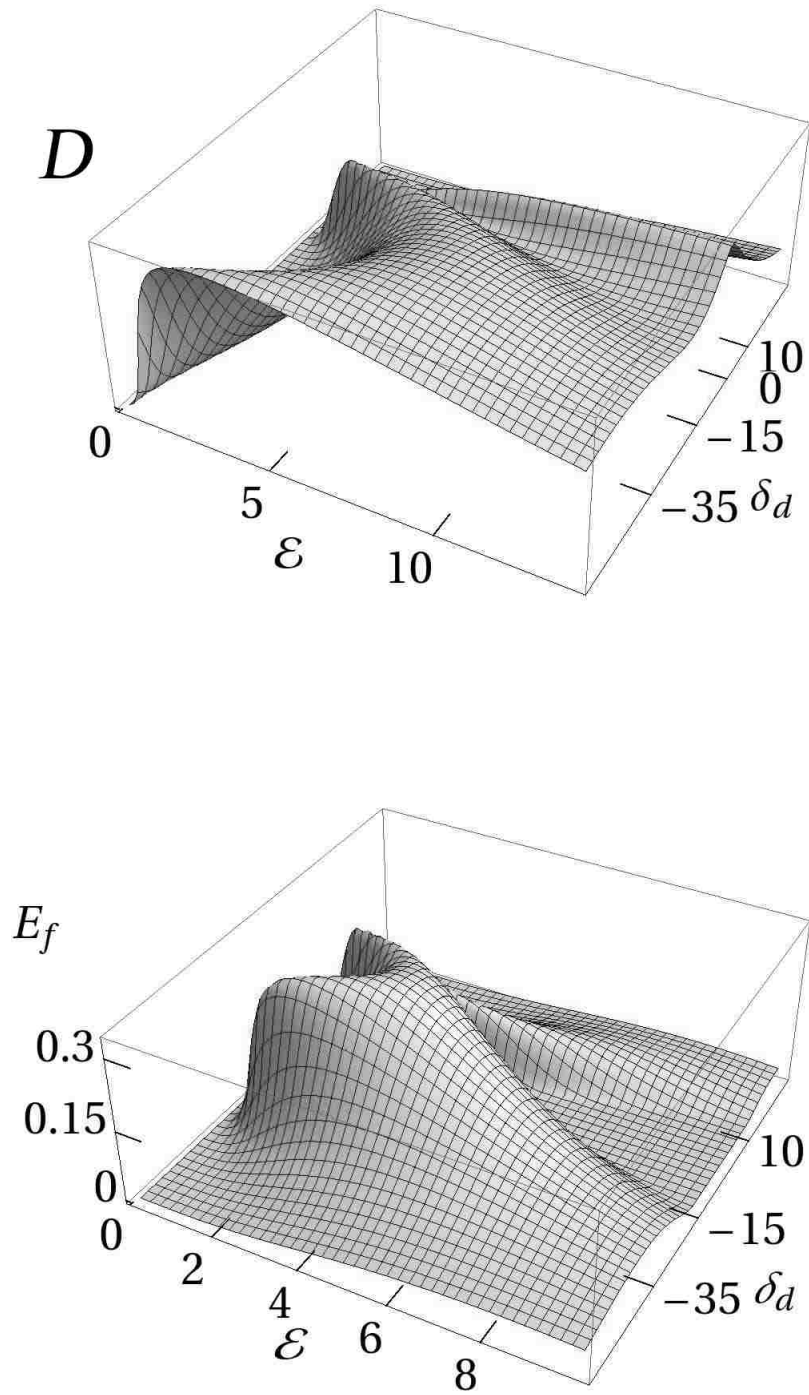


Figure 2.12: Discord and entanglement of formation as functions of dot detuning and driving field amplitude. $W = 15, \gamma = g = \kappa = 1, \delta_c = 0$

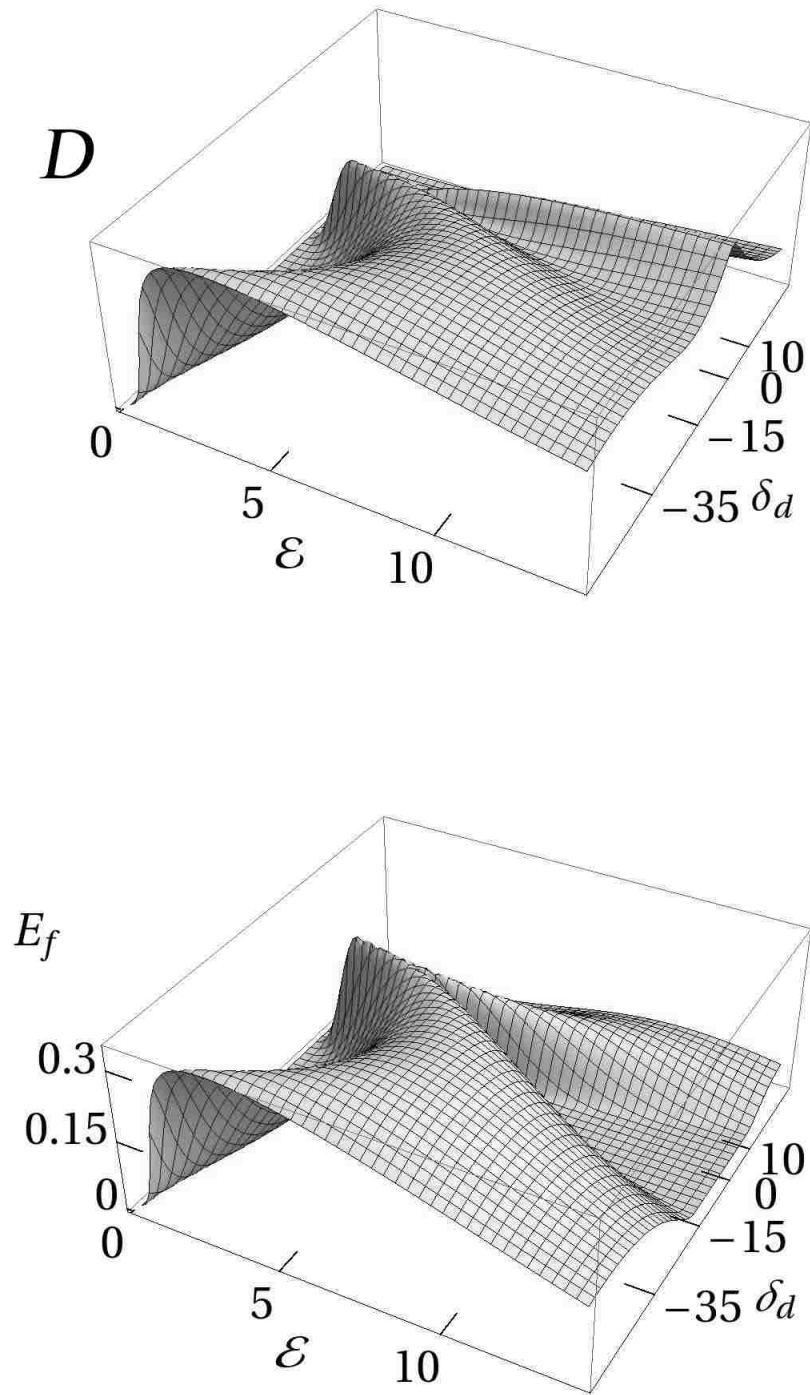


Figure 2.13: Discord and entanglement of formation as functions of dot detuning and driving field amplitude. $W = 30, \gamma = g = \kappa = 1, \delta_c = 0$

mathematically by means of a Taylor series expansion, using the solutions for the state parameters as found by Mitra and Vyas [1]. In this case, the applicable limit is $W \gg g$ and $\delta_d + 2W \rightarrow 0$. In the above limit, we find that q, r become negligible and that $x \rightarrow \frac{1}{6}$ and $y \rightarrow -\frac{1}{3}$. The dot density matrix approximation may then be written in terms of p as follows.

$$\Lambda_{highW} \approx \frac{1}{2} (1 - 4|p|^2) |\psi_0\rangle \langle \psi_0| + \frac{1}{2} (|\psi_1\rangle + 2p|\psi_0\rangle) (\langle \psi_1| + 2p^* \langle \psi_0|) \quad (2.34)$$

Though the results of this limit approximation suggest a small p , it is not negligible as such in the first order approximation. However, if one does take the simplification that $p \rightarrow 0$, then $C \rightarrow 0.5$, $E_f \rightarrow 0.354579$, $D \rightarrow 0.412154$, which corresponds well with the peaks that we see in the high W limit with optimum detuning.

2.5 Conclusion

We have studied a system of two identical quantum dots in a driven cavity with dissipation and detuning. The measure of quantum correlations known as quantum discord proves to be indeed more resilient than quantum entanglement, as measured by concurrence or entanglement of formation, in that the high driving field limit, despite approaching a separable state and having no concurrence, bears a nonzero value of quantum discord. The asymptotic limit in question is $1/3$, which can be analytically seen from the density matrix in question. This is the highest possible value of discord in a bistable regime. Exceeding this value requires both a high coupling between the dots and a negative dot detuning. The maximum value achieved for quantum discord was 0.41 and the maximum values for entanglement of formation and concurrence were 0.5 and 0.35, respectively. The optimum appears to occur around $\Delta_d = -w$. We found the values for the dot parameters in this region by means of a Taylor expansion and found the density matrix. In both cases we see a tendency for the quantum discord to initially be visually indistinguishable for low driving field indicating a relatively pure state, which purity we verify by examining this limit via a Taylor expansion.

3 Method of Calculating Global Discord of Multiple Qubits

The quantum discord discussed in the previous chapter is extendable to multiple bodies, via an extension of the mutual information. This extension, global discord, is quite difficult to calculate efficiently due to the higher number of parameters (twice the number of bodies). We have, however, developed a numerical method that calculates it efficiently and have tested it for two, three, and four qubits. This method is at its best when the system examined is symmetric in exchange of bodies, but it works well enough for asymmetric systems as well. (We use a coarse but effective search heuristic utilizing a series of meshes. We further streamline the computation by finding analytical simplifications to individual iterations, some of which sharply change how the problem scales with number of bodies provided that the bodies are identical.) The method is usable even on a desktop. We give a less efficient method employing projector matrices, known as the Matrix Method herein, and a more efficient one involving only vector operations (Vector Method). The difference in scaling between the Matrix and Vector methods is a factor of 2^{2N} for the case that the bodies are identical. The Vector Method remains faster than the alternative even if the bodies are not identical. This advantage becomes more and more critical as the number of qubits rises.

3.1 Global Discord as an Extension of Quantum Discord

3.1.1 Formal Definition

The global discord, first proposed by Rulli et al [25], is a generalization of the quantum discord. It is the minimum of the difference between the mutual information of the initial density matrix and that of the density matrix after it has been modified by a measurement on all subsystems. This is ultimately the same principle as with the pre-measurement and post-measurement mutual information functions in quantum discord, but the density matrix is modified rather than the mutual information function. As before, taking away the maximum

classical correlations from the total correlations will mean only quantum correlations remain. The mutual information of N subsystems, labeled A_1, A_2, \dots, A_N , is defined below.

$$I(\rho^{A_1 \dots A_N}) = \sum_{i=1}^N S(\rho^{A_i}) - S(\rho^{A_1 \dots A_N}) \quad (3.1)$$

where $\rho^{A_1 \dots A_N}$ is the state matrix for the whole system of N qubits, ρ^{A_n} is the density matrix for the n^{th} dot subsystem, and $S(\rho) = -\text{tr} \rho \ln \rho$ is the Von Neumann entropy. The mutual information after measurement can be defined in terms of the above function and a modified density matrix. This post measurement density matrix is with measurement outcome j is given by

$$J(\rho, j) = I(\Phi(\rho^{A_1 \dots A_n})) \quad (3.2)$$

where in the $\rho^{A_1 \dots A_N}$ space and $\Phi(\rho^{A_1 \dots A_n}) = \sum_{j=1}^{2^N} \Pi_j \rho^{A_1 \dots A_N} \Pi_j$ is the post measurement density matrix, and Π_j are separable projectors in the N -qubit space. There are 2^N possible ways the N pairs of projectors can be tensored into an N -body projector. For example, for three dots, there are eight possible measurement outcomes. The optimization must be done over all possible sets of Π_j to find which measurement maximizes the classical correlation. Global discord is therefore defined as

$$D(\rho^{A_1 \dots A_n}) = \min_{\{\Pi\}} (I(\rho^{A_1 \dots A_n}) - I(\Phi(\rho^{A_1 \dots A_n}))) \quad (3.3)$$

Discord of two qubits is not an intrinsically symmetric quantity in exchange of qubits, which is to say that the value of discord for an asymmetric two body system can change depending on which body is designated A or B [20]. This asymmetry is due to quantum discords reliance on just one subspace to determine the conditional entropy involved. However, it is apparent that global discord uses all N subspaces, creating N pairs of orthogonal two-dimensional projectors, giving a

$2N$ parameter optimization. The global discord can be defined for two qubits as well as higher numbers of bodies. In the case of two bodies, however, it makes more sense in applications to use quantum discord as there are half as many parameters. The increase in parameters is due to the symmetric nature of global discord. We nevertheless include the case of global discord of two quantum dots to give a fuller understanding of our numerical method. This optimization is considered numerically intensive [25] and has been studied in limited cases such as spin chains [74]. A generalization based in the Tsallis- q entropy [76], known as q Global Quantum Discord, or q -GGD was proposed by Chi et al [77], replacing the Von Neumann entropy with

$$S_q(\rho) = -\text{Tr} \rho^q \ln_q \rho \quad (3.4)$$

where $\ln_q x = \frac{x^{1-q}-1}{1-q}$. A single 2×2 projector can be parameterized as follows [41].

$$|b_{n\pm}\rangle\langle b_{n\pm}| = \frac{I \pm \mathbf{a} \cdot \boldsymbol{\sigma}}{2} \quad (3.5)$$

where $a_1 = \sin \theta_n \cos \phi_n$, $a_2 = \sin \theta_n \sin \phi_n$, $a_3 = \cos \theta_n$. Equivalently, the projectors can be parameterized in the following vector-based form.

$$|b_{n+}\rangle = \cos \frac{\theta_n}{2} |0\rangle_n + e^{i\phi_n} \sin \frac{\theta_n}{2} |1\rangle_n \quad (3.6)$$

$$|b_{n-}\rangle = \sin \frac{\theta_n}{2} |0\rangle_n - e^{-i\phi_n} \cos \frac{\theta_n}{2} |1\rangle_n \quad (3.7)$$

In both cases, n runs from 1 to N . Both parameterizations will be used in the development of our numerical method, with the latter being related to the faster numerical method.

3.1.2 Limited Known Cases

Like its predecessor quantum discord, global discord can only be analytically found in a limited set of special case density matrices. These analytical cases will serve as test cases for the method we develop in this chapter.

Xu [26] showed that the global discord of a Werner-GHZ state, which is a superposition of the N-qubit identity and a GHZ state, can be expressed as

$$D(\rho_{W-GHZ}) = \left(\frac{1-\mu}{2^N} + \mu \right) \log_2 \left(\frac{1-\mu}{2^N} + \mu \right) + \frac{1-\mu}{2^N} \log_2 \frac{1-\mu}{2^N} - 2 \left(\frac{1-\mu}{2^N} + \frac{\mu}{2} \right) \log_2 \left(\frac{1-\mu}{2^N} + \frac{\mu}{2} \right) \quad (3.8)$$

Here the Werner state ρ_{W-GHZ} defined as

$$\rho_{W-GHZ} = (1-\mu) \frac{I^{\otimes N}}{2^N} + \mu |\psi_{GHZ}\rangle \langle \psi_{GHZ}| \quad (3.9)$$

and μ is a real constant between 0 and 1 inclusive, I is the identity operator for a single dot, and $|\psi_{GHZ}\rangle$ is the N-body GHZ state as defined below.

$$|\psi_{GHZ}\rangle = \frac{|00\dots 0\rangle + |11\dots 1\rangle}{\sqrt{2}} \quad (3.10)$$

Xu [26] also analyzed a second class of multiqubit states defined below.

$$\rho = \frac{1}{2^N} (I^{\otimes N} + c_1 \sigma_x^{\otimes N} + c_2 \sigma_y^{\otimes N} + c_3 \sigma_z^{\otimes N})$$

where c_i are real constants restricted by the overall normalization of ρ and $\sigma_{x,y,z}$ are the Pauli spin matrices. Xu was able to show that the global discord of this state is

$$D(\rho) = f(\rho) - g(\rho) \quad (3.11)$$

where

$$f(\rho) = -\frac{1+c}{2} \log_2 \frac{1+c}{2} - \frac{1-c}{2} \log_2 \frac{1-c}{2} \quad (3.12)$$

and

$$g(\rho) = -\frac{1+d}{2} \log_2 \frac{1+d}{2} - \frac{1-d}{2} \log_2 \frac{1-d}{2} \quad (3.13)$$

if N is odd or

$$g(\rho) = -1 - \sum_{j=1}^4 \lambda_j \log_2 \lambda_j \quad (3.14)$$

and

$$c = \max(|c_i|), \quad d = \sqrt{\sum c_i^2} \quad (3.15)$$

$$\begin{aligned} \lambda_1 &= [1 + c_3 + c_1 + (-1)^{N/2} c_2]/4 \\ \lambda_2 &= [1 + c_3 - c_1 - (-1)^{N/2} c_2]/4 \\ \lambda_3 &= [1 - c_3 + c_1 - (-1)^{N/2} c_2]/4 \\ \lambda_4 &= [1 - c_3 - c_1 + (-1)^{N/2} c_2]/4 \end{aligned} \quad (3.16)$$

In addition, Braga et al [27] studied a tripartite W-GHZ state defined as

$$\rho_{W-GHZ} = \lambda |W\rangle \langle W| + (1 - \lambda) |GHZ\rangle \langle GHZ| \quad (3.17)$$

where the W-state is defined as

$$|W\rangle = \frac{|001\rangle + |010\rangle + |100\rangle}{\sqrt{3}} \quad (3.18)$$

For this case, Braga et al [27] were able to numerically solve the system based on the fact that the solution in this case would involve identical measurement projectors for all three qubits. We are able to reproduce the graph by Braga et al and the analytical solutions found by Xu [26].

3.2 A Brief Overview of Some Applications Involving Asymmetric Sets of Qubits

The scheme used to produce the systems of coupled quantum dots in chapters 2 and 4 requires that the dots are equidistant and identical [1, 16, 28, 29, 72]. This requirement imposes a hard limit of four qubits in the form of quantum dots. For a k dimensional space, at most a $k + 1$ dimensional simplex will fit [75]. Additionally, as noted by Quiroga and Johnson [13], the coupling between dots would not be the same for all dots if the quantum dots in question were

non-identical, regardless of whether they were vertices on a regular simplex, thereby resulting in a multi-level system rather than qubits. However, the method we develop for calculation of global discord of N qubits does not depend on how an N qubit density matrix was formed and will be perfectly functional regardless. Classical base three computing is possible [79] and there has been some degree of study of qutrits [80], which is to say three-level quantum information units. However, base three quantum computers are beyond the scope of this work, and qutrits are incompatible with the method we develop.

However, it is possible to create systems of qubits whose density matrices are not symmetric in exchange of bodies. To begin with, both of the DQC1 methods we have discussed [21, 22, 23] have non-identical qubits. Additionally, Altintas and Eryigit studied a system of non-interacting atoms in a cavity with dissipation for both identical atoms and non-identical atoms [81].

3.3 Outline of Numerical Method

3.3.1 Search Method

Despite the reputation the quantity Global Discord has for being quite computationally expensive we find that the function $I(\Phi(\rho))$ exhibits some properties that are readily exploitable to simplify the optimization. To begin with, consider the parameterizations of the projectors that were given above. We can see that the function depends entirely on sinusoidal functions and complex exponentials, none of which have a high frequency. Therefore, we expect the function is not particularly bumpy. Indeed, when we take the cross section of the function in which all variables except one are held constant, we get a sinusoidal pattern as seen in Figure 3.1 with θ_1 as the parameter allowed to vary and the system being that of three qubits.

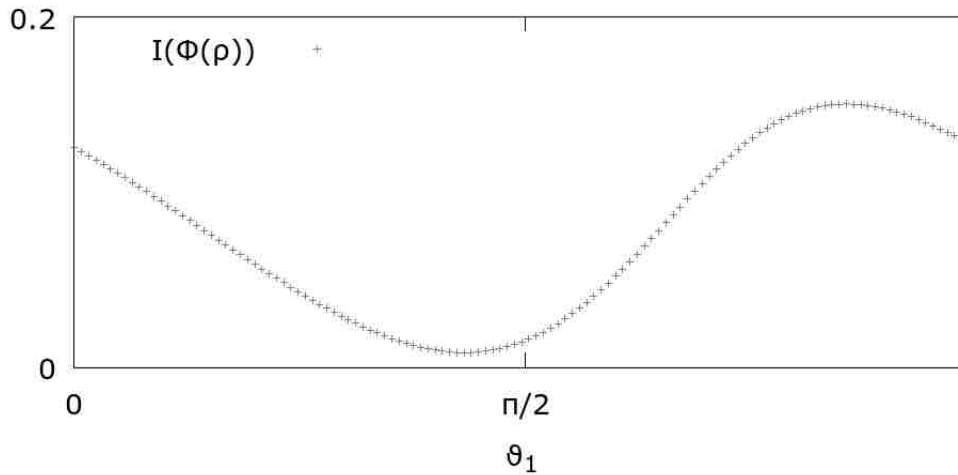


Figure 3.1: One dimensional cross section of a randomly chosen asymmetric three-body density matrix ρ_r . In this figure all $\theta_i, i \neq 1$ and all $\phi_j, j \in \{1, 2, 3\}$ are set to zero.

This by itself is suggestive but let us take this a bit further. Suppose that at each point on the sinusoid, we optimize the function with respect to all other parameters except θ_1 . While the result is not a perfect sinusoid, we can see some similarity and it is still quite well behaved, as seen in Figure 3.2.

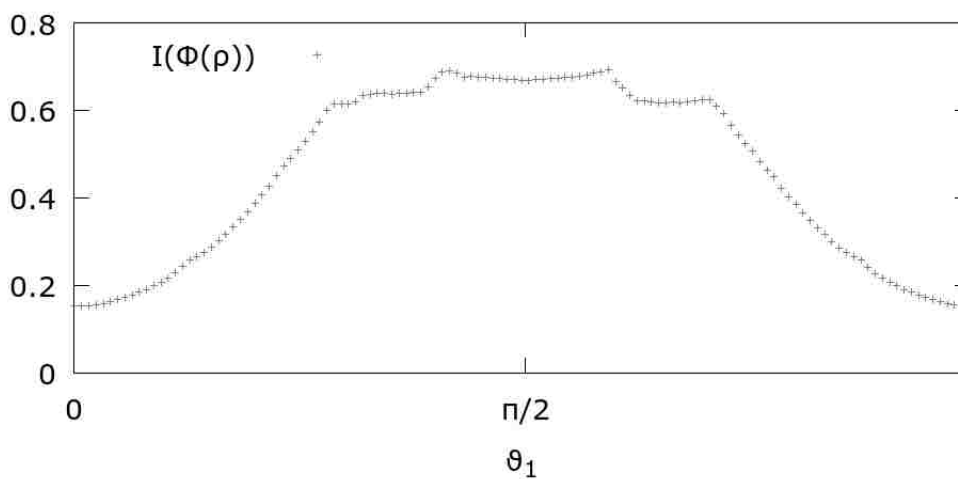


Figure 3.2: The same density matrix ρ_r as chosen in Fig 3.1, with all parameters except θ_1 optimized given input θ_1

While the above figure was created with a uniform search, this is not the most efficient search

method. So instead, let's divide the near sinusoid into five points evenly spaced and then center on the best point and divide that point's share of the area into five points centered around it, recenter on the best point, subdivide again, and then find the best point from that. This process finds the best point out of 125 points but only explores fifteen points. The process is illustrated below with an exact sinusoidal function.

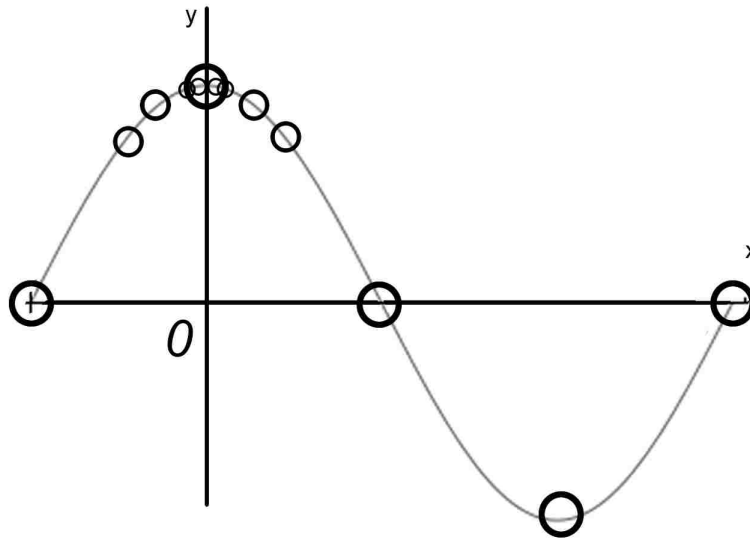


Figure 3.3: Illustration of process used to find optimum point in a sinusoidal function of arbitrary phase, amplitude, and frequency. Larger circles indicate points chosen in earlier stages of the search. Not actual data.

We have tested this method against a full uniform search in the case of three qubits. In addition, it gives the same result as the mesh-based method that we later develop.

This pattern of multidimensional sinusoidal functions allows us to realize that there is just one local maximum in the search space. While it finds the optimum in what can be considered equivalent to a uniform 125^{2N} point search (or 3.81 trillion points in the case of three qubits) but in far fewer iterations, we find that it is slower than still another method. Suppose all $2N$ dimensions were subdivided into five points to produce a $2N$ -dimensional hypercube mesh containing 5^{2N} points. This would be a very coarse uniform search and isn't by itself adequate. However, we know that there is just one local maximum, so let us create a similar mesh centered around the best point in the first mesh and reduced in length by some factor. The optimum point

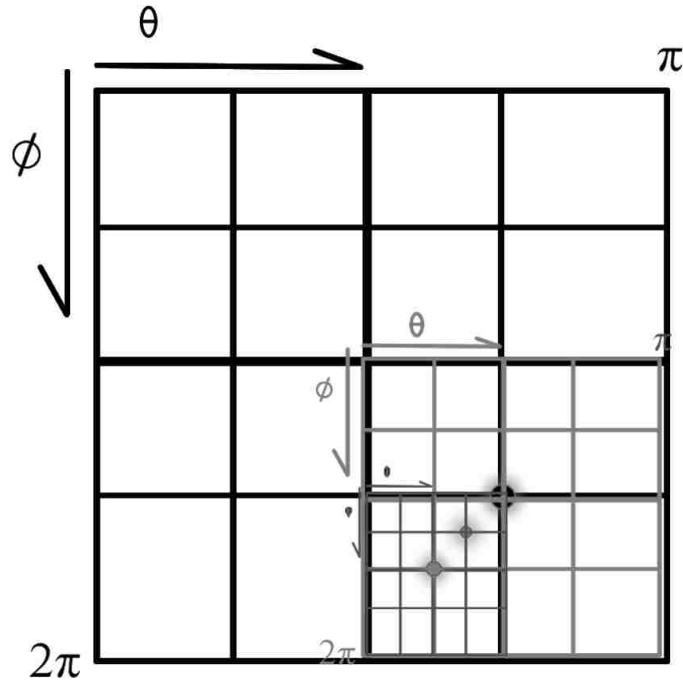


Figure 3.4: Illustration of search heuristic utilizing successively smaller meshes

on this new mesh will be closer to the proper maximum than the previous optimal point was. We can then produce yet another mesh and continue doing this until the optimum stops changing significantly. This search heuristic finds the maximum quicker than the sinusoid based search described above. The mesh-based search is illustrated in Figure 3.4 with a dimensionally suppressed diagram in which there is just a single θ and a single ϕ . In actuality, the process is carried out on a series of successively smaller $2N$ dimensional hypercubes with five points to a side.

This search pattern has some distinct advantages besides speed. Once a center point is chosen, all possible values for $\{\theta_n\}$ and $\{\phi_n\}$ (the sets of variables θ_n and ϕ_n , for $n = 1, \dots, N$) are known prior to exploration of the space, allowing for some reductions in calculations needed. For example, if $N = 3$, we have θ_n , $n = 1, 2, 3$ and ϕ_n , $n = 1, 2, 3$ and have five possible values for each variable, and hence 125 combinations of $\{\theta_n\}$ values, and 125 possible combinations of $\{\phi_n\}$ values. Furthermore, the search ends after a consistent number of nested meshes for all

density matrices so long as the number of qubits involved are the same, making the search method overall quite predictable. In the next sections we discuss ways in which the evaluation of the individual points on the mesh-grid can be reduced in computational complexity and discuss the test results for up to four qubits.

3.3.2 Matrix Method and Preliminary simplifications

The basis of the system is determined by the process of producing projectors by tensoring single body projectors together. The most natural manner in which the calculation will come out without forcing a different basis and making the logic of the program needlessly convoluted is in the binary sequence. This is to say that for a state $\psi_{i_1, i_2, \dots, i_N}$, where i_1 through i_N are treated as digits of a number in binary with i_1 being the left most digit. Examples of the basis needed in ρ are shown below.

$$\rho_{2QD} = \begin{pmatrix} \rho_{00,00} & \rho_{00,01} & \rho_{00,10} & \rho_{00,11} \\ \rho_{01,00} & \rho_{01,01} & \rho_{01,10} & \rho_{01,11} \\ \rho_{10,00} & \rho_{10,01} & \rho_{10,10} & \rho_{10,11} \\ \rho_{11,00} & \rho_{11,01} & \rho_{11,10} & \rho_{11,11} \end{pmatrix} \quad (3.19)$$

$$\rho_{3QD} = \begin{pmatrix} \rho_{000,000} & \rho_{000,001} & \rho_{000,010} & \rho_{000,011} & \rho_{000,100} & \rho_{000,101} & \rho_{000,110} & \rho_{000,111} \\ \rho_{001,000} & \rho_{001,001} & \rho_{001,010} & \rho_{001,011} & \rho_{001,100} & \rho_{001,101} & \rho_{001,110} & \rho_{001,111} \\ \rho_{010,000} & \rho_{010,001} & \rho_{010,010} & \rho_{010,011} & \rho_{010,100} & \rho_{010,101} & \rho_{010,110} & \rho_{010,111} \\ \rho_{011,000} & \rho_{011,001} & \rho_{011,010} & \rho_{011,011} & \rho_{011,100} & \rho_{011,101} & \rho_{011,110} & \rho_{011,111} \\ \rho_{100,000} & \rho_{100,001} & \rho_{100,010} & \rho_{100,011} & \rho_{100,100} & \rho_{100,101} & \rho_{100,110} & \rho_{100,111} \\ \rho_{101,000} & \rho_{101,001} & \rho_{101,010} & \rho_{101,011} & \rho_{101,100} & \rho_{101,101} & \rho_{101,110} & \rho_{101,111} \\ \rho_{110,000} & \rho_{110,001} & \rho_{110,010} & \rho_{110,011} & \rho_{110,100} & \rho_{110,101} & \rho_{110,110} & \rho_{110,111} \\ \rho_{111,000} & \rho_{111,001} & \rho_{111,010} & \rho_{111,011} & \rho_{111,100} & \rho_{111,101} & \rho_{111,110} & \rho_{111,111} \end{pmatrix} \quad (3.20)$$

where $\rho_{ij,kl}$ is the element of the density matrix for two qubits corresponding to states $|ij\rangle$ and $\langle kl|$ and $\rho_{ijk,lmn}$ is the element of the density matrix for three qubits corresponding to states $|ijk\rangle$ and $\langle lmn|$.

The matrix for the four quantum dot asymmetric case is a matrix with sixteen elements to a side and is therefore too large to be shown, but the basis follows the same pattern as with the previous two cases, ordering states of the form $|ijkl\rangle$ in the binary sequence, so that the states should be put in the following order.

$$\begin{aligned} &|0000\rangle, |0001\rangle, |0010\rangle, |0011\rangle, |0100\rangle, |0101\rangle, |0110\rangle, |0111\rangle, \\ &|1000\rangle, |1001\rangle, |1010\rangle, |1011\rangle, |1100\rangle, |1101\rangle, |1110\rangle, |1111\rangle \end{aligned}$$

The pattern above can be seen in the general case by tensoring an arbitrary number of superpositions of $|0\rangle, |1\rangle$ together. This process is elaborated upon below

$$\begin{aligned}
\otimes_{n=1}^N (|0\rangle + |1\rangle) &= (|0\rangle + |1\rangle) (\otimes_{n=2}^N (|0\rangle + |1\rangle)) \\
&= (|00\rangle + |01\rangle + |10\rangle + |11\rangle) (\otimes_{n=3}^N (|0\rangle + |1\rangle)) \\
&= (|000\rangle + |001\rangle + |010\rangle + |011\rangle) (\otimes_{n=4}^N (|0\rangle + |1\rangle)) & (3.21) \\
&\quad + (|100\rangle + |101\rangle + |110\rangle + |111\rangle) (\otimes_{n=4}^N (|0\rangle + |1\rangle))
\end{aligned}$$

$$\begin{aligned}
&= (|0000\rangle + |0001\rangle + |0010\rangle + |1010\rangle) (\otimes_{n=5}^N (|0\rangle + |1\rangle)) & (3.22) \\
&\quad + (|1000\rangle + |1001\rangle + |1010\rangle + |1011\rangle) (\otimes_{n=5}^N (|0\rangle + |1\rangle)) \\
&\quad \vdots \\
&= \{(|000\dots 0\rangle + \dots + |011\dots 1\rangle) + \dots + (|100\dots 0\rangle + \dots |111\dots 1\rangle)\} \otimes (|0\rangle + |1\rangle)
\end{aligned}$$

By adding the next qubit's digit onto the left side each time, we produce a situation in which the next set of basis states is formed of two groups of states, in which the first is the previous set of basis states with a leading zero added on and the second is the same set of basis states with the new leftmost digit being unity, a pattern which is repeatable for arbitrary system size.

Thus, if one wishes to compute a state's global discord using the Matrix Method, the density matrices must be converted to the above form from whichever form in which they were first produced. This is particularly important if using this method for computing the global discord of a symmetric system, such as the systems examined in Chapters 2 and 4 of this work, as the density matrix may be computed in its condensed form—a $N + 1$ dimensional matrix for N qubits—thereby necessitating that the density matrix be expanded to its full form. In such an expansion, it is easy to instead put the density matrices in forms where the original compressed density matrix's elements are expanded in blocks. This method produces the right density matrix for two qubits but fails to use the right basis for three or more qubits.

Knowing the binary sequence is used in producing the basis for the density matrix leads to an even more useful convention. We can use similar reasoning for the post measurement density

matrix and the ordering of the N body projectors. In this case, noting that $\Phi(\rho) = \sum_{j=1}^{2^N} \Pi_j \rho \Pi_j$, we can show that $\Phi(\rho) = \sum_{j=1}^{2^N} p_j \Pi_j \Pi_j = \sum_{j=1}^{2^N} p_j \Pi_j$ because the projectors surrounding the density matrix will only pick out the parts that are diagonal in the basis of the projectors. The result for three qubits with the binary sequence ordering is given below as an example.

$$\begin{aligned}
\Phi(\rho) = & p_1 |b_{1,0}, b_{2,0}, b_{3,0}\rangle \langle b_{1,0}, b_{2,0}, b_{3,0}| + p_2 |b_{1,0}, b_{2,0}, b_{3,1}\rangle \langle b_{1,0}, b_{2,0}, b_{3,1}| \\
& + p_3 |b_{1,0}, b_{2,1}, b_{3,0}\rangle \langle b_{1,0}, b_{2,1}, b_{3,0}| + p_4 |b_{1,0}, b_{2,1}, b_{3,1}\rangle \langle b_{1,0}, b_{2,1}, b_{3,1}| \quad (3.23) \\
& + p_5 |b_{1,1}, b_{2,0}, b_{3,0}\rangle \langle b_{1,1}, b_{2,0}, b_{3,0}| + p_6 |b_{1,1}, b_{2,0}, b_{3,1}\rangle \langle b_{1,1}, b_{2,0}, b_{3,1}| \\
& + p_7 |b_{1,1}, b_{2,1}, b_{3,0}\rangle \langle b_{1,1}, b_{2,1}, b_{3,0}| + p_8 |b_{1,1}, b_{2,1}, b_{3,1}\rangle \langle b_{1,1}, b_{2,1}, b_{3,1}|
\end{aligned}$$

where p_j are the probabilities of finding the post measurement density matrix in the corresponding projector state, so that for example p_1 corresponds to the projector for state vector $|b_{1,0}, b_{2,0}, b_{3,0}\rangle$, and

$$|b_{n,0}\rangle = |b_{n-}\rangle$$

$$|b_{n,1}\rangle = |b_{n+}\rangle$$

a notation we briefly adopt to more clearly illustrate the connection between this ordering of projectors and the binary sequence. Because the post measurement density matrix is diagonal in the basis of $\{\Pi_j\}$, the probability of finding the i^{th} dot in the $|b_{i,0}\rangle$ state can be found by adding up all probabilities p_j in which the i^{th} dot is found in that state. For example, for three qubits we can find the probabilities with the prescription below.

$$b_{1,0} = \sum_{k=1}^4 p_k, \quad b_{2,0} = p_1 + p_2 + p_5 + p_6, \quad b_{3,0} = p_1 + p_3 + p_5 + p_7$$

These three probabilities are sufficient as the $|b_{i,1}\rangle$ states may be derived by normalization constraints. Note also that even if the original density matrix is symmetric in exchange of qubits, $\Phi(\rho)$ will often not be similarly symmetric and all N sets of single dot subspace probabilities

must be calculated to achieve a correct result. So long as the projectors are ordered in the binary sequence we can generalize results for the probabilities $b_{i,0}$ as follows.

$$\begin{aligned}
b_{1,0} &= \sum_{j=1}^{2^{N-1}} p_j \\
b_{2,0} &= \sum_{\ell=0}^1 \sum_{j=2^{N-1}\ell+1}^{2^{N-2}(2\ell+1)} p_j \\
&\vdots \\
b_{n,0} &= \sum_{\ell=0}^{2^{n-1}-1} \sum_{j=2^{N-n+1}\ell+1}^{2^{N-n}(2\ell+1)} p_j \\
&\vdots \\
b_{N,0} &= \sum_{\ell=0}^{2^{N-1}-1} p_{2\ell+1}
\end{aligned} \tag{3.24}$$

This generalization allows one to find the global discord for N qubits without ever producing the full $\Phi(\rho)$ matrix at all, meaning that one can use the cyclic property of the trace and the idempotency of projectors to find $Tr \Pi_j \rho$ to obtain each measurement probability p_j and then use the p_j to calculate the $b_{i,0}$ probabilities. There is no such shortcut for evaluating the mutual information of the original density matrix ρ , but the various partial traces of this density matrix only need to be evaluated once each. Furthermore, it is not necessary to produce the entire matrix multiplication $\Pi_j \rho$ as we only need the diagonal terms. This is counter intuitive as the definition of the mutual information involves eigenvalues, but at no point in the optimization is an eigenvalue call necessary as we can gain the probabilities p_j much more rapidly and equally accurately simply by taking $Tr \Pi_j \rho \Pi_j$ [52]. The only time the eigenvalues are needed is at the beginning of the process when we take the eigenvalues of ρ , which only needs to be done once per density matrix evaluated. The simplifications discussed above can greatly improve the computational time and open up the possibility of further simplifications which we will detail in the next section, which concerns the Vector Method for global discord. The Matrix Method scales as $O((2^N)^3)$ regardless of symmetry or lack thereof. This scaling comes from the fact that the

creation of the various projectors and the process of taking the trace of $\Pi_j \rho$ scale at 2^{2N} each and the number of projectors scales with 2^N , the number of eigenvalues of an N body density matrix with no dimensional reductions from symmetry.

3.3.3 Use of Vectors to Greatly Diminish Computational Time

While the simplifications in the preceding section already improve the optimization process markedly, the method discussed, as our name for said method suggests, still relies on matrix operations. This initially may appear to be a necessity, but now that we have shown that it is never necessary to evaluate the partial traces of $\Pi_j \rho \Pi_j$, the path to further, more significant simplifications is opened up. Consider the eigendecomposition of ρ , where we write $\rho = \sum_i q_i |\psi_i\rangle \langle \psi_i|$, wherein q_i are the eigenvalues of ρ . Let us define scaled eigenvectors $|\psi'_i\rangle$

$$|\psi'_i\rangle \equiv \sqrt{q_i} |\psi_i\rangle \quad (3.25)$$

We can then rewrite post measurement density matrix as follows

$$\Phi(\rho) = \sum_{j=1}^{2^N} |B_j\rangle \langle B_j| \left(\sum_i |\psi'_i\rangle \langle \psi'_i| \right) |B_j\rangle \langle B_j| \quad (3.26)$$

where we have defined $|B_j\rangle \langle B_j| \equiv \Pi_j$. The probabilities p_j can then be written as follows, noting that the sum is independent of the projectors.

$$p_j = Tr \left(|B_j\rangle \langle B_j| \left(\sum_i |\psi'_i\rangle \langle \psi'_i| \right) |B_j\rangle \langle B_j| \right) = \sum_i |\langle \psi'_i | B_j \rangle|^2 \quad (3.27)$$

We can see then that it is only necessary to calculate the overlaps of the measurement vectors with the scaled eigenvectors. The scaled eigenvectors need only be computed once prior to the optimization. Further streamlining can be achieved by noting that

$$|B_j\rangle = |b_{1,r(1,j)}\rangle \otimes |b_{2,r(2,j)}\rangle \otimes \cdots \otimes |b_{N,r(2,j)}\rangle \quad (3.28)$$

where the index $r(n, j)$ denotes whether the n^{th} dot space measurement vector is $|b_{n,0}\rangle$ or $|b_{n,1}\rangle$ for global outcome j [25]. For example, if we have three dots and the outcome is 6, then $|B_6\rangle = |b_{1,0}\rangle \otimes |b_{2,0}\rangle \otimes |b_{3,1}\rangle$. The aforementioned single dot measurement vectors may be written as follows

$$|b_{n,+}\rangle = \cos \frac{\theta_n}{2} |0\rangle_n + e^{i\phi_n} \sin \frac{\theta_n}{2} |1\rangle_n \quad (3.29)$$

$$|b_{n,-}\rangle = \sin \frac{\theta_n}{2} |0\rangle_n - e^{-i\phi_n} \cos \frac{\theta_n}{2} |1\rangle_n \quad (3.30)$$

Therefore, all that is being multiplied by $|\psi'_i\rangle$ is products of sines and/or cosines with argument $\frac{\theta_n}{2}$ and products of complex exponentials in the $\{\phi_n\}$ variables. While these functions will change when a new mesh is created based on the prior mesh's optimal lattice point, the values of these functions will not change for a given mesh. It is therefore useful to precalculate these functions on each mesh iteration and use tables of their values and tables of products to eliminate redundant steps. Put more formally, we can define the probabilities as expressions in placeholder functions $C_{m,j}(\{\theta_n\})$ and $D_{m,j}(\{\phi_n\})$ where m indicates the m^{th} element of $|\psi'_i\rangle$.

$$\langle \psi'_i | B_j \rangle = \sum_{m=1}^{2^N} \psi'_{im} C_{m,j}(\{\theta_n\}) D_{m,j}(\{\phi_n\}) \quad (3.31)$$

$$p_j = \sum_{i=1}^{2^N} \left| \langle \psi'_i | B_j \rangle \right|^2 \quad (3.32)$$

The values for $C_{m,j}(\{\theta_n\})$ and $D_{m,j}(\{\phi_n\})$ can and should be computed ahead of time to whatever extent memory allows for speed. Even in the four quantum dot case, we find that the extent to which memory allows us to precalculate $C_{m,j}(\{\theta_n\})$ and $D_{m,j}(\{\phi_n\})$ is that they can be precalculated in their entirety without any discernable memory-related difficulty whatsoever. For a full calculation of the overlaps $\langle \psi'_i | B_j \rangle$ for up to four qubits, see Appendix A.

Some states may be symmetric in exchange of qubits. Such states are summarizable by a smaller density matrix and fewer nonzero eigenvalues. We can take advantage of this phenomenon in a simple way. Consider the eigenvectors of a general symmetric density matrix.

$$\begin{aligned}
|\psi'_i\rangle &= \psi'_{i_1} |000\dots 0\rangle + \psi'_{i_2} \frac{|100\dots 0\rangle + |010\dots 0\rangle + \dots + |000\dots 1\rangle}{\sqrt{r_2}} \\
&+ \dots + \psi'_{i_N} \frac{|011\dots 1\rangle + |101\dots 1\rangle + \dots + |111\dots 0\rangle}{\sqrt{r_N}} + \psi'_{i_{N+1}} |111\dots 1\rangle
\end{aligned} \tag{3.33}$$

where $\sqrt{r_m}$ is a normalization factor. We can then include the normalization factors in the scaled eigenvectors

$$\psi''_{i_m} \equiv \frac{\psi'_{i_m}}{\sqrt{r_m}} \tag{3.34}$$

We also note that in this case, several terms of the form $C_{m,j}(\{\theta_n\})D_{m,j}(\{\phi_n\})$ are actually multiplied by identical ψ'_{i_m} and therefore can be combined to reduce the number of multiplications in the innermost loop. In other words

$$p_j = \sum_{i=1}^N \left| \sum_{m=1}^N \psi''_{i_m} F_{i,j}(\{\theta_n\}, \{\phi_n\}) \right|^2 \tag{3.35}$$

where $F_{m,j}(\{\theta_n\}, \{\phi_n\})$ is a sum of several products of the form $C_{m,j}(\{\theta_n\})D_{m,j}(\{\phi_n\})$, except in cases where $\psi''_{i_m} = \psi'_{i_m}$, in which case the expression reduces to a single product $C_{m,j}(\{\theta_n\})D_{m,j}(\{\phi_n\})$ if $m = N$ or simply $C_{m,j}(\{\theta_n\})$ if $m = 1$. This change not only reduces the number of multiplications needed, but also allows us to move a number of operations outside of the innermost loop that would otherwise have to be performed therein.

3.3.4 Verification of Density Matrices with Known Global Discord

Using our numerical method for global discord, we are able to reproduce known results for global discord found either through analytical means, as in the case of Xu [26], or more limited case numerical means, as in the case of Braga et al [27], who studied a matrix whose global discord optimization can be reduced to a two parameter problem. Our results, shown in Figures 3.5 to 3.9, match in all cases.

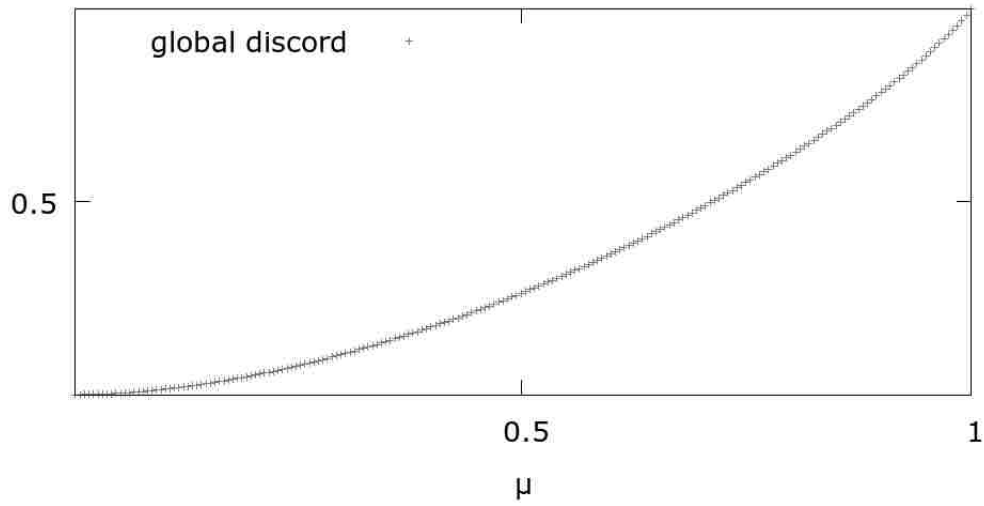


Figure 3.5: Global discord of a two qubit density matrix of the form $\rho_{Werner-Bell} = \mu\rho_{Bell} + (1 - \mu)\frac{I_4}{4}$ as a function of μ . This matches the analytically produced graph produced by Xu [26].

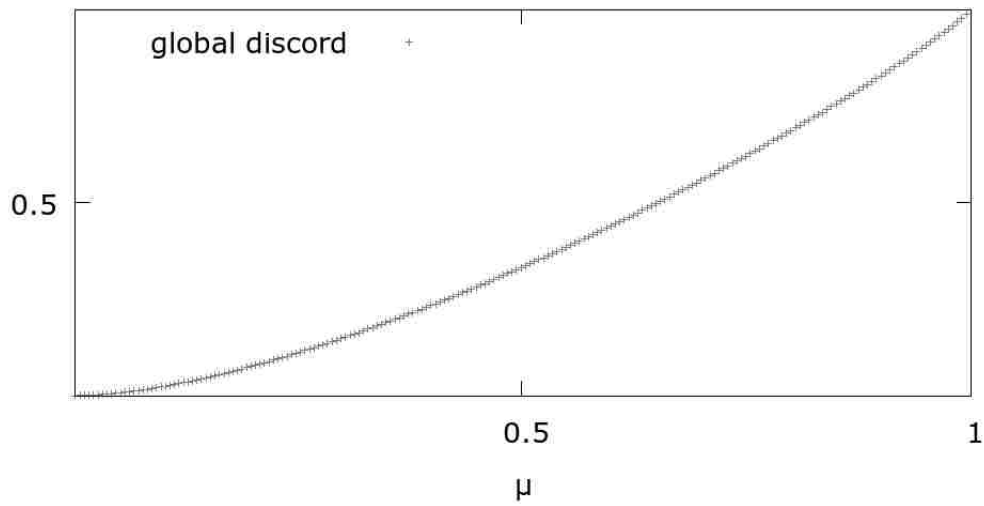


Figure 3.6: Global discord of a three qubit density matrix of the form $\rho_{Werner-GHZ_3} = \mu\rho_{GHZ_3} + (1 - \mu)\frac{I_8}{8}$ as a function of μ . This matches the analytically produced graph produced by Xu [26].

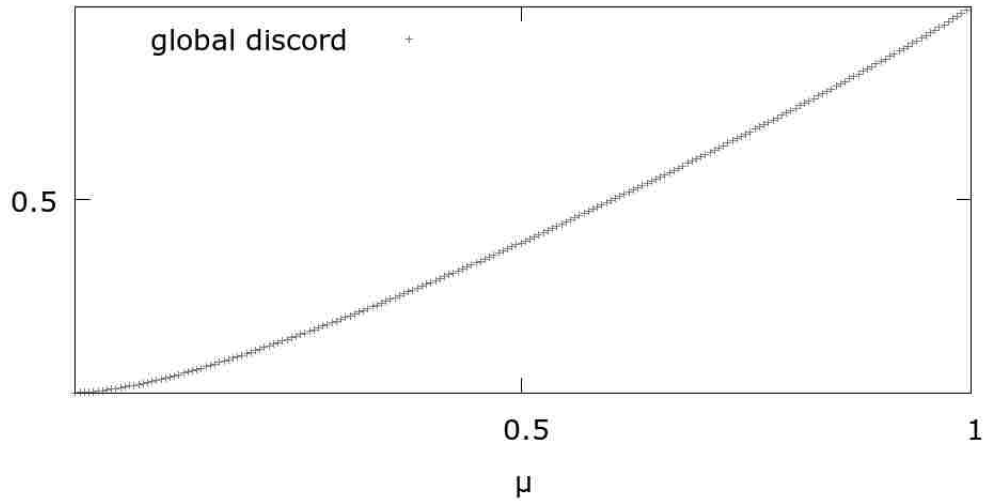


Figure 3.7: Global discord of a four qubit density matrix of the form $\rho_{Werner-GHZ_4} = \mu\rho_{GHZ_4} + (1 - \mu)\frac{I_{16}}{16}$ as a function of μ . This matches the analytically produced graph found by Xu [26].

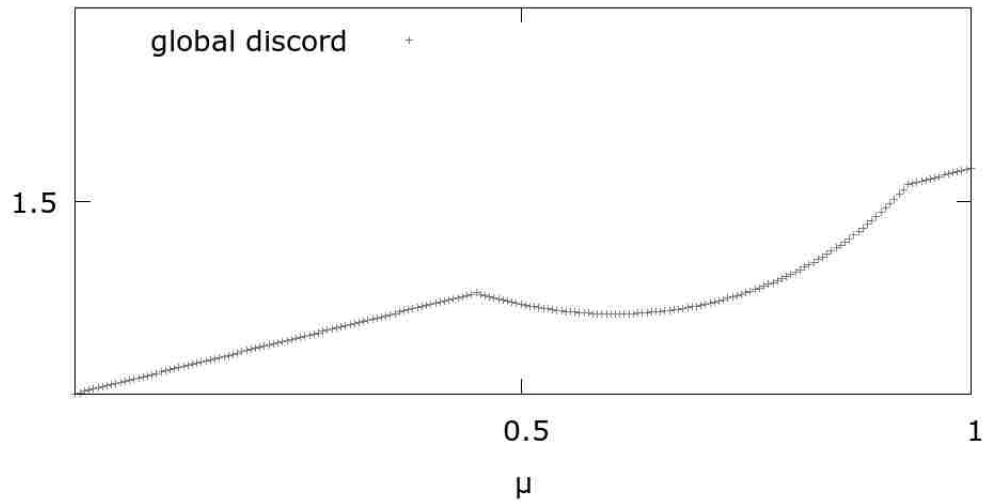


Figure 3.8: Global discord of a three qubit density matrix of the form $\rho_{W-GHZ_3} = \mu\rho_W + (1 - \mu)\rho_{GHZ_3}$ as a function of μ . This result concurs with the plot produced by Braga et al [27]

3.4 Speed Comparison for Matrix and Vector Methods

The global discord method has been tested for up to four qubits, meaning that it will work well in the event that the global discord of a system of four quantum dots is studied in the same fashion that the systems of two and three dots are studied in chapters 2 and 4 respectively. While the Hamiltonian and master equation are not able to support five or more qubits due to the

equidistance requirement, the numerical method for quantum global discord is extendable to arbitrary numbers of qubits. Additionally, while the method was originally developed in the context of identical dots, it also applies to non-identical qubit systems. In this section, we give test results for both methods in two, three, and four qubit systems using random density matrices created by the construction of random orthogonal vectors and random choice of valid probabilities.

3.4.1 Generation of Random Density Matrices

To employ a speed test for our algorithm under various conditions, we must create a large number of random valid density matrices. To understand the process of generating these matrices, consider the pure state decomposition of our random density matrix ρ_r into eigenstates

$$\rho_r = \sum_{i=1}^{2^N} q_i |\psi_i\rangle \langle \psi_i| \quad (3.36)$$

where q_i are the eigenvalues corresponding to eigenstates $|\psi_i\rangle$. We know that for a valid density matrix for a physical system, the eigenvalues will all be non-negative and sum to 1. We also know that the eigenvectors must be orthonormal. If we were to generate random state vectors $|\chi_i\rangle$, they will in all likelihood violate the constraints on the eigenvectors. However, it is likely the vectors are linearly independent (and if a pair isn't, one can be thrown out and a new one can be generated to take its place). We can create the first vector simply by taking

$$|\psi_1\rangle = \frac{|\chi_1\rangle}{\langle \chi_1 | \chi_1 \rangle} \quad (3.37)$$

Then we may use the Gram-Schmidt algorithm [78] to orthogonalize the vectors.

$$|\psi_{i+1}\rangle = \frac{|\phi_{i+1}\rangle}{\langle \phi_{i+1} | \phi_{i+1} \rangle} \quad (3.38)$$

where $|\phi_{i+1}\rangle = |\chi_{i+1}\rangle - \sum \langle \psi_i | \chi_{i+1} \rangle |\psi_i\rangle$. We then implement a failsafe against linearly dependent vectors, such that if $|\chi_i\rangle = \langle \psi_j | \chi_i \rangle |\psi_j\rangle$, for some i and j , then a new vector is randomly chosen to replace it. This algorithm therefore produces a set of randomly chosen, mutually orthonormal vectors. From these we construct a density matrix whose eigenvalues q_i are chosen such that q_1 is a random number from 0 to 1 and that q_i is a random number chosen from 0 to $1 - \sum_{j=1}^{i-1} q_j$, guaranteeing non-negative normalized eigenvalues of the density matrix. The amount of time consumed by creating the density matrices in this fashion is trivial relative to the computational time of the global discord numerical methods presented in this chapter.

3.4.2 Two Qubits

In the case of two qubits, we have a four parameter problem, creating a $5^4 = 625$ point mesh on each iteration, requiring six iterations per density matrix, and both of the methods run in a fraction of a second. This is done in both the asymmetric case, which has a 4×4 density matrix, and the symmetric case, which can be reduced to a 3×3 density matrix. A good optimum for $I(\Phi(\rho))$ may be reached in just six mesh search iterations. We can derive the overlap expressions needed for the vector based method in both asymmetric and symmetric cases with ease. The asymmetric expressions are derived in detail in Appendix A.

This produces a minor reduction in mathematical operations to be performed compared to what will be seen in later sections. In the following test runs, we used an AMD FX8350 processor, single core with Fortran 90 as the programming language used and gfortran as the compiler. To run 100,000 density matrices with the matrix method takes 688 seconds, using randomly produced density matrices. In contrast, the asymmetric vector method case takes 281 seconds, and the symmetric vector method takes 258 seconds. If we instead split the job evenly over all eight cores, which is 12,500 matrices per core, we find that the matrix method requires 130 seconds; the asymmetric vector method requires 52 seconds; and the symmetric vector method requires 45 seconds.

We then move on to the supercomputer known as Razor at the University of Arkansas. We use three nodes and sixteen parts per node. We evaluate random matrices once more and we choose the number of randomly generated matrices to be 12,000,000, which is 250,000 matrices per processing core, and the code was compiled via Intel Fortran Compiler, or IFORT. The CPUs involved are a pair of eight-core Intel Xeon E5-2670 processors, clocked at 2.60GHz, on each node. This process takes 41 minutes and 30 seconds for the matrix method. For the asymmetric vector method, the time is 29 minutes and 10 seconds. In contrast, the symmetric vector method requires 28 minutes and 47 seconds.

3.4.3 Three Qubits

For three qubits, there are six parameters, creating a $5^6 = 15625$ point mesh on each successive iteration, with twelve iterations needed to converge. The asymmetric states require an 8×8 matrix, while the symmetric states may be reduced to a 4×4 matrix. The derivation of the overlap expressions for the asymmetric and symmetric cases are derived in detail in Appendix A.

Running on an AMD FX8350 with a single core and generating 10,000 random valid density matrices, we find that the matrix method requires 18324 seconds to complete, or 5.09 hours. In contrast, the asymmetric vector method requires 4561 seconds to complete, or 76.02 minutes, whereas the symmetric vector method requires 2324 seconds to complete, or 38.73 minutes.

We perform the same test on the same processor but with parallelization, so that the code is running on all eight cores of the device. In this case, the matrix method requires only 5402 seconds or 90.03 minutes. The asymmetric vector method requires 954 seconds or 15.9 minutes. The symmetric vector method requires 361 seconds, or 6.02 minutes.

Using the same set of cores on the university supercomputer as in the case of two qubits and choosing to process 2500 density matrices per core for a total of 120,000 matrices, we find that the matrix method requires 1 hour, 43 minutes, and 36 seconds; the asymmetric vector method requires 17 minutes and 1 second; and the symmetric vector method requires 9 minutes and 43

seconds.

3.4.4 Four Qubits

Four qubit systems entail eight parameters and a $5^8 = 390625$ point mesh on each iteration. The number of meshes required to reach a good maximum is twelve. The system requires at most a 16×16 matrix, but a symmetric matrix may be reduced to a 5×5 matrix. The analytical expressions for the overlaps between the sixteen projectors and the scaled eigenvectors are derived in detail in Appendix A.

For test runs performed on a single core of an AMD FX8350 on a desktop with Fortran as the language, the matrix method requires 323,872 seconds, or 89.96 hours, to complete a thousand randomly generated density matrices. In contrast, the asymmetric vector method takes 65,250 seconds, or 18.13 hours, to complete the same test, and the symmetric vector method, which applies only to density matrices that can be rewritten as 5×5 matrices only requires 17,445 seconds, which is to say 4.85 hours.

If we use the same machine, but utilize all eight cores, which is to say that each core must process 125 of the randomly generated density matrices, then for the matrix method we get 53,624 seconds, or 14.90 hours; for the asymmetric vector method we get 12624 seconds, which is 3.51 hours; and for the symmetric vector method we get 2909 seconds, which is to say 48.48 minutes, which is also to say 0.81 hours.

Using the same nodes on the university supercomputer as in the previous sections, we consider 1200 density matrices split evenly over 48 cores. For the matrix method we find that it takes 3 hours, 18 minutes, and 37 seconds. For the asymmetric vector method it takes 30 minutes and 54 seconds. For the symmetric vector method it takes 7 minutes and 44 seconds.

3.4.5 Tabulated Speedtest Results

A full summary of our speed test results for the three different processor configurations is given in this section. In symmetric systems, the Vector Method becomes more and more efficient than the Matrix method with system size, making for an order of magnitude difference in the case of four qubits.

	2 Qubits	3 Qubits	4 Qubits
Sym Vector Time (s)	258	2324	17445
Asym Vector Time (s)	281	4561	65250
Matrix Time (s)	688	18324	323872
Number of Random Matrices	100,000	10,000	1,000

Table 1: Collected results for numerical method using a single core of desktop AMD FX8350 processor

	2 Qubits	3 Qubits	4 Qubits
Sym Vector Time (s)	45	361	2909
Asym Vector Time (s)	52	954	12624
Matrix Time (s)	130	5402	53624
Number of Random Matrices	100,000	10,000	1,000

Table 2: Collected results for numerical method using a desktop AMD FX8350 processor with all cores

	2 Qubits	3 Qubits	4 Qubits
Sym Vector Time (s)	1727	583	464
Asym Vector Time (s)	1750	1021	1854
Matrix Time (s)	2490	6216	11917
Number of Random Matrices	12,000,000	120,000	1,200

Table 3: Collected results for numerical method using two sixteen core nodes on the supercomputer

3.5 Conclusion

In all cases, our numerical method has proved capable of producing an accurate solution for the problem of quantum discord of two, three, and four qubits and can be extended to larger numbers of qubits. It is readily possible, albeit less fast, to perform these calculations on a high end home

desktop computer in a reasonable time frame. We have seen considerable speedup via the use of the vector-based method we developed, wherein iteration level mathematical simplifications are used in conjunction with the search heuristic. We have demonstrated that if we restrict the density matrices to those which are symmetric in exchange of bodies, we reduce the computation time even further, and that this advantage only grows with system size. However, even without the advantage in scaling, there is no reason to ever employ matrix based iterations in calculating the global discord, as such would be a waste of time. We have used this method in past projects, as will be seen in the following chapter, and this methodology will be especially crucial in the event of studying four qubits.

4 Examining Global Discord of Three Quantum Dots in a Driven Cavity with Dissipation

In chapter 2 we examined quantum discord for a system of two quantum dots in a driven cavity with dissipation in the steady state. One might wonder how such a system may look in the case of three quantum dots instead of two. The model used for two quantum dots is straightforward to extend to multiple dots with the restriction that all the dots have to be identical and equidistant. This means there can be up to four dots under that Hamiltonian. In this chapter we extend the model to three quantum dots and study this system in the steady state. Several new features are found including tristability in the cavity field, global discord peaks in a bistable regime, inflection points, and changes in the effects of high W and detuning adjustment compared to the case of two quantum dots.

4.1 Multibody Entanglement

Extensions of entanglement to multiple bodies is easier with even number of bodies [6], wherein the concurrence of two dots is expanded to the N concurrence and has the pure state definition below.

$$C_N = \langle \psi | \sigma_y^{\otimes N} | \psi^* \rangle \quad (4.1)$$

This extension has been shown in the aforementioned reference to have the mixed state solution seen below.

$$C_N = \max[0, \lambda_1 - \sum_{i=2}^{2^N} \lambda_i] \quad (4.2)$$

As before, λ_i are the square roots of the eigenvalues of the matrix $\rho \tilde{\rho}$, where $\tilde{\rho} \equiv (\sigma_y^{\otimes N}) \rho^* (\sigma_y^{\otimes N})$, λ_1 is larger than all other λ_i and N is the number of bodies in the system. However, this extension has one critical flaw: it only works for the case that the number of bodies

is even. For odd number of bodies, the problem becomes multilinear and requires other extensions, such as the three tangle [7]. Attempting to use the N-concurrence expression for odd numbers of dots results in zero entanglement, meaning the measurement is invalidated in $2K + 1$ body cases by the very fact that entanglement of odd numbers of bodies exists to begin with [6].

It is possible, however, to extend the idea of concurrence of two bodies in a different fashion. Consider the pure state expression shown above for the concurrence of a two body system. This expression may be rewritten as a determinant in the following way [51].

$$C_{pure} = \det \begin{pmatrix} \psi_{00} & \psi_{01} \\ \psi_{10} & \psi_{11} \end{pmatrix} \quad (4.3)$$

The determinant is a function in linear algebra and therefore only works with a two dimensional matrix. However, there is an extension of the determinant to a cube-shaped hypermatrix. This extension is known as Cayley's Second Hyperdeterminant and is defined below [82].

$$H_3(a) = d_1 - 2d_2 + 4d_3 \quad (4.4)$$

$$\begin{aligned} d_1 &= a_{000}^2 a_{111}^2 + a_{001}^2 a_{110}^2 + a_{010}^2 a_{101}^2 + a_{100}^2 a_{011}^2 \\ d_2 &= a_{000} a_{111} a_{011} a_{100} + a_{000} a_{111} a_{101} a_{010} + a_{000} a_{111} a_{110} a_{001} \\ &\quad + a_{011} a_{100} a_{101} a_{010} + a_{011} a_{100} a_{110} a_{001} + a_{101} a_{010} a_{110} a_{001} \\ d_3 &= a_{000} a_{110} a_{101} a_{011} + a_{111} a_{001} a_{010} a_{100} \end{aligned} \quad (4.5)$$

Geometrically, Cayley's Second Hyperdeterminant corresponds to a three-dimensional hypermatrix shown in Fig 4.1 [83]

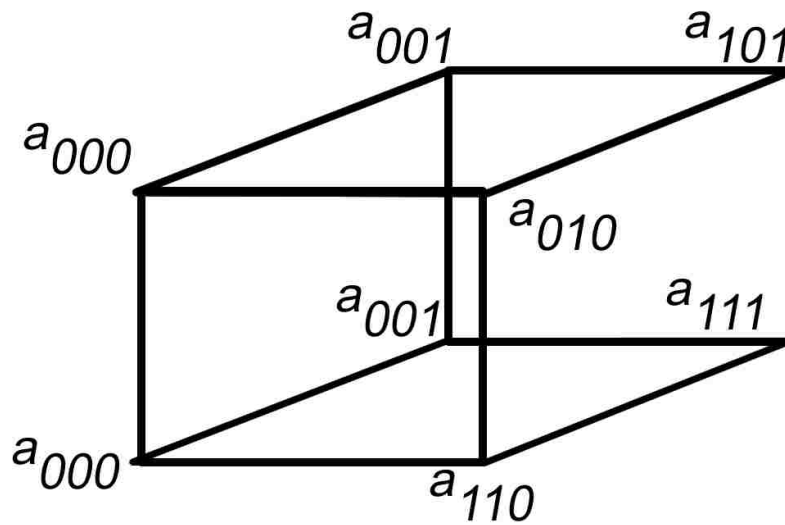


Figure 4.1: Three-dimensional hypermatrix used in the calculation of Caley's Second Hyperdeterminant, based on a previously produced figure [83]

Coffman et al extended the concurrence to three bodies by taking the hyperdeterminant of the following cube-shaped hypermatrix [7].

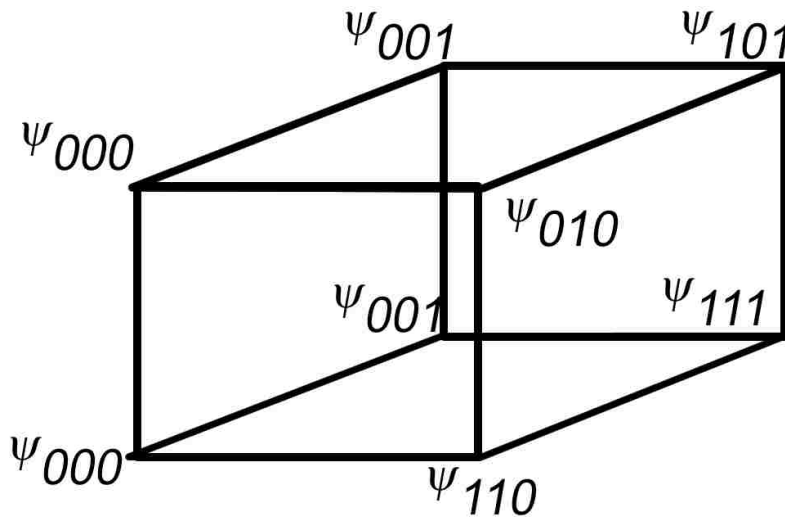


Figure 4.2: Hypermatrix used in calculation of 3-tangle based on a previously produced figure [7]

The 3-tangle, as defined by Coffman et al, then, is given as follows for a pure state.

$$\tau_3(\psi) = d_1 - 2d_2 + 4d_3 \quad (4.6)$$

$$\begin{aligned} d_1 &= \psi_{000}^2 \psi_{111}^2 + \psi_{001}^2 \psi_{110}^2 + \psi_{010}^2 \psi_{101}^2 + \psi_{100}^2 \psi_{011}^2 \\ d_2 &= \psi_{000} \psi_{111} \psi_{011} \psi_{100} + \psi_{000} \psi_{111} \psi_{101} \psi_{010} + \psi_{000} \psi_{111} \psi_{110} \psi_{001} \\ &\quad + \psi_{011} \psi_{100} \psi_{101} \psi_{010} + \psi_{011} \psi_{100} \psi_{110} \psi_{001} + \psi_{101} \psi_{010} \psi_{110} \psi_{001} \\ d_3 &= \psi_{000} \psi_{110} \psi_{101} \psi_{011} + \psi_{111} \psi_{001} \psi_{010} \psi_{100} \end{aligned} \quad (4.7)$$

where ψ_{ijk} is the component of the wavefunction corresponding to the basis state $|ijk\rangle$. It can readily be shown that for both the determinant corresponding to the concurrence and the hyperdeterminant used in 3-tangle, the measure will vanish if an arbitrary separable state is used. Additionally, Verstraete et al have shown that the concurrence and the 3-tangle are special cases of a general method for producing entanglement monotones [84].

This gives an analytical expression for the entanglement of a pure three body state. However, as was the case in the two body system, we have a mixed state for at least some parameters. As with the concurrence this measure can be extended to mixed states by means of a convex roof extension. However, unlike the concurrence there exists no known analytical solution for the three tangle of an arbitrary mixed state, due to the multilinear nature of the problem, whereas concurrence is merely an antilinear problem [85]. Some limited case analytical solutions have been devised for the 3-tangle of select mixed states [86, 87, 88]. Some progress has been made in the numerical study of the 3-tangle using a large number of interacting simulated annealing processes [89]. Additionally, there has been a proposed extension of the 3-tangle to arbitrary odd numbers of bodies [90].

The hyperdeterminant approach quickly becomes impractical with higher numbers of dots. Beyond the above difficulties with the 3-tangle, one notices that while a third rank

hyperdeterminant was discovered in the 1800s [82], there was no fourth rank hyperdeterminant known until the 2000s [91, 92]. Further, the fourth-rank hyperdeterminant expression that was found is a high degree polynomial in 16 unknowns with close to three million terms [92].

A simple way to glean some information regarding entanglement without directly calculating entanglement was exhibited in the study by Quiroga and Johnson [13], in which the overlap between the density matrix and the probabilities of orthogonal maximally entangled states was used in place of any measure of entanglement per se. The system in this case is a 4×4 density matrix and therefore can be given in terms of four orthogonal maximally entangled states that span the space. In tripartite entanglement, there are two types of entanglement which the system can have, the GHZ-type entanglement and the W-type entanglement, named for states which exhibit these types of entanglement [93].

A simpler to compute, albeit less accurate, method of estimating the entanglement is to examine the system state's overlap with a set of maximally entangled states which span the space. This method was used by Quiroga and Johnson [13], but was determined to be inferior to the concurrence measure when a modified version of their system was studied by Mitra et al [1]. For our system, there are four orthogonal maximally entangled states which span the space. The first two are GHZ, or Greeneberger-Horne-Zeilinger states and are defined as follows [94].

$$|GHZ_{\pm}\rangle \equiv \frac{|000\rangle \pm |111\rangle}{\sqrt{2}} \quad (4.8)$$

The second set are the W and \tilde{W} states, which exhibit W type entanglement [95, 93, 87]. These are shown below. The 3-tangle does not detect this type of entanglement [85].

$$|W\rangle \equiv \frac{|001\rangle + |010\rangle + |100\rangle}{\sqrt{3}} \quad (4.9)$$

$$|\tilde{W}\rangle \equiv \frac{|110\rangle + |101\rangle + |011\rangle}{\sqrt{3}} \quad (4.10)$$

We denote the probabilities of these states in our system as follows

$$P_{\pm} \equiv Tr \langle GHZ_{\pm} | \rho | GHZ_{\pm} \rangle \quad (4.11)$$

$$P_W \equiv Tr \langle W | \rho | W \rangle \quad (4.12)$$

$$P_{\tilde{W}} \equiv Tr \langle \tilde{W} | \rho | \tilde{W} \rangle \quad (4.13)$$

4.2 Model

As noted in chapter 2, the master equation used for two quantum dots earlier is readily extended to more bodies, provided that the dots in question are equidistant, a restriction that prevents this model from applying to five or more dots. In this case, we use three dots. Once again, the dots are identical and there is a driving field, dissipation, detuning, coupling between the dots and the field, and coupling amongst dots. The master equation is

$$\begin{aligned} \dot{\rho} = & -i\Delta_c[a^\dagger a, \rho] - i\Delta_d[J_z, \rho] + g[aJ_- - aJ_+, \rho] \\ & + \epsilon[a^\dagger - a, \rho] - iw[T, \rho] + \frac{\gamma}{2}[2J_- \rho J_+ - J_+ J_- \rho - \rho J_+ J_-] \\ & + \kappa[2a\rho a^\dagger - a^\dagger a \rho - \rho a^\dagger a] \end{aligned} \quad (4.14)$$

where w is the coupling amongst dots, g is the coupling between dots and internal field, γ, κ are the decay rates for the dots and the cavity, Δ_d, Δ_c are the dot detuning ($\omega_d - \omega_0$) and the cavity detuning ($\omega_c - \omega_0$), ϵ is the driving field amplitude, α is the complex cavity field amplitude, J, J_{\pm} are the quasispin dot operators, and $a^{(\dagger)}$ is the cavity field annihilation(creation) operator. The operator T in this case may be given by

$$T = I + J_{1+}J_{2-} + J_{1-}J_{2+} + J_{1+}J_{3-} + J_{1-}J_{3+} + J_{2+}J_{3-} + J_{2-}J_{3+} \quad (4.15)$$

where I is the identity operator and $J_{i\pm}$ are the quasispinor ladder operators in the i^{th} dot space.

By operating the Hamiltonian on an arbitrary superposition of symmetric states $\psi_A = a |GHZ_+\rangle + b |GHZ_-\rangle + c |W\rangle + d |\tilde{W}\rangle$, we can readily see that the result will always be of the form $\psi_B = a_1 |GHZ_+\rangle + b_1 |GHZ_-\rangle + c_1 |W\rangle + d_1 |\tilde{W}\rangle$, regardless of the coefficients used in the first state, making the such state vectors and matrices representing statistical mixtures thereof optically isolated from states which are orthogonal to the symmetric states. Similar to the procedure employed by Mitra and Vyas [1], we parameterize the dot density matrix to expedite its solution. The parameterization in this case is as follows.

$$\Lambda = \begin{pmatrix} \frac{1}{4} + x & p & q & s \\ p^* & \frac{1}{4} + y & r & u \\ q^* & r^* & \frac{1}{4} + z & v \\ s^* & u^* & v^* & \frac{1}{4} - x - y - z \end{pmatrix} \quad (4.16)$$

We derive the equations of motion and their solution in the steady state with the low noise approximation. The equations of motion found are given below (see Appendix B for derivation).

$$\begin{aligned}
\langle \dot{\alpha} \rangle &= -\varsigma + (p^* + v^*) + \frac{2}{\sqrt{3}}r^* \\
\langle \dot{x} \rangle &= \sqrt{3}g(p^*\alpha^* + p\alpha) + 3\gamma\left(y + \frac{1}{4}\right) \\
\langle \dot{y} \rangle &= g\left(2r^*\alpha^* - \sqrt{3}p\alpha - \sqrt{3}p^*\alpha^* + 2r\alpha\right) + \gamma\left(4z - 3y + \frac{1}{4}\right) \\
\langle \dot{z} \rangle &= g\left(\sqrt{3}(v^*\alpha^* + v\alpha) - 2(r\alpha + r^*\alpha^*)\right) + \gamma\left(3\left(\frac{1}{4} - x - y - z\right) - 4\left(\frac{1}{4} + z\right)\right) \\
\langle \dot{p} \rangle &= g\left(\sqrt{3}\alpha^*(y - x) + 2q\alpha\right) + \gamma 2\sqrt{3}r + \xi_1 p \\
\langle \dot{q} \rangle &= g\left(\sqrt{3}\alpha^*r - 2\alpha^*p + \sqrt{3}\alpha s\right) + 3\gamma u + \xi_2 q \\
\langle \dot{r} \rangle &= g\left(2\alpha^*(z - y) - \sqrt{3}q\alpha + \sqrt{3}u\alpha\right) + 2\sqrt{3}\gamma v + \xi_3 r \\
\langle \dot{s} \rangle &= \sqrt{3}g(\alpha^*u - \alpha^*q) + \xi_4 s \\
\langle \dot{u} \rangle &= g\left(2\alpha^*v - \sqrt{3}\alpha s - \sqrt{3}\alpha^*r\right) + \xi_5 u \\
\langle \dot{v} \rangle &= g\left(\sqrt{3}\alpha^*(-x - y - 2z) - 2u\alpha\right) + \xi_6 v
\end{aligned} \tag{4.17}$$

where we have defined the function ς and the constants ξ_i , $1 \leq i \leq 6$ as follows.

$$\begin{aligned}
\varsigma &\equiv \frac{(\kappa + i\Delta_c)\alpha - \varepsilon}{\sqrt{3}} \\
\xi_1 &\equiv -\frac{3}{2}\gamma + 2iw + i\Delta_d, \quad \xi_2 \equiv -2\gamma + 2iw + 2i\Delta_d \\
\xi_3 &\equiv -\frac{7}{2}\gamma + i\Delta_d, \quad \xi_4 \equiv \frac{-3\gamma}{2} + 3i\Delta_d \\
\xi_5 &\equiv 2i\Delta_d - 3\gamma - 2iw, \quad \xi_6 \equiv i\Delta_d - \frac{7\gamma}{2} - 2iw
\end{aligned}$$

If the system were solved entirely numerically, the parameter space would be seventeen-dimensional (seven complex parameters and three real ones). This would be needlessly cumbersome as, just like in the case of two quantum dots, it is possible to solve these equations in the steady state with the low noise approximation that $\langle AB \rangle \approx \langle A \rangle \langle B \rangle$. However, unlike the earlier case where the solutions are readily written and analytically informative, these solutions involve significant abstraction and are primarily useful for speeding up the computation time. The

steady state solutions are derived in Appendix C.

Once again, because these solutions are derived with the approximation that $\langle AB \rangle \approx \langle A \rangle \langle B \rangle$ we avoid having to produce equations of motion for $\langle AB \rangle$ and then equations of motion for higher and higher order averaged products arising in the new equations of motion ad infinitum, in much a similar way to the case of two quantum dots under the same approximation as studied by Mitra and Vyas [1, 72]. It is possible to truncate the hierarchy of equations of motion later to produce more accurate results, but these would involve ever more convoluted solutions even than the above. The derivation of the above solutions and of the equations of motion can be found in one of the appendices, and the other appendix derives the equations of motion in the four quantum dot case, but not the solutions.

The above solutions, however convoluted, reduce the dot parameters to functions of α alone, creating a two parameter numerical problem as it is not possible to find an analytical solution for α from the above equations. This is a much simpler numerical problem. If the system were studied in the time dependent regime, there would be no such reduction in complexity as the time derivatives would be nonzero. The solutions above have been checked against a program devised to create the time dependent density matrix via fourth order Runge-Kutta, allowing the time to become large enough to produce an approximate steady state. The solutions above match said time dependent solution in the long-time limit. However, it is faster to produce the solutions this way. The author recommends that any work regarding the time dependent solution in this system be done with a higher order Runge-Kutta method than described above for the sake of expediency.

In searching for proper values of α , two obstacles present themselves. The first and simpler one is that there can be more than one mathematical solution, a difficulty readily solved. A larger challenge is presented by the large number of dips found while exploring the parameter space. We parameterize the problem numerically by finding the magnitude and phase of α separately, thereby narrowing the range of one of the two parameters to a finite space, namely 0 to 2π .

4.3 Results

In this section we will outline our findings for the global discord and maximally entangled state probabilities for the previously stated three quantum dot system. We compare our results to the similar two quantum dot system and see new interesting phenomena which were not exhibited in the two dot case. As before, we explore the system in both low interdot and high interdot coupling ranges.

4.3.1 Low Interdot Coupling Range

Once again we see that the system can show bistability in the cavity field amplitude as a function of the driving field strength (see Figure 4.3). Additionally, much like the case with two quantum dots, the system will approach a statistical mixture of separable states if the field is high enough. We are not able to analytically prove this; however, we have tested a variety of system configurations for high driving field and find the steady state solution appears to always approach the following density matrix

$$\Lambda_{high\ field} = \frac{1}{4} \begin{pmatrix} 1 & 0 & 0 & 0 \\ 0 & 1 & 0 & 0 \\ 0 & 0 & 1 & 0 \\ 0 & 0 & 0 & 1 \end{pmatrix} \quad (4.18)$$

where we have used the compact 4×4 matrix form of the symmetric system state. This state is clearly unentangled. Yet, as before, we find that the system exhibits a high value asymptotic limit for global discord. In this case the asymptotic limit is approximately 0.79, which is a larger proportion of the total possible global discord $\log_2 3$ than the asymptotic limit for two quantum dots, namely $\frac{1}{3}$ was when compared to the maximal quantum discord value of 1 (See figures 4.3, 4.4, and 4.6). Additionally, we find that in some bistable regions, there exists a peak in the upper branch of the global discord curve (Figure 4.3). This feature is absent for two quantum dots.

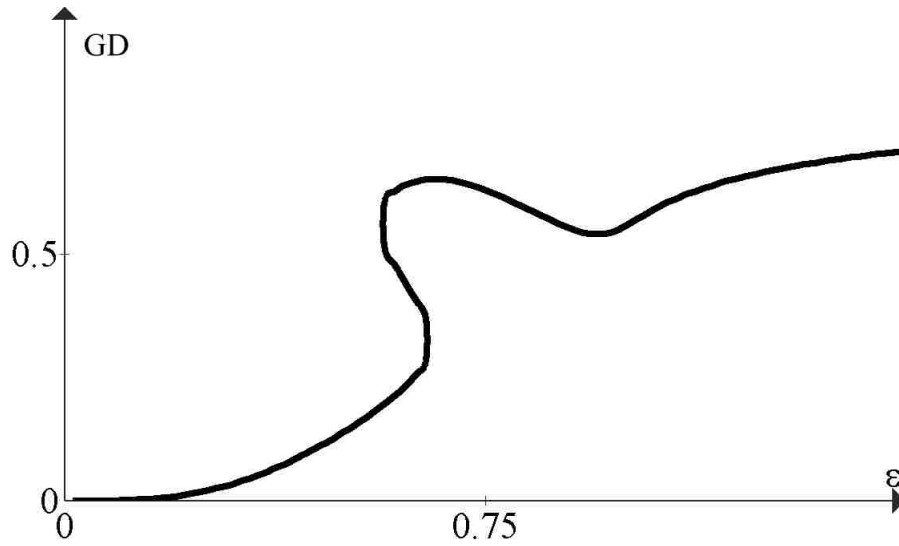


Figure 4.3: Example of the asymptotic limit of global discord, herein abbreviated GD, as well as the peak exhibited in the upper branch of certain bistable systems and the dip that follows prior to the curve asymptotically approaching $GD \approx 0.79$. Parameters used are $g = 1$, $\gamma = 0.3$, $\Delta_d = -1.25$, $\Delta_c = 0$, $w = 1.5$, $\kappa = 0.2$

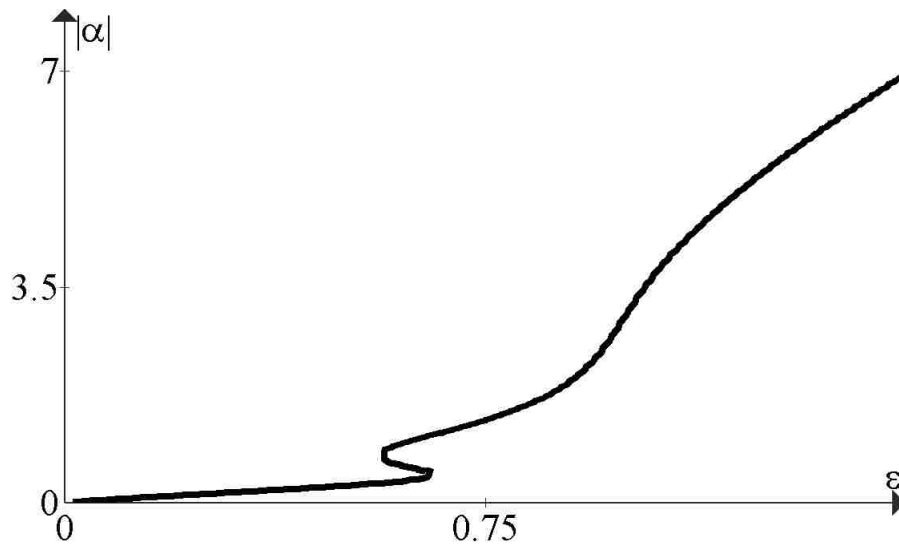


Figure 4.4: The magnitude of the complex cavity field amplitude for the system shown in the previous figure. Note the inflection point corresponding in placement to the dip found in the global discord curve of said system.

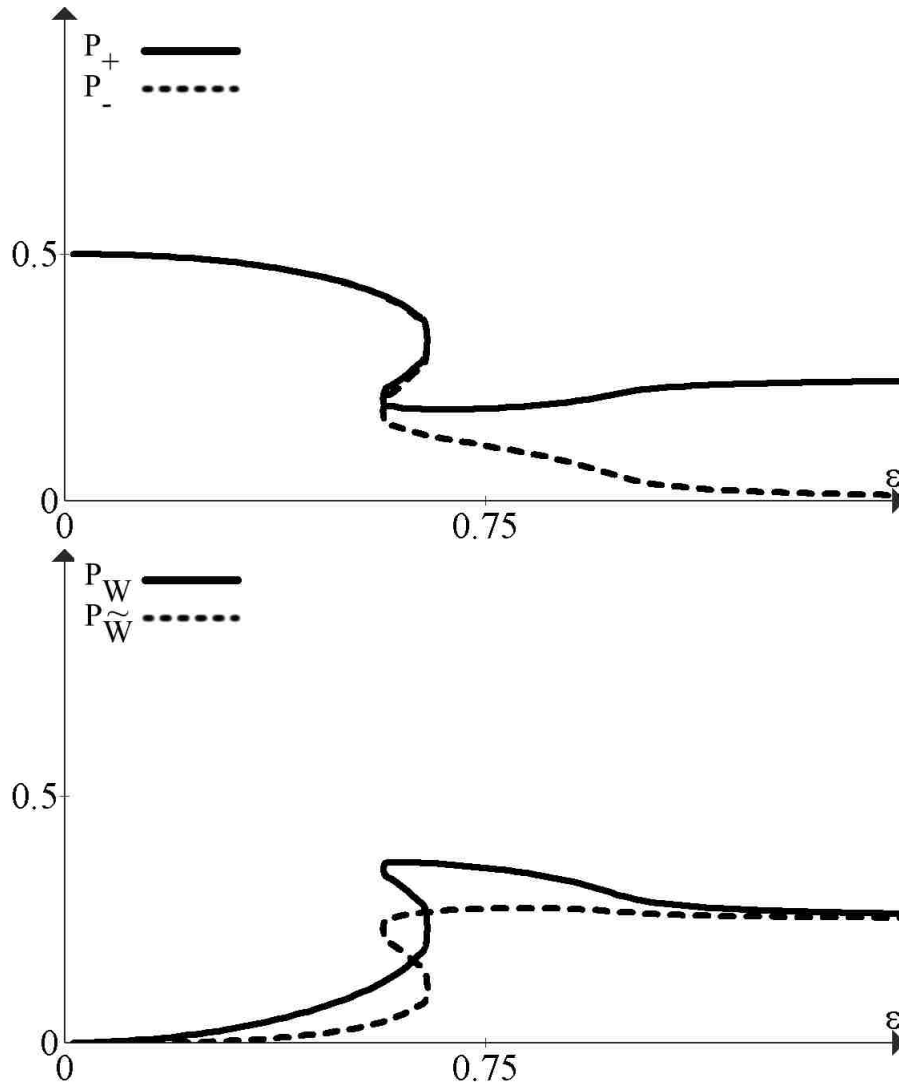


Figure 4.5: The GHZ state probabilities for the same system as in the previous two figures, as well as the probabilities of the W and \tilde{W} states. Note the growing separation in the GHZ state probabilities in the region corresponding to the upper branch of the bistability curve.

In addition to the bistability seen above we are able to find some sets of system parameters in which the cavity field amplitude actually displays tristability (Figure 4.6). In these cases there is a region of the graph in which there are five mathematically valid solutions. However, the system may only physically be found in three of them as the others are unstable. This interesting phenomenon appears to be found in parameter regimes in which the decay rates are low compared to other parameters. In other words, the cooperativity parameter [66]

$$C = \frac{g^2}{\gamma\kappa} \quad (4.19)$$

which has been connected to the phenomenon of multistability, is high in these cases [66, 96].

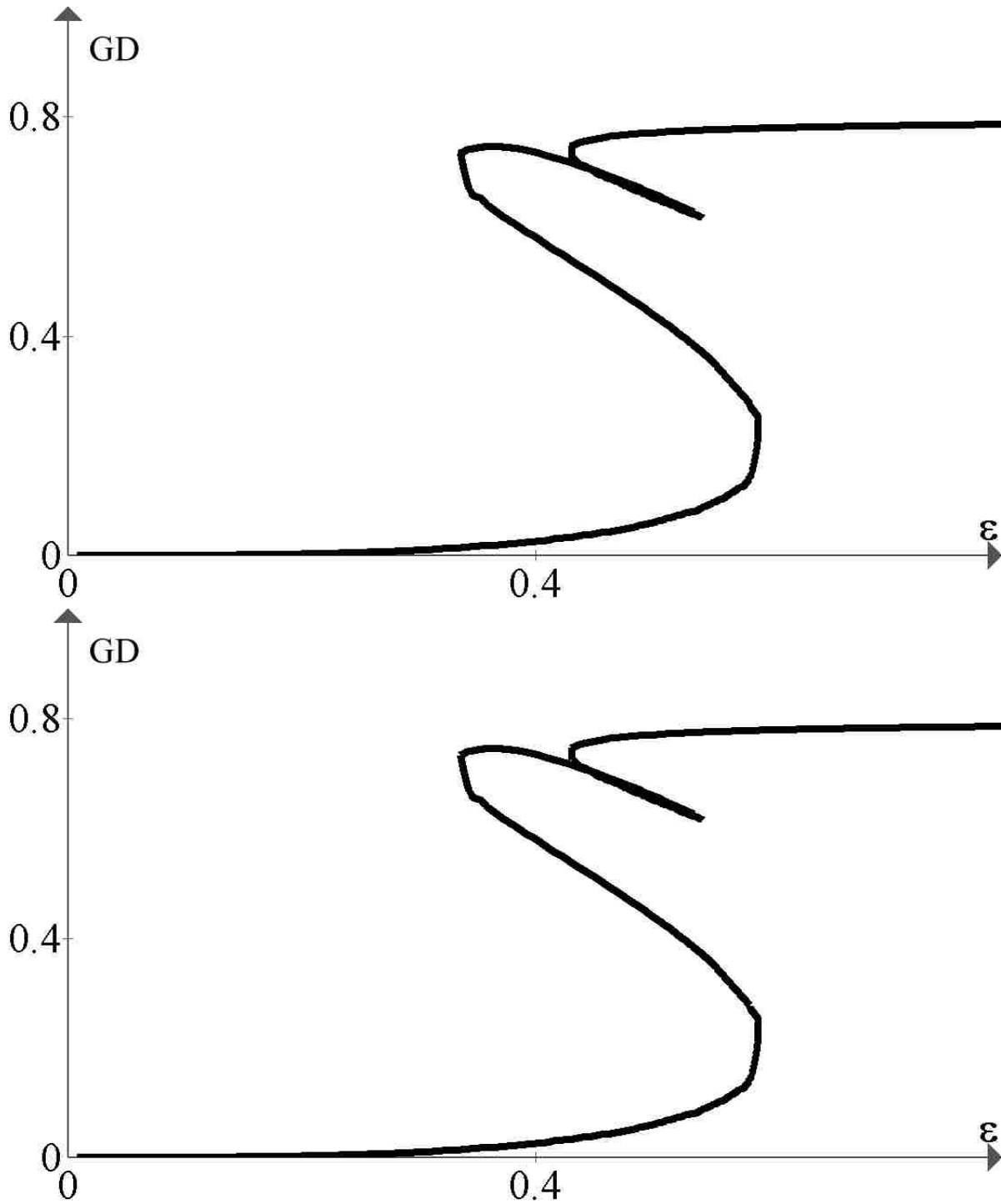


Figure 4.6: An example of tristability, GD and cavity field curves shown. $g = 1$, $\gamma = 0.3$, $\Delta_d = -0.6$, $\Delta_c = 0$, $w = 1.5$, $\kappa = 0.05$

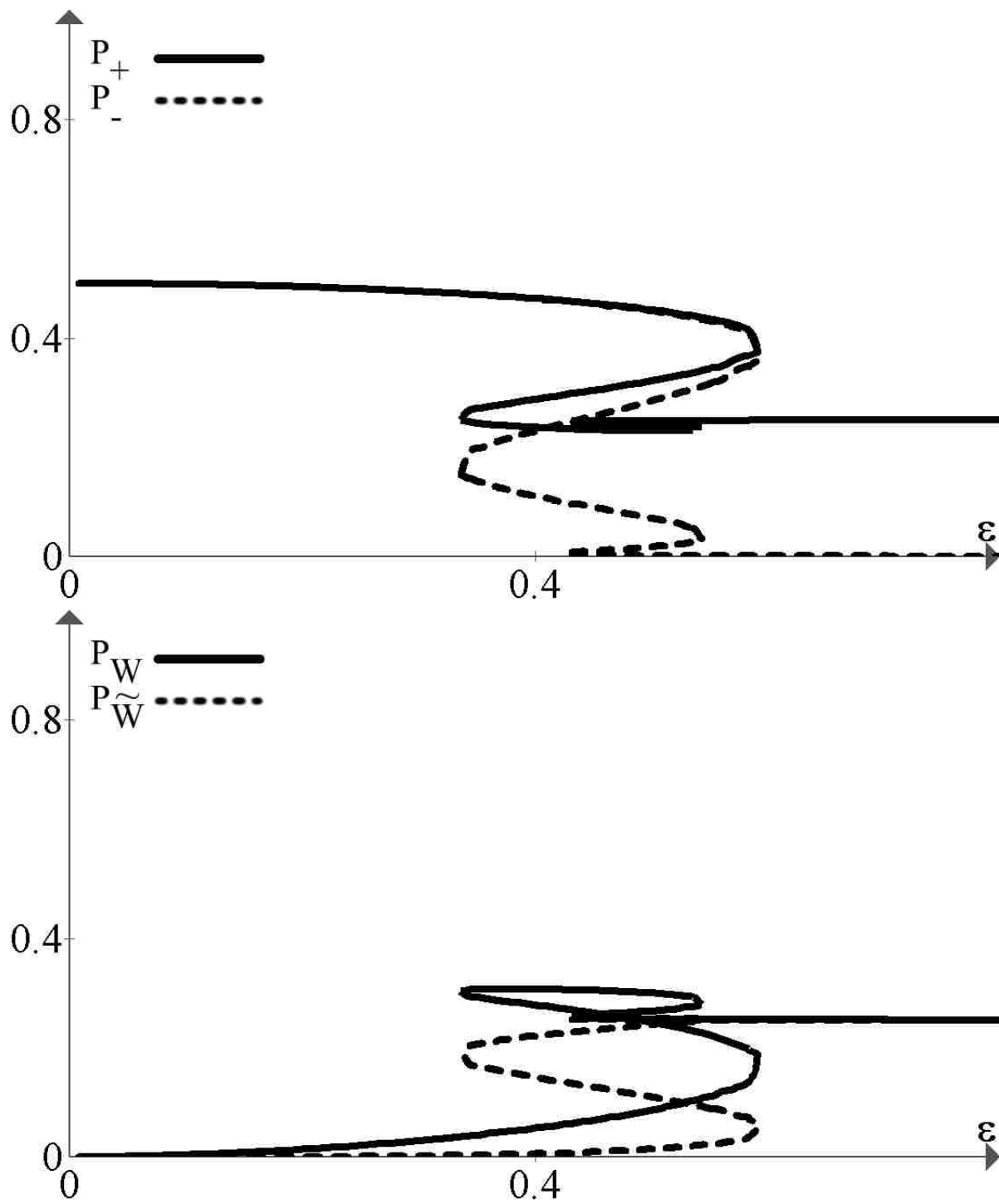


Figure 4.7: Maximally entangled state probabilities for the system described in the previous figure.

4.3.2 High Interdot Coupling and the Effects of Detuning

We had seen in chapter 2 that when the coupling between the two dots was high enough, a peak in global discord formed, one which was not as high as the asymptotic limit in the absence of detuning. It was also found that by adjusting the dot detuning in the negative direction, the peak would grow markedly higher and eventually hit an optimum near $\delta_d \approx -2W$, wherein the discord peak was higher than the asymptotic limit of $\frac{1}{3}$. It is of interest to study the same limit in the three quantum dot system and see how the behaviors compare.

As we saw in the case of the two quantum dot system, the cavity field as a function of the driving field becomes almost linear in this region.

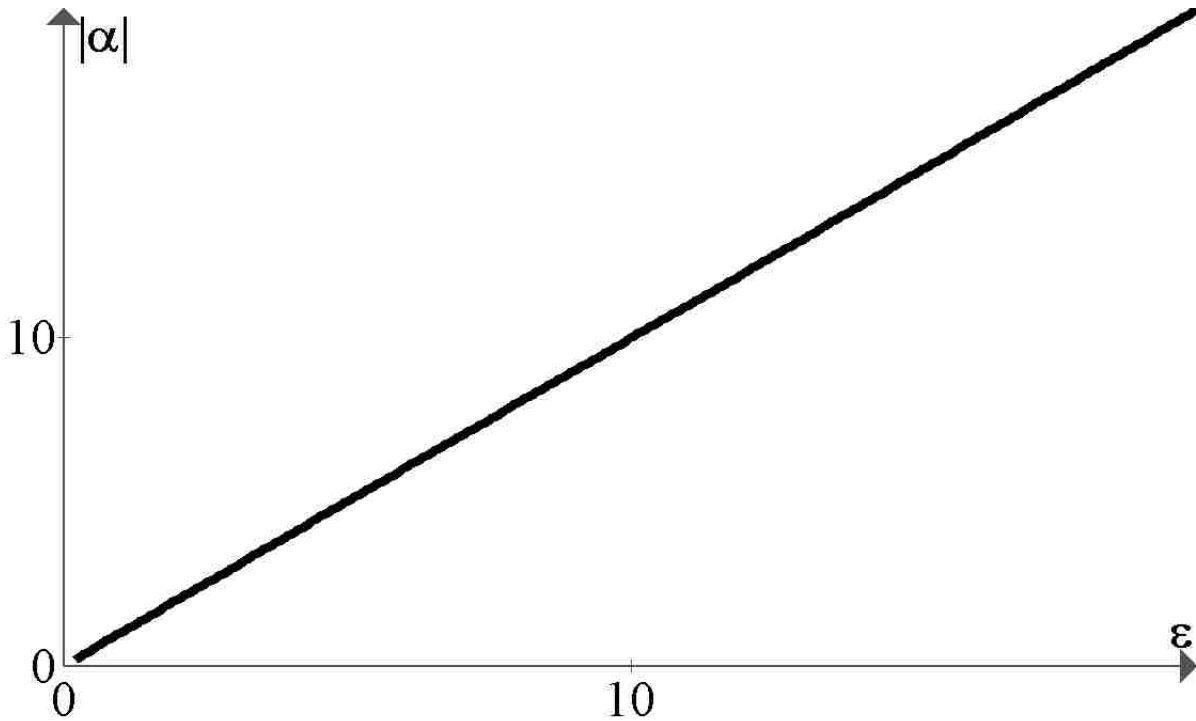


Figure 4.8: Example of the linearity of the cavity field curve in the realm of high w . Here, $g = 1$, $\gamma = 1$, $\Delta_d = 0$, $\Delta_c = 0$, $w = 50$, $\kappa = 1$

We also find that in this region, the global discord reaches above the asymptotic limit, which was not the case for a similar regime in the case of two quantum dots.

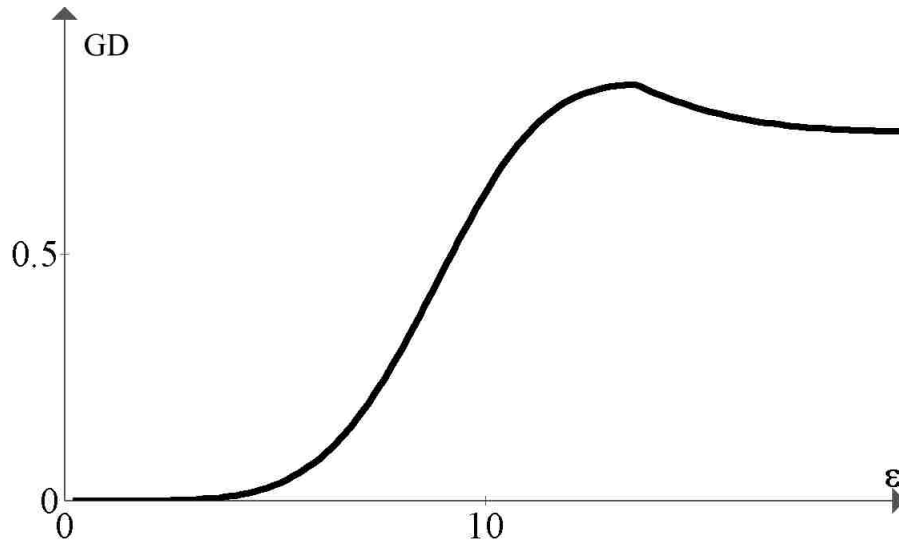


Figure 4.9: Global discord for high w with no detuning. $g = 1$, $\gamma = 1$, $\Delta_d = 0$, $\Delta_c = 0$, $w = 50$, $\kappa = 1$

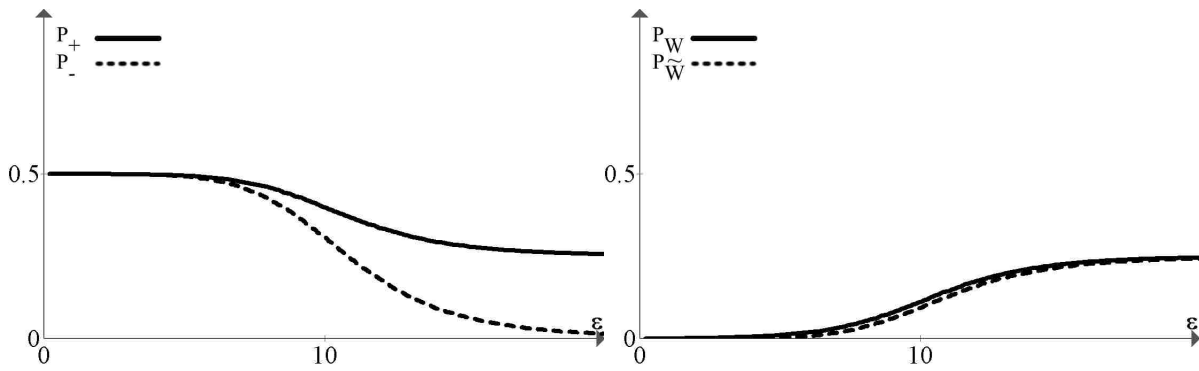


Figure 4.10: Entangled state probabilities for the system in the previous figure.

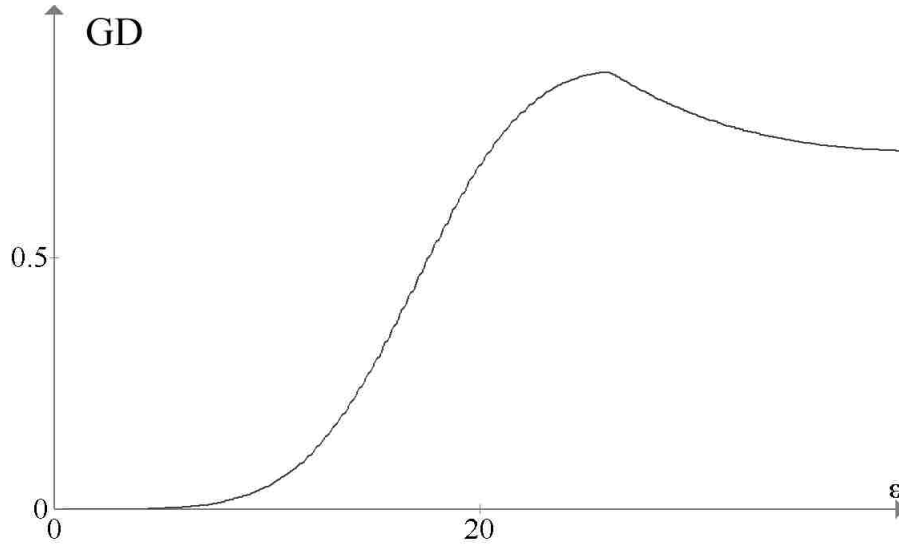


Figure 4.11: Global discord with quite slight enhancement via detuning adjustment. $g = 1$, $\gamma = 1$, $\Delta_d = -3.75$, $\Delta_c = 0$, $w = 50$, $\kappa = 1$

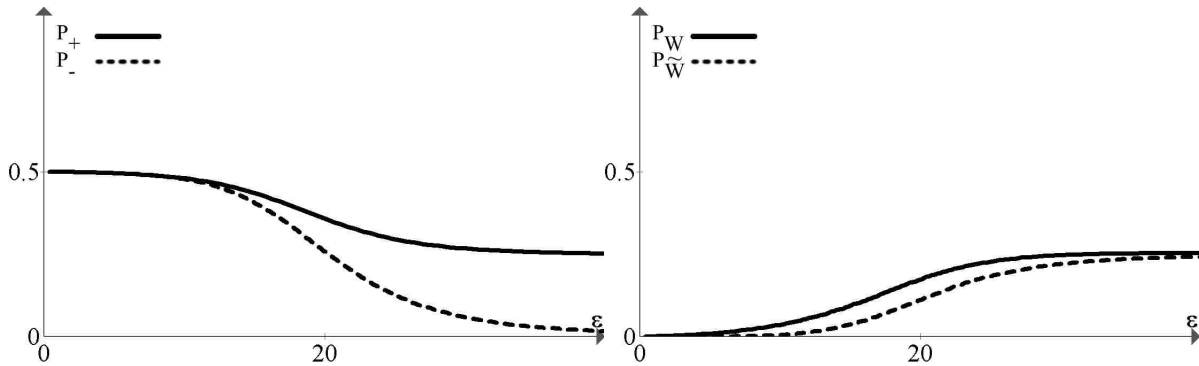


Figure 4.12: Entangled state probabilities for the system shown in the previous figure.

4.4 Conclusion

Much as with the two quantum dot system that was studied in chapter 2, our system has high global discord in a high driving field range, which can be seen to have no entanglement, though we were only able to numerically obtain the density matrix in this regime, unlike in the two quantum dot case where it was found analytically [1]. The asymptotic high field limit for global discord of three quantum dots in the steady state is approximately 0.79. In a low interdot coupling range this is the highest that the global discord found in all such systems tested. We find peaks in

global discord in the bistable regime of the three dot system (Figure 4.3), a phenomenon that was never seen in the two quantum dot system. We find tristability (Figure 4.6) in the cavity field amplitude as a function of driving field in the case that the three dot system has low decay rates and therefore high cooperativity parameter [66, 96]. For a high interdot coupling range with no detuning, the two quantum dot system had exhibited a peak in quantum discord that was not as high as the asymptotic limit of $\frac{1}{3}$, whereas for three quantum dots in similar conditions we see a peak which exceeds the value of the asymptotic limit of 0.79 without the aid of detuning. The effect of adjusting detuning on this peak is much less marked for the three quantum dot system than for the two dot system, and the optimum happens for a smaller value of $|\frac{\Delta_d}{w}|$ than in the two dot system.

5 Conclusion

We have studied the quantum discord of two identical coupled quantum dots in a driven cavity with detuning and losses in the steady state regime and compared it to the entanglement of the system as previously explored by Mitra and Vyas [1]. We have also developed a numerical method to calculate global discord and tested it for small numbers of bodies. Finally, we have extended the system of identical quantum dots in a driven cavity to a similar system of three quantum dots and studied that system using the numerical method we developed.

In examining the system of two identical coupled quantum dots in a driven cavity in the steady state, we found that the quantum discord is high in the limit of high driving field, asymptotically approaching a value of $1/3$, a value which we verified analytically using the density matrix in that limit and a known analytical method for determining the quantum discord of Bell Diagonal states. This result holds true regardless of whether the system is in a bistable regime or not, and in the bistable regime it is the highest value of quantum discord we were able to find. For the nonbistable regime, we find that a peak in quantum discord begins to form for sufficiently high interdot coupling constant W . This peak is still not above the asymptotic limit; however, by adjusting the dot detuning in the negative direction until an optimum is found, we can exceed the asymptotic limit, giving a value of 0.40 for discord, 0.49 for concurrence, and 0.34 for entanglement of formation. The value for concurrence was higher than that previously thought to be the highest for this system.

In the process of preparing to examine the system of three identical quantum dots in a driven cavity with losses in the steady state, we created a numerical method to calculate global discord, one which proved to be efficient enough to be worth examining further in its own right, as this quantity is considered numerically intensive and our method ran rapidly on a desktop computer. The method was tested for two, three, and four quantum dots. Two different versions of the numerical method were developed, one which, known in this work as the matrix method, primarily relies on the search heuristic for speed and only involves some elementary iteration

level optimizations, still treating the measurements as matrix optimizations, while the other, known herein as the vector method, takes advantage of the lack of any need to take partial traces and therefore treats the measurement of the system as a simple vector problem. The latter method is much faster and presents a particularly compelling advantage in speed in the case that the system consists of identical bodies, in which case the vector method scales 2^{2N} times faster than the matrix method. In all cases, the search used was a succession of coarse hypercube meshes that got smaller as the search recentered on each successive best point. These meshes had five points to a side, for 5^{2N} total points explored per iteration. The search pattern was verified against known analytical cases and validated through comparison to less efficient searches.

The method of finding global discord was applied to a system of three quantum dots which, as was the case when we studied two quantum dots, were identical, equidistant, coupled, and inside of a driven cavity in the steady state, with dissipation and detuning accounted for but not noise terms.

5.1 Future Work

While the time dependent quantum discord of a system of two coupled quantum dots in a driven cavity with dissipation was studied by Freed et al [29], a similar study has not yet been produced for three quantum dots in similar conditions. With the numerical method for global discord of three quantum dots already in place, such a project is mostly already built, requiring only the use of a Runge-Kutta method in seventeen parameters to produce the time dependent density matrices. While we used such a Runge-Kutta in verifying our steady state solution for the dot parameters in terms of α it was not efficient and it is likely that a higher order Runge-Kutta algorithm would be needed to explore the system properly.

In both the two quantum dot system explored in chapter 2 and the three quantum dot system explored in chapter 4, the system was studied in a noiseless approximation, so that $\langle AB \rangle \approx \langle A \rangle \langle B \rangle$. Mitra studied the entanglement of the two quantum dot system with noise accounted for using a correlation matrix, finding reductions in the steady state concurrence of the

system when noise was introduced [72]. A similar procedure could be done for three quantum dots, but there is a different way to account for noise in the two quantum dot regime as well, simply by a more conservative truncation of the infinite sets of equations needed to fully solve the equations of motion without using the noiseless approximation. This is done by finding equations of motion for the averages of products introduced, then finding equations for the higher terms produced with the preceding step, and so on [1, 72, 16]. This could be done for two or more quantum dots.

With the numerical method having been developed and tested up to four quantum dots, one obvious next step is to consider systems of four quantum dots, particularly identical coupled quantum dots forming a regular tetrahedron interacting with a field of light. As the Hamiltonian used in our past works on the discord and global discord of two and three dots requires that the dots be equidistant and equidistance is only geometrically possible for four bodies in a three dimensional space (or more generally, $N+1$ bodies in an N -dimensional space), this is the most that the system complexity may be increased solely by changing the number of bodies involved. The equations of motion of this system have already been derived via the same procedure as in Chapter 4 and are included in Appendix A. As stated in Appendix A, this produces a problem with twenty-six real parameters and therefore it is that much more critical to solve the equations of motion in terms of α alone in the steady state, and the solutions will be even more abstracted and inscrutable than in the case of three quantum dots, once again only useful in decreasing the computation times involved in creating the density matrix in the steady state. Also of interest, as a preliminary project, would be the study of the system of four identical coupled quantum dots interacting with a quantized field of light in a lossless cavity. Counter-intuitively, the entanglement will actually be easier to calculate in this system due to the N -concurrence of even numbers of bodies having a simple analytical solution for mixed states, as seen in chapter 4.

References

- [1] A. Mitra and R. Vyas Phys. Rev. A 81, 012329 (2010) A. Einstein, B. Podolsky, and N. Rosen, Phys. Rev. 47, 777 (1935)
- [2] A. Einstein, B. Podolsky, and N. Rosen, Phys. Rev. 47, 777 (1935)
- [3] J.S. Bell, Physics 1, 195 (1964)
- [4] J.F. Clauser, M.A. Horne, A. Shimony, and R.A. Holt, Phys. Rev. Lett. 24, 549 (1970)
- [5] W.K. Wootters, Phys. Rev. Lett. 80, 2245 (1998)
- [6] A Uhlmann, Phys. Rev. A Third Series 62 032307 (2000)
- [7] V. Coffman, J. Kundu, and W.K. Wootters, Phys. Rev. A 61, 052306 (2000)
- [8] M.A. Nielsen and I.L.Chuang, “Quantum Computation and Quantum Information” (Cambridge University Press, Cambridge, England, 2000)
- [9] R. Feynman, International Journal of Theoretical Physics 21, 467 (1982)
- [10] P. Shor, SIAM J. Comput., 26(5), 1484–1509 (1997)
- [11] A.K. Ekert, Phys. Rev. Lett. 67, 661 (1991)
- [12] Z. Merali, Nature 474, 24 (2011).
- [13] L. Quiroga and N.F. Johnson, Phys. Rev. Lett. 83, 2270 (1999)
- [14] J.H. Reina, L. Quiroga, and N.F. Johnson, Phys. Rev. A. 62, 012305 (2000)
- [15] A. Mitra, R. Vyas, and D. Erenso Phys. Rev. A 76, 052317 (2007)
- [16] H. Shiao, A. Mitra, and R. Vyas, J. of Mod. Opt., 60, 1273 (2013)
- [17] W. Rawlinson, A. Mitra, R. Vyas, OSA Technical Digest (Optical Society of America, 2011), paper JTua39
- [18] C. Gerry and P. Knight, Introductory Quantum Optics (Cambridge University Press, Cambridge, England, 2005).
- [19] L.M.K. Vandersypen, M. Steffen, G. Breyta, C.S. Yan- noni, M.H. Sherwood, and I.L. Chuang, Nature 414, 883-887 (2001)
- [20] H. Oliver and W.H. Zurek, Phys. Rev. Lett. 88, 017901 (2001).
- [21] E. Knill and R. Laflamme, Phys. Rev. Lett. 81, 5672 (1998)
- [22] A. Datta, A. Shaji, and C.M. Caves, Phys. Rev. Lett. 100, 050502 (2008)
- [23] A. Datta, and A. Shaji, Int. J. of Quant. Inf. 9, 1787 (2011)

- [24] B. Dakić, V. Vedral, C. Brukner, Phys. Rev. Lett. 105, 190502 (2010)
- [25] C.C. Rulli and M.S. Sarandy, Phys. Rev. A 84, 210904 (2011)
- [26] J. Xu, Phys. Lett. A, Vol. 377, 3–4, 3 (2013), pp. 238–242
- [27] H.C. Braga, C.C. Rulli, T.R. de Oliveira, M.S. Sarandy, Phys. Rev. A 86, 062106 (2012)
- [28] W. Rawlinson and R. Vyas, J. Mod. Opt. 62, 1061-1067 (2015)
- [29] S. Freed, W. Rawlinson, and R. Vyas, “Evolution of Discord in a System of Two Coupled Quantum Dots,” Laser Science XXXI, Symposium on Undergraduate Research, San Jose, CA, October, 2015
- [30] W. Rawlinson and R. Vyas, “Global Discord of Three Quantum Dots in a Driven Cavity with Dissipation in the Steady State,” in Frontiers in Optics 2015, OSA Technical Digest (online) (OSA, 2015), paper LTh4D. 5
- [31] F.M. Paula, Thiago. R. de Oliveira, M. S. Sarandy, Phys. Rev. A 87, 064101 (2013)
- [32] A.S.M. Hassan, P.S. Joag, J. Phys. A: Math. Theor. 45 (2012) 345301
- [33] J. Jin, F. Zhang, C. Yu, H. Song, J. Phys. A: Math. Theor. 45, 115308 (2012)
- [34] M. Piani, Phys. Rev. A 86, 034101 (2012)
- [35] Y. Yao, H. Li, Z. Yin, Z. Han, Phys. Lett. A 376, 358 (2012)
- [36] M. Hu, D. Tian, Ann. Phys. 343, 132 (2014)
- [37] M. Hu, H. Lian, Ann. Phys. 362, 795 (2015)
- [38] W. Roga, D. Spehner, F. Illuminati, J. Phys. A: Math. Theor. 49, 235301 (2016)
- [39] T.M. Cover, J.A. Thomas, Elements of Information Theory (Wiley, New York, 1991)
- [40] F.M. Reza, “An Introduction to Information Theory”, (McGraw-Hill, New York, 1961)
- [41] A. Datta, “Studies on the Role of Entanglement in Mixed-state Quantum Computation”, Indian Institute of Technology, Kanpur, 2003
- [42] S. Luo, Phys. Rev. A 77, 042303 (2008)
- [43] M. Ali, A.R.P. Rau, and G. Alber, Phys. Rev. A 81, 042105 (2010)
- [44] D. Girolami and G. Adesso, 2012, Phys. Rev. Lett. 108, 150403 (2012)
- [45] D. Girolami and G. Adesso, Phys. Rev. A 83, 052108 (2011)
- [46] A. Kay Phys. Rev. Lett. 109, 080503 (2012)
- [47] Q. Quan, H. Zhu, S. Liu, S. Fei, H. Fan, W. Yang, Nature, Scientific Reports 6, 22025 (2016)

- [48] M.D. Lang and C.M. Caves Phys. Rev. Lett. 105, 150501 (2010)
- [49] D. Girolami, A.M. Souza, V. Giovannetti, T. Tufarelli, J.G. Filgueiras, R.S. Sarthour, D.O. Soares-Pinto, I.S. Oliveira, G. Adesso, Phys. Rev. Lett. 112, 210401 (2014)
- [50] Y. Wang, T. Ma, H. Fan, S. Fei, Z. Wang, Quant. Inf. Proc. 13, 283 (2014)
- [51] R. Horodecki, P. Horodecki, M. Horodecki, K. Horodecki, Rev. Mod. Phys. 81, 865 (2009)
- [52] K. Modi, A. Brodutch, H. Cable, T. Paterek, V. Vedral, Rev. Mod. Phys. 84, 1655-1707 (2012)
- [53] A. Al-Qasimi and D.F.V. James, Phys. Rev. A 83, 032101 (2011)
- [54] S. Campbell, Quant. Inf. Process, 12, pp 2623-2636 (2013).
- [55] H.M. Gibbs, Optical bistability: controlling light with light (Academic Press, New York, 1985)
- [56] A.R. Cowan and J.F. Young Phys. Rev. E 68, 046606 (2003)
- [57] R. Sawant, S.A. Rangwala, Phys. Rev. A 93, 023806 (2016)
- [58] D.A.B. Miller, S.D. Smith, and C.T. Seaton, IEEE Journ. of Quant. Elect., QE-17, 3 (1981)
- [59] A.T. Rosenberger, L.A. Orozco, and H.J. Kimble, Phys. Rev. A 28, 2569 (1983)
- [60] H.M. Gibbs, Optical Bistability, (Academic Press, Orlando, FL, 1985).
- [61] J. Gripp, S.L. Mielke, and L.A. Orozco, Phys. Rev. A 56, 3262 (1997).
- [62] A. Joshi, W. Yang, and M. Xiao, Optics Letters 30, 8 (2005)
- [63] N.R. de Melo, C.G. Wade, N. Sibalic, J.M. Kondo, C.S. Adams, K.J. Weatherill, Phys. Rev. A 93, 063863 (2016)
- [64] A. Joshi and M. Xiao, Phys. Rev. Lett. 91, 14 (2003)
- [65] S. Cecchi, G. Giusfredi, E. Petriella, and P. Salieri Phys. Rev. Lett. 49, 1928 (1982)
- [66] R. Bonifacio and L.A. Lugiato, Phys. Rev. A 11 1507 (1975)
- [67] C. Wang and R. Vyas, Phys. Rev. A 51, 2516 (1995)
- [68] C. Wang and R. Vyas, Phys. Rev. A 54, 4453 (1996)
- [69] C. Wang and R. Vyas, Phys. Rev. A 55, 823 (1997)
- [70] H.J. Carmichael, Statistical Methods in Quantum Optics 1: Master Equations and Fokker-Planck Equations (Springer, New York, 1999); Statistical Methods in Quantum Optics 2: Non- classical Fields (Springer, New York, 2007)

- [71] P.D. Drummond and C.W. Gardiner, *J. Phys. A: Math. Gen.* 13, 2353 (1980)
- [72] A. Mitra, “Entanglement in Coupled Quantum Dots Inside a Cavity and the Effect of Dissipation”, University of Arkansas, Fayetteville, AR, 1999
- [73] J. Huang, L. Wang, and S. Zhu, *New J. Phys.* 13, 063045 (2011)
- [74] Z. Sun, Y. Liao, B. Guo, H. Huang, D. Zhang, J. Xu, B. Zhan, Y. Wu, H. Cheng, G. Wen, C. Fang, C. Duan, B. Wang, arXiv:1412.5285
- [75] L.M. Blumenthal. "Theory and Applications of Distance Geometry," Clarendon Press, Oxford, 1953
- [76] C. Tsallis, *Journ. of Stat. Phys.*, 52, 1, pp. 479–487 (1998)
- [77] D.P. Chi, J.S. Kim, K. Lee, *Phys. Rev. A* 87, 062339 (2013)
- [78] W. Cheney, D. Kincaid (2009). “Linear Algebra: Theory and Applications”, Sudbury, Ma: Jones and Bartlett. pp. 544, 558.
- [79] M. Glusker, D.M. Hogan, P. Vass, *IEEE Annals of the History of Computing*, 27, 3, pp. 4–22 (2005)
- [80] C.M. Caves, G.J. Milburn, *Opt. Commun.* 179, 1–6, pp. 439–446 (2000)
- [81] F. Altintas and R. Eryigit, *J. Phys. B: At. Mol. Opt. Phys.* 44, 125501 (2011)
- [82] A. Cayley, *Cambridge Mathematical Journal* 4 (1845) 193–209
- [83] Murray R. Bremner, Mikelis G. Bickis, Mohsen Soltanifar, “Cayley’s hyperdeterminant: A combinatorial approach via representation theory”, in *Linear Algebra and its Applications* 437, 1, 2012
- [84] F. Verstraete, J. Dehaene, B. De Moor, *Phys. Rev. A* 68, 012103 (2003)
- [85] A. Osterloh, J. Siewert, *Phys. Rev. A* 72, 012337 (2005)
- [86] C. Eltschka, A. Osterloh, J. Siewert, A. Uhlmann, *New J. Phys.* 10, 043014 (2008)
- [87] E. Jung, M. Hwang, D. Park, J. Son, *Phys. Rev. A* 79 (2009) 024306
- [88] S. He, X. Wang, S. Fei, H. Sun, Q. Wen, *Commun. Theor. Phys.* 55 (2011) 251-256
- [89] K. Cao, Z. Zhou, G. Guo, and L. He *Phys. Rev. A* 81, 034302 (2010)
- [90] D. Li, *Quantum Inf Process* 11, 481-492 (2012)
- [91] S.P. Tsarev and T. Wolf, *Journ. Phys. A: Mathematical and Theoretical*, 42, 45 (2009)
- [92] P. Huggins, B. Sturmfels, J. Yu, D. Yuster *Mathematics of Computation* 77, 263, pp. 1653–1679 (2008)

- [93] M. Walter, B. Doran, D. Gross, M. Christandl, *Science*, vol. 340, no. 6137, pp. 1205-1208 (2013)
- [94] D. M. Greenberger, M. A. Horne, and A. Zeilinger, "Going Beyond Bell's Theorem," in *Bell's Theorem, Quantum Theory, and Conceptions of the Universe* (Kluwer, 1989) p. 69
- [95] W. Dür, G. Vidal, J.I. Cirac *Phys. Rev. A* 62, 062314 (2000)
- [96] Y. Ji and F. Lin, *J. Opt. Soc. Am. B* 12, 1595-1601 (1995)

A Probability Amplitudes of $\Phi(\rho)$ for Two, Three, and Four Qubits

We devote this first appendix to the derivation of expressions for probability amplitudes for post-measurement density matrices in the case of two, three, and four qubits, both symmetric and asymmetric cases, for use in the method outlined in Chapter 3.

A.1 Two Qubits

$|B_1\rangle$ represents the $|b_{A-}\rangle |b_{B-}\rangle$ measurement vector, and the overlap with the scaled eigenvectors is as follows.

$$\begin{aligned} \langle \psi'_i | B_1 \rangle &= \psi''_{i00} \cos \frac{\theta_1}{2} \cos \frac{\theta_2}{2} + \psi''_{i01} \cos \frac{\theta_1}{2} \sin \frac{\theta_2}{2} e^{i\phi_2} \\ &\quad + \psi''_{i10} \sin \frac{\theta_1}{2} e^{i\phi_1} \cos \frac{\theta_2}{2} + \psi''_{i11} \sin \frac{\theta_1}{2} e^{i\phi_1} \sin \frac{\theta_2}{2} e^{i\phi_2} \end{aligned}$$

$|B_2\rangle$ represents the $|b_{A-}\rangle |b_{B+}\rangle$ measurement vector and the overlap in this case may be found by applying the following transformation to the result for $|B_1\rangle$. In the B space, simply change cosines to sines and sines to negative cosines.

$$\begin{aligned} \langle \psi'_i | B_2 \rangle &= \psi''_{i00} \cos \frac{\theta_1}{2} \sin \frac{\theta_2}{2} - \psi''_{i01} \cos \frac{\theta_1}{2} \cos \frac{\theta_2}{2} e^{i\phi_2} \\ &\quad + \psi''_{i10} \sin \frac{\theta_1}{2} e^{i\phi_1} \sin \frac{\theta_2}{2} - \psi''_{i11} \sin \frac{\theta_1}{2} e^{i\phi_1} \cos \frac{\theta_2}{2} e^{i\phi_2} \end{aligned}$$

$|B_3\rangle$ represents the $|b_{A+}\rangle |b_{B-}\rangle$ measurement vector and the overlap in this case may be found by applying the following transformation to the result for $|B_1\rangle$. In the A space, simply change cosines to sines and sines to negative cosines.

$$\begin{aligned} \langle \psi'_i | B_3 \rangle &= \psi''_{i00} \sin \frac{\theta_1}{2} \cos \frac{\theta_2}{2} + \psi''_{i01} \sin \frac{\theta_1}{2} \sin \frac{\theta_2}{2} e^{i\phi_2} \\ &\quad - \psi''_{i10} \cos \frac{\theta_1}{2} e^{i\phi_1} \cos \frac{\theta_2}{2} - \psi''_{i11} \cos \frac{\theta_1}{2} e^{i\phi_1} \sin \frac{\theta_2}{2} e^{i\phi_2} \end{aligned}$$

It is possible to derive the overlap with the fourth projector, but it is not useful as the probabilities must add to unity. Hence these are sufficient for the calculation of the global discord of two qubits without taking advantage of symmetry. The symmetric version of these expressions is shown below

$$\begin{aligned} \langle \psi''_i | B_1 \rangle &= \psi''_{i1} \cos \frac{\theta_1}{2} \cos \frac{\theta_2}{2} + \psi''_{i2} \left(\cos \frac{\theta_1}{2} \sin \frac{\theta_2}{2} e^{i\phi_2} + \sin \frac{\theta_1}{2} e^{i\phi_1} \cos \frac{\theta_2}{2} \right) \\ &\quad + \psi''_{i3} \sin \frac{\theta_1}{2} e^{i\phi_1} \sin \frac{\theta_2}{2} e^{i\phi_2} \end{aligned}$$

$$\begin{aligned}
\langle \psi''_i | B_2 \rangle &= \psi''_{i_1} \cos \frac{\theta_1}{2} \sin \frac{\theta_2}{2} + \psi''_{i_2} \left(\sin \frac{\theta_1}{2} e^{i\phi_1} \sin \frac{\theta_2}{2} - \cos \frac{\theta_1}{2} \cos \frac{\theta_2}{2} e^{i\phi_2} \right) \\
&\quad - \psi''_{i_3} \sin \frac{\theta_1}{2} e^{i\phi_1} \cos \frac{\theta_2}{2} e^{i\phi_2} \\
\langle \psi''_i | B_3 \rangle &= \psi''_{i_1} \sin \frac{\theta_1}{2} \cos \frac{\theta_2}{2} + \psi''_{i_2} \left(\sin \frac{\theta_1}{2} \sin \frac{\theta_2}{2} e^{i\phi_2} - \cos \frac{\theta_1}{2} e^{i\phi_1} \cos \frac{\theta_2}{2} \right) \\
&\quad - \psi''_{i_3} \cos \frac{\theta_1}{2} e^{i\phi_1} \sin \frac{\theta_2}{2} e^{i\phi_2}
\end{aligned}$$

where $\psi''_{i_1}, \psi''_{i_2}, \psi''_{i_3}$ are the i^{th} elements of the scaled eigenvectors of the symmetric density matrix for the system in question.

A.2 Three Qubits: Asymmetric Case

Using the same procedure as in two qubits we find the following

$$\begin{aligned}
\langle B_1 | \psi'_i \rangle &= \psi'_{i_{000}} \cos \frac{\theta_1}{2} \cos \frac{\theta_2}{2} \cos \frac{\theta_3}{2} \\
&\quad + \psi'_{i_{001}} \cos \frac{\theta_1}{2} \cos \frac{\theta_2}{2} e^{i\phi_3} \sin \frac{\theta_3}{2} + \psi'_{i_{010}} \cos \frac{\theta_1}{2} e^{i\phi_2} \sin \frac{\theta_2}{2} \cos \frac{\theta_3}{2} + \psi'_{i_{100}} e^{i\phi_1} \sin \frac{\theta_1}{2} \cos \frac{\theta_2}{2} \cos \frac{\theta_3}{2} \\
&\quad + \psi'_{i_{011}} \cos \frac{\theta_1}{2} e^{i\phi_2} \sin \frac{\theta_2}{2} e^{i\phi_3} \sin \frac{\theta_3}{2} + \psi'_{i_{110}} e^{i\phi_1} \sin \frac{\theta_1}{2} e^{i\phi_2} \sin \frac{\theta_2}{2} \cos \frac{\theta_3}{2} \\
&\quad + \psi'_{i_{101}} e^{i\phi_1} \sin \frac{\theta_1}{2} \cos \frac{\theta_2}{2} e^{i\phi_3} \sin \frac{\theta_3}{2} + \psi'_{i_{111}} e^{i\phi_1} \sin \frac{\theta_1}{2} e^{i\phi_2} \sin \frac{\theta_2}{2} e^{i\phi_3} \sin \frac{\theta_3}{2} \\
\langle B_2 | \psi'_i \rangle &= \psi'_{i_{000}} \cos \frac{\theta_1}{2} \cos \frac{\theta_2}{2} \sin \frac{\theta_3}{2} \\
&\quad - \psi'_{i_{001}} \cos \frac{\theta_1}{2} \cos \frac{\theta_2}{2} e^{i\phi_3} \cos \frac{\theta_3}{2} + \psi'_{i_{010}} \cos \frac{\theta_1}{2} e^{i\phi_2} \sin \frac{\theta_2}{2} \sin \frac{\theta_3}{2} + \psi'_{i_{100}} e^{i\phi_1} \sin \frac{\theta_1}{2} \cos \frac{\theta_2}{2} \sin \frac{\theta_3}{2} \\
&\quad - \psi'_{i_{011}} \cos \frac{\theta_1}{2} e^{i\phi_2} \sin \frac{\theta_2}{2} e^{i\phi_3} \cos \frac{\theta_3}{2} + \psi'_{i_{110}} e^{i\phi_1} \sin \frac{\theta_1}{2} e^{i\phi_2} \sin \frac{\theta_2}{2} \sin \frac{\theta_3}{2} \\
&\quad + \psi'_{i_{101}} e^{i\phi_1} \sin \frac{\theta_1}{2} \cos \frac{\theta_2}{2} e^{i\phi_3} \cos \frac{\theta_3}{2} + \psi'_{i_{111}} e^{i\phi_1} \sin \frac{\theta_1}{2} e^{i\phi_2} \sin \frac{\theta_2}{2} e^{i\phi_3} \cos \frac{\theta_3}{2} \\
\langle B_3 | \psi'_i \rangle &= \psi'_{i_{000}} \cos \frac{\theta_1}{2} \sin \frac{\theta_2}{2} \cos \frac{\theta_3}{2} \\
&\quad + \psi'_{i_{001}} \cos \frac{\theta_1}{2} \sin \frac{\theta_2}{2} e^{i\phi_3} \sin \frac{\theta_3}{2} - \psi'_{i_{010}} \cos \frac{\theta_1}{2} e^{i\phi_2} \cos \frac{\theta_2}{2} \cos \frac{\theta_3}{2} + \psi'_{i_{100}} e^{i\phi_1} \sin \frac{\theta_1}{2} \sin \frac{\theta_2}{2} \cos \frac{\theta_3}{2} \\
&\quad - \psi'_{i_{011}} \cos \frac{\theta_1}{2} e^{i\phi_2} \cos \frac{\theta_2}{2} e^{i\phi_3} \sin \frac{\theta_3}{2} - \psi'_{i_{110}} e^{i\phi_1} \sin \frac{\theta_1}{2} e^{i\phi_2} \cos \frac{\theta_2}{2} \cos \frac{\theta_3}{2} \\
&\quad + \psi'_{i_{101}} e^{i\phi_1} \sin \frac{\theta_1}{2} \sin \frac{\theta_2}{2} e^{i\phi_3} \sin \frac{\theta_3}{2} - \psi'_{i_{111}} e^{i\phi_1} \sin \frac{\theta_1}{2} e^{i\phi_2} \cos \frac{\theta_2}{2} e^{i\phi_3} \sin \frac{\theta_3}{2} \\
\langle B_4 | \psi'_i \rangle &= \psi'_{i_{000}} \cos \frac{\theta_1}{2} \sin \frac{\theta_2}{2} \sin \frac{\theta_3}{2} \\
&\quad - \psi'_{i_{001}} \cos \frac{\theta_1}{2} \sin \frac{\theta_2}{2} e^{i\phi_3} \cos \frac{\theta_3}{2} - \psi'_{i_{010}} \cos \frac{\theta_1}{2} e^{i\phi_2} \cos \frac{\theta_2}{2} \sin \frac{\theta_3}{2} + \psi'_{i_{100}} e^{i\phi_1} \sin \frac{\theta_1}{2} \sin \frac{\theta_2}{2} \sin \frac{\theta_3}{2} \\
&\quad + \psi'_{i_{011}} \cos \frac{\theta_1}{2} e^{i\phi_2} \cos \frac{\theta_2}{2} e^{i\phi_3} \cos \frac{\theta_3}{2} - \psi'_{i_{110}} e^{i\phi_1} \sin \frac{\theta_1}{2} e^{i\phi_2} \cos \frac{\theta_2}{2} \sin \frac{\theta_3}{2} \\
&\quad - \psi'_{i_{101}} e^{i\phi_1} \sin \frac{\theta_1}{2} \sin \frac{\theta_2}{2} e^{i\phi_3} \cos \frac{\theta_3}{2} + \psi'_{i_{111}} e^{i\phi_1} \sin \frac{\theta_1}{2} e^{i\phi_2} \cos \frac{\theta_2}{2} e^{i\phi_3} \cos \frac{\theta_3}{2} \\
\langle B_5 | \psi'_i \rangle &= \psi'_{i_{000}} \sin \frac{\theta_1}{2} \cos \frac{\theta_2}{2} \cos \frac{\theta_3}{2}
\end{aligned}$$

B Equations of Motion–Three Quantum Dots

In this appendix we derive the equations of motion for the system of three quantum dots studied in Chapters 2 and 4 (equation 2.20 or equation 4.14), using the approximation that

$\langle AB \rangle \approx \langle A \rangle \langle B \rangle$ and using the fact that $\langle \dot{A} \rangle = Tr A \dot{\rho}$ in conjunction with the master equation given for this system in chapter 4. We use the following matrix parameterization.

$$\Lambda = \begin{pmatrix} \frac{1}{4} + x & p & q & s \\ p^* & \frac{1}{4} + y & r & u \\ q^* & r^* & \frac{1}{4} + z & v \\ s^* & u^* & v^* & \frac{1}{4} - x - y - z \end{pmatrix}$$

B.1 Summary of Operator Effects

The dot ladder operators' effects on different states are as follows.

$$\begin{aligned} J_+ |0\rangle &= \sqrt{3} |1\rangle, \quad J_+ |1\rangle = 2 |2\rangle, \quad J_+ |2\rangle = \sqrt{3} |3\rangle \\ J_- |3\rangle &= \sqrt{3} |2\rangle, \quad J_- |2\rangle = 2 |1\rangle, \quad J_- |1\rangle = \sqrt{3} |0\rangle \end{aligned} \quad (\text{B.1})$$

Likewise, the T operator has the following effects.

$$T |0\rangle = |0\rangle, \quad T |1\rangle = 3 |1\rangle, \quad T |2\rangle = 3 |2\rangle, \quad T |3\rangle = |3\rangle \quad (\text{B.2})$$

This means also that the operator T will commute with any diagonal element. Furthermore, for three dots, if neither the ket nor the bra is 0 or 3, or if they are only 0 and 3, then the w term ($w [T, \rho]$) will still be zero because the same coefficient will be in both terms in the derivation.

B.2 Field Parameter α Equation

Let us break down the equation $Tr a \dot{\rho}$ into terms.

$$\Delta_c \text{ term: } Tr a (-i\Delta_c[a^\dagger a, \rho]) = -i\Delta_c (Tr aa^\dagger a \rho - Tr a \rho a^\dagger a) = -i\Delta_c Tr a \rho$$

$$g \text{ term: } Tr a (g[aJ_- - aJ_+, \rho]) = g (Tr (1 + a^\dagger a) J_- \rho - Tr a^\dagger a J_- \rho) = g Tr J_- \rho$$

$$\varepsilon \text{ term: } Tr a (\varepsilon[a^\dagger - a, \rho]) = \varepsilon (Tr aa^\dagger \rho - Tr a a \rho - Tr a \rho a^\dagger + Tr a \rho a) = \varepsilon$$

$$\kappa \text{ term: } Tr a (\kappa[2a\rho a^\dagger - a^\dagger a \rho - \rho a^\dagger a]) = \kappa[2Tr a a \rho a^\dagger - Tr a a^\dagger a \rho - Tr a \rho a^\dagger a] = -\kappa \langle \alpha \rangle$$

We note that $J_- = \sqrt{3}(|0\rangle\langle 1| + |2\rangle\langle 3|) + 2|1\rangle\langle 2|$, so the expectation value of J_- is

$$Tr J_- \dot{\rho} = \sqrt{3}(\langle p^* \rangle + \langle v^* \rangle) + 2 \langle r^* \rangle$$

We can then find the overall equation of motion as follows.

$$\langle \alpha \rangle = -(\kappa + i\Delta_c) \langle \alpha \rangle + \varepsilon + \sqrt{3}(\langle p^* \rangle + \langle v^* \rangle) + 2 \langle r^* \rangle$$

B.3 Dot variable parameters: Repeatable simplifications

Any term in the master equation lacking dot operators will go to zero (by both the fact that it's an independent space, and the cyclic property of the trace allowing you to rewrite $B\rho A = AB\rho$).

Therefore, the only relevant terms for the equations of motion regarding the dot parameters will be those corresponding to the following variables: Δ_d, g, γ, w . Further terms can be eliminated in the case of diagonal elements. Since the diagonal elements commute with J_z , the diagonals will have no Δ_d term. Likewise, they commute with the T operator. So there will be no w term.

B.4 x, y, and z Equations

For the x equation, let us break down $Tr |0\rangle \langle 0| \dot{\rho}$ into individual terms.

$$g \text{ term: } Tr |0\rangle \langle 0| (g[a^\dagger J_- - a J_+, \rho]) = \sqrt{3}g (\langle p^* \alpha^* \rangle + \langle p \alpha \rangle)$$

$$\gamma \text{ term: } Tr |0\rangle \langle 0| \left(\frac{\gamma}{2} [2J_- \rho J_+ - J_+ J_- \rho - \rho J_+ J_-] \right) = \gamma (3Tr |1\rangle \langle 1| \rho) = 3\gamma (\langle y \rangle + \frac{1}{4})$$

The overall equation of motion is

$$\dot{x} = \sqrt{3}g (\langle p^* \alpha^* \rangle + \langle p \alpha \rangle) + 3\gamma (\langle y \rangle + \frac{1}{4}).$$

For the y equation, we must instead break down $Tr |1\rangle \langle 1| \dot{\rho}$ into terms.

$$g \text{ term: } Tr |1\rangle \langle 1| (g[a^\dagger J_- - a J_+, \rho]) = g (2 \langle r^* \alpha^* \rangle - \sqrt{3} \langle p \alpha \rangle - \sqrt{3} \langle p^* \alpha^* \rangle + 2 \langle r \alpha \rangle)$$

$$\gamma \text{ term: } Tr |1\rangle \langle 1| \left(\frac{\gamma}{2} [2J_- \rho J_+ - J_+ J_- \rho - \rho J_+ J_-] \right) = \gamma (4 \langle z \rangle - 3 \langle y \rangle + \frac{1}{4})$$

The overall equation of motion is as follows.

$$\dot{y} = g (2 \langle r^* \alpha^* \rangle - \sqrt{3} \langle p \alpha \rangle - \sqrt{3} \langle p^* \alpha^* \rangle + 2 \langle r \alpha \rangle) + \gamma (4 \langle z \rangle - 3 \langle y \rangle + \frac{1}{4})$$

Next, to get the z equation, let us break down $Tr |2\rangle \langle 2| \dot{\rho}$ into terms.

$$g \text{ term: } Tr |2\rangle \langle 2| (g[a^\dagger J_- - a J_+, \rho]) = g (\sqrt{3} (\langle v^* \alpha^* \rangle + \langle v \alpha \rangle) - 2 (\langle r \alpha \rangle + \langle r^* \alpha^* \rangle))$$

$$\gamma \text{ term: } Tr |2\rangle \langle 2| \left(\frac{\gamma}{2} [2J_- \rho J_+ - J_+ J_- \rho - \rho J_+ J_-] \right) = \gamma (4z - 3y + \frac{1}{4})$$

The overall equation of motion is as follows.

$$\langle \dot{y} \rangle = 0 = g (2 \langle r^* \alpha^* \rangle - \sqrt{3} \langle p \alpha \rangle - \sqrt{3} \langle p^* \alpha^* \rangle + 2 \langle r \alpha \rangle) + \gamma (4z - 3y + \frac{1}{4})$$

B.5 p, q, and r Equations

Now, in order to get the p equation, let us consider $Tr |1\rangle \langle 0| \dot{\rho}$.

$$g \text{ term: } Tr |1\rangle \langle 0| (g[a^\dagger J_- - a J_+, \rho]) = g (\sqrt{3} \langle y\alpha^* \rangle - \sqrt{3} \langle x\alpha^* \rangle + 2 \langle q\alpha \rangle)$$

$$\gamma \text{ term: } Tr |1\rangle \langle 0| \left(\frac{\gamma}{2} [2J_- \rho J_+ - J_+ J_- \rho - \rho J_+ J_-] \right) = \gamma (2\sqrt{3} \langle r \rangle - \frac{3}{2} \langle p \rangle)$$

$$w \text{ term: } -Tr |1\rangle \langle 0| (iw[T, \rho]) = -iw (Tr |1\rangle \langle 0| T\rho - Tr |1\rangle \langle 0| \rho T) = 2iw \langle p \rangle$$

$$\Delta_d \text{ term: } Tr |1\rangle \langle 0| (-i\Delta_d[J_z, \rho]) = -i\Delta_d (Tr |1\rangle \langle 0| J_z \rho - Tr |1\rangle \langle 0| \rho J_z) = i\Delta_d \langle p \rangle$$

The overall equation of motion can be written as shown below.

$$\dot{p} = g (\sqrt{3} \langle y\alpha^* \rangle - \sqrt{3} \langle x\alpha^* \rangle + 2 \langle q\alpha \rangle) + \gamma (2\sqrt{3} \langle r \rangle - \frac{3}{2} \langle p \rangle) + 2iw \langle p \rangle + i\Delta_d \langle p \rangle$$

Let us now break $Tr |2\rangle \langle 0| \dot{\rho}$ into terms in order to get the q equation.

$$g \text{ term: } Tr |2\rangle \langle 0| (g[a^\dagger J_- - a J_+, \rho]) = g (\sqrt{3} \langle \alpha^* r \rangle - 2 \langle \alpha^* p \rangle + \sqrt{3} \langle \alpha s \rangle)$$

$$\gamma \text{ term: } Tr |2\rangle \langle 0| \left(\frac{\gamma}{2} [2J_- \rho J_+ - J_+ J_- \rho - \rho J_+ J_-] \right) = \gamma (3 \langle u \rangle - 2 \langle q \rangle)$$

$$w \text{ term: } -Tr |2\rangle \langle 0| (iw[T, \rho]) = -iw (Tr |2\rangle \langle 0| T\rho - Tr |2\rangle \langle 0| \rho T) = 2iw \langle q \rangle$$

$$\Delta_d \text{ term: } Tr |2\rangle \langle 0| (-i\Delta_d[J_z, \rho]) = -i\Delta_d (Tr |2\rangle \langle 0| J_z \rho - Tr |2\rangle \langle 0| \rho J_z) = 2i\Delta_d \langle q \rangle$$

Below is the overall equation of motion.

$$\dot{q} = g (\sqrt{3} \langle \alpha^* r \rangle - 2 \langle \alpha^* p \rangle + \sqrt{3} \langle \alpha s \rangle) + \gamma (3 \langle u \rangle - 2 \langle q \rangle) + 2iw \langle q \rangle + 2i\Delta_d \langle q \rangle$$

We are now to consider the expression $Tr |2\rangle \langle 1| \dot{\rho}$, to get the equation of motion for r .

$$g \text{ term: } Tr |2\rangle \langle 1| (g[a^\dagger J_- - a J_+, \rho]) = g (2 \langle z\alpha^* \rangle - \sqrt{3} \langle q\alpha \rangle - 2 \langle y\alpha^* \rangle + \sqrt{3} \langle u\alpha \rangle)$$

$$\gamma \text{ term: } Tr |2\rangle \langle 1| \left(\frac{\gamma}{2} [2J_- \rho J_+ - J_+ J_- \rho - \rho J_+ J_-] \right) = \gamma (2\sqrt{3} \langle v \rangle - \frac{3}{2} \langle r \rangle - 2 \langle r \rangle)$$

$$w \text{ term: } -Tr |2\rangle \langle 1| (iw[T, \rho]) = -iw (Tr |2\rangle \langle 1| T\rho - Tr |2\rangle \langle 1| \rho T) = 0$$

$$\Delta_d \text{ term: } Tr |2\rangle \langle 1| (-i\Delta_d[J_z, \rho]) = -i\Delta_d (Tr |2\rangle \langle 1| J_z \rho - Tr |2\rangle \langle 1| \rho J_z) = i\Delta_d \langle r \rangle$$

We then get the following overall equation of motion.

$$\dot{r} = g (2 \langle z\alpha^* \rangle - \sqrt{3} \langle q\alpha \rangle - 2 \langle y\alpha^* \rangle + \sqrt{3} \langle u\alpha \rangle) + \gamma (2\sqrt{3} \langle v \rangle - \frac{3}{2} \langle r \rangle - 2 \langle r \rangle) + i\Delta_d \langle r \rangle$$

B.6 s , u , and v Equations

We must now break $Tr |3\rangle \langle 0| \dot{\rho}$ into terms to get the equation of motion for s .

$$g \text{ term: } Tr |3\rangle \langle 0| (g[a^\dagger J_- - aJ_+, \rho]) = \sqrt{3}g (\langle \alpha^* u \rangle - \langle \alpha^* q \rangle)$$

$$\gamma \text{ term: } Tr |3\rangle \langle 0| \left(\frac{\gamma}{2} [2J_- \rho J_+ - J_+ J_- \rho - \rho J_+ J_-] \right) = \frac{\gamma}{2} (-3 \langle s \rangle)$$

$$w \text{ term: } -Tr |3\rangle \langle 0| (iw[T, \rho]) = -iw (Tr |3\rangle \langle 0| T\rho - Tr |3\rangle \langle 0| \rho T) = 0$$

$$\Delta_d \text{ term: } Tr |3\rangle \langle 0| (-i\Delta_d[J_z, \rho]) = -i\Delta_d (Tr |3\rangle \langle 0| J_z \rho - Tr |3\rangle \langle 0| \rho J_z) = 3i\Delta_d \langle s \rangle$$

The overall equation of motion, therefore, is $\dot{s} = \sqrt{3}g (\langle \alpha^* u \rangle - \langle \alpha^* q \rangle) + \frac{\gamma}{2} (-3 \langle s \rangle) + 3i\Delta_d \langle s \rangle$.

We then must consider $Tr |3\rangle \langle 1| \dot{\rho}$, for the u equation.

$$g \text{ term: } Tr |3\rangle \langle 1| (g[a^\dagger J_- - aJ_+, \rho]) = g (2 \langle \alpha^* v \rangle - \sqrt{3} \langle \alpha s \rangle - \sqrt{3} \langle \alpha^* r \rangle)$$

$$\gamma \text{ term: } Tr |3\rangle \langle 1| \left(\frac{\gamma}{2} [2J_- \rho J_+ - J_+ J_- \rho - \rho J_+ J_-] \right) = -3\gamma \langle u \rangle$$

$$w \text{ term: } -Tr |3\rangle \langle 1| (iw[T, \rho]) = -iw (Tr |3\rangle \langle 1| T\rho - Tr |3\rangle \langle 1| \rho T) = -2iw \langle u \rangle$$

$$\Delta_d \text{ term: } Tr |3\rangle \langle 1| (-i\Delta_d[J_z, \rho]) = -i\Delta_d (Tr |3\rangle \langle 1| J_z \rho - Tr |3\rangle \langle 1| \rho J_z) = 2i\Delta_d \langle u \rangle$$

Below is the overall equation of motion.

$$\dot{u} = g (2 \langle \alpha^* v \rangle - \sqrt{3} \langle \alpha s \rangle - \sqrt{3} \langle \alpha^* r \rangle) - 3\gamma \langle u \rangle - 2iw \langle u \rangle + 2i\Delta_d \langle u \rangle$$

Now let us take $Tr |3\rangle \langle 2| \dot{\rho}$ and evaluate it one term at a time to obtain the v equation of motion.

$$g \text{ term: } Tr |3\rangle \langle 2| (g[a^\dagger J_- - aJ_+, \rho]) = g (\sqrt{3} (-\langle x\alpha^* \rangle - \langle y\alpha^* \rangle - 2 \langle z\alpha^* \rangle) - 2 \langle u\alpha \rangle)$$

$$\gamma \text{ term: } Tr |3\rangle \langle 2| \left(\frac{\gamma}{2} [2J_- \rho J_+ - J_+ J_- \rho - \rho J_+ J_-] \right) = -\frac{7\gamma}{2} \langle v \rangle$$

$$w \text{ term: } -Tr |3\rangle \langle 2| (iw[T, \rho]) = -iw (Tr |3\rangle \langle 2| T\rho - Tr |3\rangle \langle 2| \rho T) = -2iw \langle v \rangle$$

$$\Delta_d \text{ term: } Tr |3\rangle \langle 2| (-i\Delta_d[J_z, \rho]) = -i\Delta_d (Tr |3\rangle \langle 2| J_z \rho - Tr |3\rangle \langle 2| \rho J_z) = i\Delta_d \langle v \rangle$$

The overall equation of motion for v is given by

$$\dot{v} = g (\sqrt{3} (-\langle x\alpha^* \rangle - \langle y\alpha^* \rangle - 2 \langle z\alpha^* \rangle) - 2 \langle u\alpha \rangle) - \frac{7\gamma}{2} \langle v \rangle - 2iw \langle v \rangle + i\Delta_d \langle v \rangle$$

B.7 Summary of Equations of motion

For a system of three identical coupled quantum dots in a driven cavity with dissipation and detuning, we find that the equations of motion are

$$\langle \dot{\alpha} \rangle = -\varsigma + (p^* + v^*) + \frac{2}{\sqrt{3}}r^* \quad (\text{B.3})$$

$$\langle \dot{x} \rangle = \sqrt{3}g(p^*\alpha^* + p\alpha) + 3\gamma\left(y + \frac{1}{4}\right) \quad (\text{B.4})$$

$$\langle \dot{y} \rangle = g\left(2(r^*\alpha^* + r\alpha) - \sqrt{3}(p\alpha + p^*\alpha^*)\right) + \gamma\left(4z - 3y + \frac{1}{4}\right) \quad (\text{B.5})$$

$$\langle \dot{z} \rangle = g\left(\sqrt{3}(v^*\alpha^* + v\alpha) - 2(r\alpha + r^*\alpha^*)\right) + \gamma\left(3\left(\frac{1}{4} - x - y - z\right) - 4\left(\frac{1}{4} + z\right)\right) \quad (\text{B.6})$$

$$\langle \dot{p} \rangle = g\left(\sqrt{3}\alpha^*(y - x) + 2q\alpha\right) + \gamma 2\sqrt{3}r + \xi_1 p \quad (\text{B.7})$$

$$\langle \dot{q} \rangle = g\left(\sqrt{3}\alpha^*r - 2\alpha^*p + \sqrt{3}\alpha s\right) + 3\gamma u + \xi_2 q \quad (\text{B.8})$$

$$\langle \dot{r} \rangle = g\left(2\alpha^*(z - y) - \sqrt{3}q\alpha + \sqrt{3}u\alpha\right) + 2\sqrt{3}\gamma v + \xi_3 r \quad (\text{B.9})$$

$$\langle \dot{s} \rangle = \sqrt{3}g\alpha^*(u - q) + \xi_4 s \quad (\text{B.10})$$

$$\langle \dot{u} \rangle = g\left(2\alpha^*v - \sqrt{3}\alpha s - \sqrt{3}\alpha^*r\right) + \xi_5 u \quad (\text{B.11})$$

$$\langle \dot{v} \rangle = g\left(\sqrt{3}\alpha^*(-x - y - 2z) - 2u\alpha\right) + \xi_6 v \quad (\text{B.12})$$

where we have defined the function ς and the constants ξ_i , $1 \leq i \leq 6$ as follows.

$$\begin{aligned} \varsigma &\equiv \frac{(\kappa + i\Delta_c)\alpha - \varepsilon}{\sqrt{3}}, \quad \xi_1 \equiv -\frac{3}{2}\gamma + 2iw + i\Delta_d, \quad \xi_2 \equiv -2\gamma + 2iw + 2i\Delta_d \\ \xi_3 &\equiv -\frac{7}{2}\gamma + i\Delta_d, \quad \xi_4 \equiv \frac{-3\gamma}{2} + 3i\Delta_d, \quad \xi_5 \equiv 2i\Delta_d - 3\gamma - 2iw, \quad \xi_6 \equiv i\Delta_d - \frac{7\gamma}{2} - 2iw \end{aligned} \quad (\text{B.13})$$

C Steady State Solutions of the Equations of Motion for Three Quantum Dots

In this appendix, we derive the steady state solutions for the system of three quantum dots studied in Chapter 4 of this work, solving all equations of motion algebraically in terms of α and constant system parameters alone. Extensive abstraction is needed to keep the expressions in a manageable form. Due to the high levels of abstraction, this exercise is mainly useful in reducing the numerical complexity of the problem, rather than in granting insight into the system itself. We use the same notation as developed in Appendix B

C.1 Preparation

Using the definitions for ς, ξ_i employed in Appendix B (equation B.13) and the definition of a steady state we write the steady state equations of motion for the system studied in Chapter 4 as follows.

$$\langle \dot{\alpha} \rangle = 0 = -\zeta + (p^* + v^*) + \frac{2}{\sqrt{3}}r^* \quad (\text{C.1})$$

$$\langle \dot{x} \rangle = 0 = \sqrt{3}g(p^*\alpha^* + p\alpha) + 3\gamma\left(y + \frac{1}{4}\right) \quad (\text{C.2})$$

$$\langle \dot{y} \rangle = 0 = g\left(2(r^*\alpha^* + r\alpha) - \sqrt{3}(p\alpha + p^*\alpha^*)\right) + \gamma\left(4z - 3y + \frac{1}{4}\right) \quad (\text{C.3})$$

$$\langle \dot{z} \rangle = 0 = g\left(\sqrt{3}(v^*\alpha^* + v\alpha) - 2(r\alpha + r^*\alpha^*)\right) + \gamma\left(3\left(\frac{1}{4} - x - y - z\right) - 4\left(\frac{1}{4} + z\right)\right) \quad (\text{C.4})$$

$$\langle \dot{p} \rangle = 0 = g\left(\sqrt{3}\alpha^*(y - x) + 2q\alpha\right) + \gamma 2\sqrt{3}r + \xi_1 p \quad (\text{C.5})$$

$$\langle \dot{q} \rangle = 0 = g\left(\sqrt{3}\alpha^*r - 2\alpha^*p + \sqrt{3}\alpha s\right) + 3\gamma u + \xi_2 q \quad (\text{C.6})$$

$$\langle \dot{r} \rangle = 0 = g\left(2\alpha^*(z - y) - \sqrt{3}q\alpha + \sqrt{3}u\alpha\right) + 2\sqrt{3}\gamma v + \xi_3 r \quad (\text{C.7})$$

$$\langle \dot{s} \rangle = 0 = \sqrt{3}g\alpha^*(u - q) + \xi_4 s \quad (\text{C.8})$$

$$\langle \dot{u} \rangle = 0 = g\left(2\alpha^*v - \sqrt{3}\alpha s - \sqrt{3}\alpha^*r\right) + \xi_5 u \quad (\text{C.9})$$

$$\langle \dot{v} \rangle = 0 = g\left(\sqrt{3}\alpha^*(-x - y - 2z) - 2u\alpha\right) + \xi_6 v \quad (\text{C.10})$$

C.2 Solve Eqn C.1 for p, Solve Eqn C.8 for s, and Solve Eqn C.9 for u

Taking the equations of motion in the steady state (equations C.1 through C.10) we solve

$$0 = -\zeta + (p^* + v^*) + \frac{2}{\sqrt{3}}r^* \Rightarrow p = \zeta^* - v - \frac{2r}{\sqrt{3}}$$

$$0 = \sqrt{3}g\alpha^*(u - q) + \xi_4 s \Rightarrow s = \frac{\sqrt{3}g\alpha^*}{\xi_4}(q - u)$$

$$0 = g\left(2\alpha^*v - \sqrt{3}\alpha s - \sqrt{3}\alpha^*r\right) + \xi_5 u$$

To solve the above equation for u , first we must substitute the current expression for s into the above.

$$0 = g \left(2\alpha^* v - 3 \frac{g\alpha\alpha^*}{\xi_4} q - \sqrt{3}\alpha^* r \right) + \left(3g \frac{g\alpha\alpha^*}{\xi_4} + \xi_5 \right) u$$

Solving for u and simplifying, we obtain the following.

$$u = \frac{1}{3 \frac{g\alpha\alpha^*}{\xi_4} + \frac{\xi_5}{g}} \left(3 \frac{g\alpha\alpha^*}{\xi_4} q + \sqrt{3}\alpha^* r \right) - \frac{2\alpha^*}{3g \frac{g\alpha\alpha^*}{\xi_4} + \frac{\xi_5}{g}} v$$

Now it is wise to eliminate u from our expression for s which we previously found. For brevity,

let us define the notation $\xi_{i,j} \equiv \xi_i \xi_j$, $\xi_{i,j,k} \equiv \xi_i \xi_j \xi_k$, $\xi_{i,j,k,\dots,\mathcal{N}} \equiv \xi_i \xi_j \xi_k \dots \xi_{\mathcal{N}}$

$$s = \frac{\sqrt{3}g\alpha^*}{\xi_4} (q - u) = \frac{\sqrt{3}g\alpha^*}{\xi_4} q - \frac{\sqrt{3}}{3\alpha + \frac{\xi_{4,5}}{g^2\alpha^*}} \left(3 \frac{g\alpha\alpha^*}{\xi_4} q + \sqrt{3}\alpha^* r \right) + \alpha^* \frac{2\sqrt{3}}{3\alpha + \frac{\xi_{4,5}}{g^2\alpha^*}} v$$

C.3 Solve Eqn C.10 for v

$$0 = g(\sqrt{3}\alpha^*(-x-y-2z) - 2u\alpha) + \xi_6 v$$

Substituting u and collecting v terms, we obtain the following.

$$0 = g(\sqrt{3}\alpha^*(-x-y-2z)) - 2g\alpha \left(\frac{1}{3g\frac{\alpha\alpha^*}{\xi_4} + \frac{\xi_5}{g}} \left(3\frac{g\alpha\alpha^*}{\xi_4}q + \sqrt{3}\alpha^*r \right) \right) + \left(\xi_6 + 2g\alpha \frac{2\alpha^*}{3g\frac{\alpha\alpha^*}{\xi_4} + \frac{\xi_5}{g}} \right) v$$

By isolating v, we obtain

$$v = -\frac{\sqrt{3}g\alpha^*(-x-y-2z)}{\xi_6 + 4g\alpha \frac{\alpha^*}{3g\frac{\alpha\alpha^*}{\xi_4} + \frac{\xi_5}{g}}} + \frac{2g\alpha}{\xi_6 \left(3g\frac{\alpha\alpha^*}{\xi_4} + \frac{\xi_5}{g} \right) + 4g\alpha\alpha^*} \left(3\frac{g\alpha\alpha^*}{\xi_4}q + \sqrt{3}\alpha^*r \right)$$

It is useful to simplify the remaining expressions before continuing. If we define

$$\Upsilon_1 \equiv 3\alpha + \frac{\xi_{4,5}}{g^2\alpha^*}$$

for simplicity and then use that and the expression we just found for v to eliminate v from all the expressions we have considered so far for the dot variables, we find the following expressions for p, s, u, v.

$$\begin{aligned} p &= \varsigma^* - \frac{2r}{\sqrt{3}} + \frac{\sqrt{3}g\alpha^*(-x-y-2z)}{\xi_6 + 4\alpha \frac{\xi_4}{\Upsilon_1}} - \frac{2\alpha\xi_4}{\xi_6\Upsilon_1 + 4\alpha\xi_4} \left(3\frac{g\alpha}{\xi_4}q + \sqrt{3}r \right) \\ s &= \sqrt{3}g\alpha^* \left(\frac{1}{\xi_4} - \frac{3}{\Upsilon_1} \frac{\alpha}{\xi_4} + \frac{1}{\Upsilon_1} \frac{12\alpha}{\xi_6 \frac{\Upsilon_1}{\alpha} + 4\xi_4} \right) q - \alpha^* \frac{6}{\Upsilon_1} \frac{g\alpha^*(-x-y-2z)}{\xi_6 + 4\alpha \frac{\xi_4}{\Upsilon_1}} + \frac{3\alpha^*}{\Upsilon_1} \left(\frac{4\alpha\xi_4}{\xi_6\Upsilon_1 + 4\alpha\xi_4} - 1 \right) r \\ u &= \frac{\xi_4}{g\Upsilon_1} \left(1 - \frac{4\alpha\xi_4}{\xi_6\Upsilon_1 + 4\alpha\xi_4} \right) \left(3\frac{g\alpha}{\xi_4}q + \sqrt{3}r \right) + \frac{2\xi_4}{g\Upsilon_1} \frac{\sqrt{3}g\alpha^*(-x-y-2z)}{\xi_6 + 4\alpha \frac{\xi_4}{\Upsilon_1}} \\ v &= -\frac{\sqrt{3}g\alpha^*(-x-y-2z)}{\xi_6 + 4\alpha \frac{\xi_4}{\Upsilon_1}} + \frac{2\alpha\xi_4}{\xi_6\Upsilon_1 + 4\alpha\xi_4} \left(3\frac{g\alpha}{\xi_4}q + \sqrt{3}r \right) \end{aligned}$$

C.4 Solve Eqn C.5 for r

$$0 = g(\sqrt{3}\alpha^*(y-x) + 2q\alpha) + \gamma 2\sqrt{3}r + \xi_1 p$$

The only variable expression we need substitute in this instance is that of p.

$$0 = g(\sqrt{3}\alpha^*(y-x) + 2q\alpha) + \gamma 2\sqrt{3}r + \xi_1 \left(\varsigma^* - \frac{2r}{\sqrt{3}} + \frac{\sqrt{3}g\alpha^*(-x-y-2z)}{\xi_6 + 4\alpha\frac{\xi_4}{\mathcal{Y}_1}} - \frac{2\alpha\xi_4\left(3\frac{g\alpha}{\xi_4}q + \sqrt{3}r\right)}{\xi_6\mathcal{Y}_1 + 4\alpha\xi_4} \right)$$

We now collect the r terms and the q terms.

$$0 = g(\sqrt{3}\alpha^*(y-x)) + \left(2g\alpha - \frac{6\xi_1 g\alpha^2}{\xi_6\mathcal{Y}_1 + 4\alpha\xi_4}\right) q + \xi_1 \left(\varsigma^* + \frac{\sqrt{3}g\alpha^*(-x-y-2z)}{\xi_6 + 4\alpha\frac{\xi_4}{\mathcal{Y}_1}} \right) + \left(\gamma 2\sqrt{3} - \xi_1 \left(\frac{2}{\sqrt{3}} + \frac{2\alpha\xi_4}{\xi_6\mathcal{Y}_1 + 4\alpha\xi_4} \sqrt{3} \right) \right) r$$

Then we must solve for r and simplify the result.

$$r = -\frac{g\alpha^*(y-x)}{2\gamma - \xi_1 \left(\frac{2}{\sqrt{3}} + \frac{2\alpha\xi_4}{\xi_6\mathcal{Y}_1 + 4\alpha\xi_4} \right)} - \frac{1}{\sqrt{3}} \frac{2g\alpha - \frac{6\xi_1 g\alpha^2}{\xi_6\mathcal{Y}_1 + 4\alpha\xi_4}}{2\gamma - \xi_1 \left(\frac{2}{\sqrt{3}} + \frac{2\alpha\xi_4}{\xi_6\mathcal{Y}_1 + 4\alpha\xi_4} \right)} q - \frac{\xi_1}{\sqrt{3}} \left(\frac{\varsigma^* + \frac{\sqrt{3}g\alpha^*(-x-y-2z)}{\xi_6 + 4\alpha\frac{\xi_4}{\mathcal{Y}_1}}}{2\gamma - \xi_1 \left(\frac{2}{\sqrt{3}} + \frac{2\alpha\xi_4}{\xi_6\mathcal{Y}_1 + 4\alpha\xi_4} \right)} \right)$$

Let us define $\mathcal{Y}_2 \equiv \xi_6\mathcal{Y}_1 + 4\alpha\xi_4 = \xi_6 \left(3\alpha + \frac{\xi_4\xi_5}{g^2\alpha^*} \right) + 4\alpha\xi_4$. By eliminating r from the expressions for v, p, u, s, we find the following expressions.

$$\begin{aligned} v &= -\mathcal{Y}_1 \frac{\sqrt{3}g\alpha^*(-x-y-2z)}{\mathcal{Y}_2} + \frac{6g\alpha^2}{\mathcal{Y}_2} \left(1 - \frac{\xi_4 \left(\frac{1}{3} - \frac{\xi_1\alpha}{\mathcal{Y}_2} \right)}{\gamma - \xi_1 \left(\frac{1}{3} + \frac{\alpha\xi_4}{\mathcal{Y}_2} \right)} \right) q \\ &\quad + \frac{g\alpha^* \frac{\sqrt{3}\alpha\xi_4}{\mathcal{Y}_2}}{\gamma - \xi_1 \left(\frac{1}{3} + \frac{\alpha\xi_4}{\mathcal{Y}_2} \right)} \left(-y + x - \mathcal{Y}_1 \frac{\xi_1(-x-y-2z)}{\mathcal{Y}_2} - \frac{\xi_1\varsigma^*}{\sqrt{3}g\alpha^*} \right) \\ r &= -\frac{g\alpha^*(y-x)}{2\gamma - \xi_1 \left(\frac{2}{\sqrt{3}} + \frac{2\alpha\xi_4}{\mathcal{Y}_2} \right)} - \frac{1}{\sqrt{3}} \frac{g\alpha - \frac{3\xi_1 g\alpha^2}{\mathcal{Y}_2}}{\gamma - \xi_1 \left(\frac{1}{3} + \frac{\alpha\xi_4}{\mathcal{Y}_2} \right)} q - \frac{\xi_1}{\sqrt{3}} \frac{\varsigma^* + \mathcal{Y}_1 \frac{\sqrt{3}g\alpha^*(-x-y-2z)}{\mathcal{Y}_2}}{2\gamma - \xi_1 \left(\frac{2}{\sqrt{3}} + \frac{2\alpha\xi_4}{\mathcal{Y}_2} \right)} \\ p &= \varsigma^* + \left(\mathcal{Y}_1 \frac{\sqrt{3}g\alpha^*}{\mathcal{Y}_2} + \left(\frac{2}{\sqrt{3}} + \frac{2\sqrt{3}\alpha\xi_4}{\mathcal{Y}_2} \right) \frac{\mathcal{Y}_1 \frac{\xi_1 g\alpha^*}{\mathcal{Y}_2}}{2\gamma - \xi_1 \left(\frac{2}{\sqrt{3}} + \frac{2\alpha\xi_4}{\mathcal{Y}_2} \right)} \right) (-x - y - 2z) + \frac{\xi_1}{\sqrt{3}} \frac{\left(\frac{2}{\sqrt{3}} + \frac{2\sqrt{3}\alpha\xi_4}{\mathcal{Y}_2} \right) \varsigma^*}{2\gamma - \xi_1 \left(\frac{2}{\sqrt{3}} + \frac{2\alpha\xi_4}{\mathcal{Y}_2} \right)} \\ &\quad + \left(\frac{2}{\sqrt{3}} + \frac{2\sqrt{3}\alpha\xi_4}{\mathcal{Y}_2} \right) \frac{g\alpha^*(y-x)}{2\gamma - \xi_1 \left(\frac{2}{\sqrt{3}} + \frac{2\alpha\xi_4}{\mathcal{Y}_2} \right)} + \left(-\frac{6g\alpha^2}{\mathcal{Y}_2} + \left(\frac{2}{\sqrt{3}} + \frac{2\sqrt{3}\alpha\xi_4}{\mathcal{Y}_2} \right) \frac{1}{\sqrt{3}} \frac{g\alpha - \frac{3\xi_1 g\alpha^2}{\mathcal{Y}_2}}{\gamma - \xi_1 \left(\frac{1}{3} + \frac{\alpha\xi_4}{\mathcal{Y}_2} \right)} \right) q \\ u &= \frac{\left(1 - \frac{4\alpha\xi_4}{\mathcal{Y}_2} \right) \alpha}{\mathcal{Y}_1} \left(3 - \xi_4 \frac{1 - \frac{3\xi_1\alpha}{\mathcal{Y}_2}}{\gamma - \xi_1 \left(\frac{1}{3} + \frac{\alpha\xi_4}{\mathcal{Y}_2} \right)} \right) q + \xi_4 \frac{\sqrt{3}\alpha^*}{\mathcal{Y}_2} \left(2 - \frac{\left(1 - \frac{4\alpha\xi_4}{\mathcal{Y}_2} \right) \xi_1}{2\gamma - \xi_1 \left(\frac{2}{\sqrt{3}} + \frac{2\alpha\xi_4}{\mathcal{Y}_2} \right)} \right) (-x - y - 2z) \\ &\quad + \frac{\sqrt{3}\xi_4}{g\mathcal{Y}_1} \left(1 - \frac{4\alpha\xi_4}{\mathcal{Y}_2} \right) \left(-\frac{g\alpha^*(y-x)}{2\gamma - \xi_1 \left(\frac{2}{\sqrt{3}} + \frac{2\alpha\xi_4}{\mathcal{Y}_2} \right)} - \frac{\frac{\xi_1}{\sqrt{3}}\varsigma^*}{2\gamma - \xi_1 \left(\frac{2}{\sqrt{3}} + \frac{2\alpha\xi_4}{\mathcal{Y}_2} \right)} \right) \\ s &= \frac{\sqrt{3}g\alpha^*}{\mathcal{Y}_1} \left(\frac{\mathcal{Y}_1}{\xi_4} - 3\frac{\alpha}{\xi_4} + \frac{12\alpha^2}{\mathcal{Y}_2} - \left(\frac{4\alpha\xi_4}{\mathcal{Y}_2} - 1 \right) \frac{\alpha - \frac{3\xi_1\alpha^2}{\mathcal{Y}_2}}{\gamma - \xi_1 \left(\frac{1}{3} + \frac{\alpha\xi_4}{\mathcal{Y}_2} \right)} \right) q - \frac{6g\alpha^{*2}(-x-y-2z)}{\mathcal{Y}_2} \\ &\quad + \frac{3\alpha^*}{\mathcal{Y}_1} \left(\frac{4\alpha\xi_4}{\mathcal{Y}_2} - 1 \right) \left(-\frac{g\alpha^*(y-x)}{2\gamma - \xi_1 \left(\frac{2}{\sqrt{3}} + \frac{2\alpha\xi_4}{\mathcal{Y}_2} \right)} - \frac{\xi_1}{\sqrt{3}} \frac{\varsigma^* + \mathcal{Y}_1 \frac{\sqrt{3}g\alpha^*(-x-y-2z)}{\mathcal{Y}_2}}{2\gamma - \xi_1 \left(\frac{2}{\sqrt{3}} + \frac{2\alpha\xi_4}{\mathcal{Y}_2} \right)} \right) \end{aligned}$$

C.5 Solve Eqn C.7 for q

$$0 = 2g\alpha^*(z - y) + \sqrt{3}g\alpha u - \sqrt{3}g\alpha q + 2\sqrt{3}\gamma v + \xi_3 r$$

Substitute r and v

$$\begin{aligned} 0 = & 2g\alpha^*(z - y) + \sqrt{3}g\alpha u - \sqrt{3}g\alpha q \\ & + 2\sqrt{3}\gamma \left(-\mathcal{Y}_1 \frac{\sqrt{3}g\alpha^*(-x-y-2z)}{\mathcal{Y}_2} + \frac{6g\alpha^2}{\mathcal{Y}_2} \left(1 - \frac{\xi_4 \left(\frac{1}{3} - \frac{\xi_1 \alpha}{\mathcal{Y}_2} \right)}{\gamma - \xi_1 \left(\frac{1}{3} + \frac{\alpha \xi_4}{\mathcal{Y}_2} \right)} \right) q \right) \\ & + \gamma \frac{g\alpha^* \frac{6\alpha \xi_4}{\mathcal{Y}_2}}{\gamma - \xi_1 \left(\frac{1}{3} + \frac{\alpha \xi_4}{\mathcal{Y}_2} \right)} \left(-y + x - \mathcal{Y}_1 \frac{\xi_1(-x-y-2z)}{\mathcal{Y}_2} - \frac{\xi_1 \varsigma^*}{\sqrt{3}g\alpha^*} \right) \\ & + \frac{g\xi_3}{2\gamma - \xi_1 \left(\frac{2}{3} + \frac{2\alpha \xi_4}{\mathcal{Y}_2} \right)} \left(-\frac{\alpha^*(y-x)}{1} - 2\frac{\alpha - \frac{3\xi_1 \alpha^2}{\mathcal{Y}_2}}{\sqrt{3}} q - \xi_1 \frac{\frac{\varsigma^*}{g} + \mathcal{Y}_1 \frac{\sqrt{3}\alpha^*(-x-y-2z)}{\mathcal{Y}_2}}{\sqrt{3}} \right) \end{aligned}$$

$$\text{Let us define } \mathcal{Y}_3 \equiv \gamma - \xi_1 \left(\frac{1}{3} + \frac{\alpha \xi_4}{\mathcal{Y}_2} \right) = \gamma - \xi_1 \left(\frac{1}{3} + \frac{\alpha \xi_4}{\xi_6 \left(3\alpha + \frac{\xi_4 \xi_5}{g^2 \alpha^*} \right) + 4\alpha \xi_4} \right)$$

Using the above definition we can rewrite the expression for u with the definition of \mathcal{Y}_3 .

$$\begin{aligned} u = & \frac{\left(1 - \frac{4\alpha \xi_4}{\mathcal{Y}_2} \right) \alpha}{\mathcal{Y}_1} \left(3 - \xi_4 \frac{1 - \frac{3\xi_1 \alpha}{\mathcal{Y}_2}}{\mathcal{Y}_3} \right) q + \xi_4 \frac{\sqrt{3}\alpha^*}{\mathcal{Y}_2} \left(2 - \frac{\left(1 - \frac{4\alpha \xi_4}{\mathcal{Y}_2} \right) \xi_1}{2\mathcal{Y}_3} \right) (-x - y - 2z) \\ & + \frac{\frac{\sqrt{3}\xi_4}{g\mathcal{Y}_1} \left(1 - \frac{4\alpha \xi_4}{\mathcal{Y}_2} \right)}{2\mathcal{Y}_3} \left(-g\alpha^*(y-x) - \frac{\xi_1}{\sqrt{3}} \varsigma^* \right) \end{aligned}$$

Now we shall substitute the new expression for u into equation [7] and simplify.

$$\begin{aligned} 0 = & \sqrt{3}g\alpha \left(\frac{\left(1 - \frac{4\alpha \xi_4}{\mathcal{Y}_2} \right) \alpha}{\mathcal{Y}_1} \left(3 - \xi_4 \frac{1 - \frac{3\xi_1 \alpha}{\mathcal{Y}_2}}{\mathcal{Y}_3} \right) - 1 - \frac{\xi_3}{\mathcal{Y}_3} \frac{1 - \frac{3\xi_1 \alpha}{\mathcal{Y}_2}}{3} + \frac{12\gamma \alpha \left(1 - \frac{\xi_4 \left(\frac{1}{3} - \frac{\xi_1 \alpha}{\mathcal{Y}_2} \right)}{\mathcal{Y}_3} \right)}{\mathcal{Y}_2} \right) q \\ & 2g\alpha^*(z - y) + \sqrt{3}g\alpha \xi_4 \frac{\sqrt{3}\alpha^*}{\mathcal{Y}_2} \left(2 - \frac{\left(1 - \frac{4\alpha \xi_4}{\mathcal{Y}_2} \right) \xi_1}{2\mathcal{Y}_3} \right) (-x - y - 2z) \\ & + \sqrt{3}g\alpha \left(\frac{\frac{\sqrt{3}\xi_4}{g\mathcal{Y}_1} \left(1 - \frac{4\alpha \xi_4}{\mathcal{Y}_2} \right)}{2\mathcal{Y}_3} \left(-g\alpha^*(y-x) - \frac{\xi_1}{\sqrt{3}} \varsigma^* \right) \right) - 2\sqrt{3}\gamma \left(\mathcal{Y}_1 \frac{\sqrt{3}g\alpha^*(-x-y-2z)}{\mathcal{Y}_2} \right) \\ & + \gamma \frac{g\alpha^* \frac{6\alpha \xi_4}{\mathcal{Y}_2}}{\mathcal{Y}_3} \left(x - y + \frac{\xi_1 \mathcal{Y}_1 (x+y+2z)}{\mathcal{Y}_2} - \frac{\xi_1 \varsigma^*}{\sqrt{3}g\alpha^*} \right) - \frac{g\xi_3}{2\mathcal{Y}_3} \left(\alpha^*(y-x) + \xi_1 \frac{\frac{\varsigma^*}{g} + \mathcal{Y}_1 \frac{\sqrt{3}\alpha^*(-x-y-2z)}{\mathcal{Y}_2}}{\sqrt{3}} \right) \end{aligned}$$

Realistically speaking, this expression could stand some simplification beyond that which is afforded by the current level of abstraction. Consider the portion of the above expression which is multiplied by q . Within this expression, let us collect terms in $\frac{1 - \frac{3\xi_1 \alpha}{\mathcal{Y}_2}}{\mathcal{Y}_3}$ and define

$$\mathcal{Y}_4 \equiv \frac{\left(3 - \frac{12\alpha \xi_4}{\mathcal{Y}_2} \right) \alpha}{\mathcal{Y}_1} - \left(\alpha \xi_4 \left(\frac{1 - \frac{4\alpha \xi_4}{\mathcal{Y}_2}}{\mathcal{Y}_1} + \frac{4\gamma}{\mathcal{Y}_2} \right) + \frac{\xi_3}{3} \right) \frac{1 - \frac{3\xi_1 \alpha}{\mathcal{Y}_2}}{\mathcal{Y}_3} + \gamma \frac{12\alpha}{\mathcal{Y}_2} - 1,$$

$$\mathcal{Y}_5 \equiv \frac{3\xi_4}{\mathcal{Y}_1} \left(1 - \frac{4\alpha \xi_4}{\mathcal{Y}_2} \right) + \frac{12\gamma \xi_4}{\mathcal{Y}_2} + \frac{\xi_3}{\alpha}, \text{ and } \mathcal{Y}_6 \equiv \xi_4 \left(6 - \frac{\left(3 - \frac{12\alpha \xi_4}{\mathcal{Y}_2} \right) \xi_1}{2\mathcal{Y}_3} \right) - 6\gamma \mathcal{Y}_1 \left(\frac{1}{\alpha} + \frac{\xi_4 \xi_1}{\mathcal{Y}_2 \mathcal{Y}_3} \right) - \frac{\xi_1 \mathcal{Y}_1 \xi_3}{2\mathcal{Y}_3 \alpha}$$

After considerable simplification and solving for q , we obtain

$$q = -\frac{2\alpha^*}{\sqrt{3}\alpha \mathcal{Y}_4} (z - y) + \frac{1}{6} \frac{\xi_1 \mathcal{Y}_5}{g \mathcal{Y}_3 \mathcal{Y}_4} \varsigma^* - \frac{\alpha^* \mathcal{Y}_6}{\sqrt{3} \mathcal{Y}_2 \mathcal{Y}_4} (-x - y - 2z) + \frac{\alpha^*}{2\sqrt{3} \mathcal{Y}_3 \mathcal{Y}_4} \mathcal{Y}_5 (y - x)$$

Now we will substitute the q expression into the current expressions for p, r, s, u, v . To assist in this matter, we further define the following.

$$\mathcal{Y}_7 \equiv \frac{3\alpha}{\mathcal{Y}_2} + \frac{\mathcal{Y}_3 - \gamma}{\xi_1} \frac{1 - \frac{3\xi_1\alpha}{\mathcal{Y}_2}}{\mathcal{Y}_3}, \mathcal{Y}_8 \equiv \frac{\xi_5}{g^2\alpha^*} + \frac{12\alpha^2}{\mathcal{Y}_2} + \alpha \frac{\xi_6\mathcal{Y}_1}{\mathcal{Y}_2} \frac{1 - \frac{3\xi_1\alpha}{\mathcal{Y}_2}}{\mathcal{Y}_3}, \text{ and simplify.}$$

We can then rewrite our expressions for the dot variables p, q, r, s, u, v as follows, with q eliminated from the expressions for the variables p, q, r, s, u, v .

$$\begin{aligned} p &= \left(\frac{\gamma}{\mathcal{Y}_3} - \frac{\mathcal{Y}_7}{3} \frac{\alpha\xi_1\mathcal{Y}_5}{\mathcal{Y}_3\mathcal{Y}_4} \right) \zeta^* - \frac{g\alpha^*}{\mathcal{Y}_3} \left(\mathcal{Y}_7 \frac{\alpha\mathcal{Y}_5}{\sqrt{3}\mathcal{Y}_4} + \sqrt{3} \frac{\mathcal{Y}_3 - \gamma}{\xi_1} \right) (y - x) \\ &\quad + \mathcal{Y}_7 \frac{4g\alpha^*}{\sqrt{3}\mathcal{Y}_4} (z - y) + \sqrt{3}g\alpha^* \left(\frac{2\alpha\mathcal{Y}_6}{3\mathcal{Y}_2\mathcal{Y}_4} \mathcal{Y}_7 + \frac{\mathcal{Y}_1}{\mathcal{Y}_2} \frac{\gamma}{\mathcal{Y}_3} \right) (-x - y - 2z) \\ q &= -\frac{2\alpha^*}{\sqrt{3}\alpha\mathcal{Y}_4} (z - y) + \frac{1}{6} \frac{\xi_1\mathcal{Y}_5}{g\mathcal{Y}_3\mathcal{Y}_4} \zeta^* - \frac{\alpha^*\mathcal{Y}_6}{\sqrt{3}\mathcal{Y}_2\mathcal{Y}_4} (-x - y - 2z) + \frac{\alpha^*}{2\sqrt{3}\mathcal{Y}_3\mathcal{Y}_4} \mathcal{Y}_5 (y - x) \\ r &= \frac{g\alpha^*}{\sqrt{3}\mathcal{Y}_2} \left(\frac{1 - \frac{3\xi_1\alpha}{\mathcal{Y}_2}}{\mathcal{Y}_3} \frac{\alpha\mathcal{Y}_6}{\sqrt{3}\mathcal{Y}_4} - \xi_1 \frac{\sqrt{3}\mathcal{Y}_1}{2\mathcal{Y}_3} \right) (-x - y - 2z) - \frac{\xi_1}{2\sqrt{3}\mathcal{Y}_3} \left(1 + \frac{\alpha}{3} \frac{1 - \frac{3\xi_1\alpha}{\mathcal{Y}_2}}{\mathcal{Y}_3} \frac{\mathcal{Y}_5}{\mathcal{Y}_4} \right) \zeta^* \\ &\quad - \frac{g\alpha^*}{2\mathcal{Y}_3} \left(1 + \frac{1 - \frac{3\xi_1\alpha}{\mathcal{Y}_2}}{\mathcal{Y}_3} \frac{\alpha\mathcal{Y}_5}{3\mathcal{Y}_4} \right) (y - x) + \frac{1 - \frac{3\xi_1\alpha}{\mathcal{Y}_2}}{\mathcal{Y}_3} \frac{2g\alpha^*}{3\mathcal{Y}_4} (z - y) \\ s &= -\frac{g\alpha^{*2}}{\mathcal{Y}_2} \left(3 \left(2 - \frac{\xi_6\mathcal{Y}_1}{\mathcal{Y}_2} \frac{\xi_1}{2\mathcal{Y}_3} \right) + \frac{\mathcal{Y}_8\mathcal{Y}_6}{\mathcal{Y}_1\mathcal{Y}_4} \right) (-x - y - 2z) + \frac{\alpha^*\xi_1}{2\mathcal{Y}_3} \left(\frac{\sqrt{3}\xi_6}{\mathcal{Y}_2} + \frac{1}{\sqrt{3}} \frac{\mathcal{Y}_8}{\mathcal{Y}_1} \frac{\mathcal{Y}_5}{\mathcal{Y}_4} \right) \zeta^* \\ &\quad + \frac{g\alpha^{*2}}{2\mathcal{Y}_3} \left(\frac{3\xi_6}{\mathcal{Y}_2} + \frac{\mathcal{Y}_8\mathcal{Y}_5}{\mathcal{Y}_1\mathcal{Y}_4} \right) (y - x) - \frac{g\alpha^{*2}}{\mathcal{Y}_1} \frac{2\mathcal{Y}_8}{\alpha\mathcal{Y}_4} (z - y) \\ u &= \frac{\alpha^*}{\mathcal{Y}_2} \left(\sqrt{3}\xi_4 \left(2 - \frac{\xi_6\mathcal{Y}_1}{\mathcal{Y}_2} \frac{\xi_1}{2\mathcal{Y}_3} \right) - \frac{\alpha}{\sqrt{3}} \frac{\xi_6\mathcal{Y}_6}{\mathcal{Y}_2\mathcal{Y}_4} \left(3 - \xi_4 \frac{1 - \frac{3\xi_1\alpha}{\mathcal{Y}_2}}{\mathcal{Y}_3} \right) \right) (-x - y - 2z) \\ &\quad + \frac{\xi_6\xi_1}{2g\mathcal{Y}_3\mathcal{Y}_2} \left(\left(3 - \xi_4 \frac{1 - \frac{3\xi_1\alpha}{\mathcal{Y}_2}}{\mathcal{Y}_3} \right) \frac{\alpha}{3} \frac{\mathcal{Y}_5}{\mathcal{Y}_4} - \xi_4 \right) \zeta^* + \frac{\sqrt{3}\xi_6\alpha^*}{2\mathcal{Y}_2\mathcal{Y}_3} \left(\left(3 - \xi_4 \frac{1 - \frac{3\xi_1\alpha}{\mathcal{Y}_2}}{\mathcal{Y}_3} \right) \frac{\alpha\mathcal{Y}_5}{3\mathcal{Y}_4} - \xi_4 \right) (y - x) \\ &\quad - \left(3 - \xi_4 \frac{1 - \frac{3\xi_1\alpha}{\mathcal{Y}_2}}{\mathcal{Y}_3} \right) \frac{2\alpha^*}{\sqrt{3}\mathcal{Y}_4} \frac{\xi_6}{\mathcal{Y}_2} (z - y) \\ v &= \sqrt{3}g\alpha^* \left(-\frac{\mathcal{Y}_1}{\mathcal{Y}_2} \left(1 + \frac{\alpha\xi_1\xi_4}{\mathcal{Y}_2\mathcal{Y}_3} \right) - \left(1 - \frac{\xi_4 \left(\frac{1}{3} - \frac{\xi_1\alpha}{\mathcal{Y}_2} \right)}{\mathcal{Y}_3} \right) \frac{2\alpha^2\mathcal{Y}_6}{\mathcal{Y}_2^2\mathcal{Y}_4} \right) (-x - y - 2z) \\ &\quad + \frac{\xi_1}{\mathcal{Y}_2} \left(\alpha^2 \left(1 - \frac{\xi_4 \left(\frac{1}{3} - \frac{\xi_1\alpha}{\mathcal{Y}_2} \right)}{\mathcal{Y}_3} \right) \frac{\mathcal{Y}_5}{\mathcal{Y}_3\mathcal{Y}_4} - \frac{\alpha\xi_4}{\mathcal{Y}_3} \right) \zeta^* - \left(1 - \frac{\xi_4 \left(\frac{1}{3} - \frac{\xi_1\alpha}{\mathcal{Y}_2} \right)}{\mathcal{Y}_3} \right) \frac{12\alpha^*}{\sqrt{3}\mathcal{Y}_4} \frac{g\alpha}{\mathcal{Y}_2} (z - y) \\ &\quad + \left(\frac{6g\alpha^2}{\mathcal{Y}_2} \left(1 - \frac{\xi_4 \left(\frac{1}{3} - \frac{\xi_1\alpha}{\mathcal{Y}_2} \right)}{\mathcal{Y}_3} \right) \frac{\alpha^*\mathcal{Y}_5}{2\sqrt{3}\mathcal{Y}_3\mathcal{Y}_4} - \frac{g\alpha^*}{\mathcal{Y}_3} \frac{\sqrt{3}\alpha\xi_4}{\mathcal{Y}_2} \right) (y - x) \end{aligned}$$

C.6 Solve Eqn C.2 for y

$$0 = \sqrt{3}g2\mathcal{R} [p\alpha] + 3\gamma \left(y + \frac{1}{4} \right)$$

Let us focus on $\mathcal{R} [p\alpha]$. We find the following expression.

$$\mathcal{R} [p\alpha] = \mathcal{R} \left[\left(\frac{\gamma}{\mathcal{Y}_3} - \frac{\mathcal{Y}_7}{3} \frac{\alpha\xi_1\mathcal{Y}_5}{\mathcal{Y}_3\mathcal{Y}_4} \right) \alpha\zeta^* \right] - \mathcal{R} \left[\frac{g\alpha^*\alpha}{\mathcal{Y}_3} \left(\frac{\alpha\mathcal{Y}_5\mathcal{Y}_7}{\sqrt{3}\mathcal{Y}_4} + \sqrt{3} \frac{\mathcal{Y}_3 - \gamma}{\xi_1} \right) \right] (y - x)$$

$$+\mathcal{R} \left[\frac{4g\alpha^* \alpha \mathcal{Y}_7}{\sqrt{3}\mathcal{Y}_4} \right] (z - y) + \sqrt{3}g\alpha^* \alpha \mathcal{R} \left[\frac{2\alpha\mathcal{Y}_6\mathcal{Y}_7}{3\mathcal{Y}_2\mathcal{Y}_4} \mathcal{Y}_7 + \frac{\mathcal{Y}_1}{\mathcal{Y}_2} \frac{\gamma}{\mathcal{Y}_3} \right] (-x - y - 2z)$$

Therefore, the equation of motion is given as follows.

$$0 = \left(3\gamma - 2\sqrt{3}g^2|\alpha|^2 \left(\mathcal{R} \left[\frac{\alpha\mathcal{Y}_5\mathcal{Y}_7}{\sqrt{3}\mathcal{Y}_4} + \sqrt{3} \frac{\mathcal{Y}_3 - \gamma}{\xi_1} + \frac{4\mathcal{Y}_7}{\sqrt{3}\mathcal{Y}_4} + \frac{\sqrt{3}}{\mathcal{Y}_2} \left(\frac{2\alpha\mathcal{Y}_6\mathcal{Y}_7}{3\mathcal{Y}_4} + \frac{\gamma\mathcal{Y}_1}{\mathcal{Y}_3} \right) \right] \right) \right) y \\ + 2\sqrt{3}g \left(\mathcal{R} \left[\left(\gamma - \frac{\mathcal{Y}_7}{3} \frac{\alpha\xi_1\mathcal{Y}_5}{\mathcal{Y}_4} \right) \frac{\alpha\xi^*}{\mathcal{Y}_3} \right] + \mathcal{R} \left[\frac{g|\alpha|^2}{\mathcal{Y}_3} \left(\frac{\alpha\mathcal{Y}_5\mathcal{Y}_7}{\sqrt{3}\mathcal{Y}_4} + \sqrt{3} \frac{\mathcal{Y}_3 - \gamma}{\xi_1} \right) \right] \right) x \\ + g^2|\alpha|^2 \left(\mathcal{R} \left[\frac{8\mathcal{Y}_7}{\mathcal{Y}_4} \right] z + 6\mathcal{R} \left[\frac{2\alpha\mathcal{Y}_6\mathcal{Y}_7 + \frac{\gamma\mathcal{Y}_1}{\mathcal{Y}_3}}{\mathcal{Y}_2} \right] (-x - 2z) \right) + 3\gamma \frac{1}{4}$$

Let us define $\mathcal{Y}_9 \equiv \frac{\alpha\mathcal{Y}_5\mathcal{Y}_7}{\sqrt{3}\mathcal{Y}_4} + \sqrt{3} \frac{\mathcal{Y}_3 - \gamma}{\xi_1}$ and $\mathcal{Y}_{10} \equiv \frac{2\alpha\mathcal{Y}_6\mathcal{Y}_7}{3\mathcal{Y}_4} + \frac{\gamma\mathcal{Y}_1}{\mathcal{Y}_3}$. We then find the following expression.

$$0 = 3 \left(\gamma - \frac{2g^2|\alpha|^2}{\sqrt{3}} \mathcal{R} \left[\frac{\mathcal{Y}_9}{\mathcal{Y}_3} + \frac{4\mathcal{Y}_7}{\sqrt{3}\mathcal{Y}_4} + \frac{\sqrt{3}}{\mathcal{Y}_2} \mathcal{Y}_{10} \right] \right) y \\ + 2\sqrt{3}g \left(\mathcal{R} \left[\left(\gamma - \frac{\mathcal{Y}_7}{3} \frac{\alpha\xi_1\mathcal{Y}_5}{\mathcal{Y}_4} \right) \frac{\alpha\xi^*}{\mathcal{Y}_3} \right] + \mathcal{R} \left[\frac{g|\alpha|^2}{\mathcal{Y}_3} \mathcal{Y}_9 \right] \right) x \\ + g^2|\alpha|^2 \left(\mathcal{R} \left[\frac{8\mathcal{Y}_7}{\mathcal{Y}_4} \right] z + 6\mathcal{R} \left[\frac{\mathcal{Y}_{10}}{\mathcal{Y}_2} \right] (-x - 2z) \right) + 3\gamma \frac{1}{4}$$

It occurs to one to try to simplify $\gamma - \frac{\mathcal{Y}_7}{3} \frac{\alpha\xi_1\mathcal{Y}_5}{\mathcal{Y}_4}$

$$\gamma - \frac{\mathcal{Y}_7}{3} \frac{\alpha\xi_1\mathcal{Y}_5}{\mathcal{Y}_4} = \gamma - \frac{\xi_1}{\sqrt{3}} \frac{\alpha\mathcal{Y}_5\mathcal{Y}_7}{\sqrt{3}\mathcal{Y}_4} = \gamma - \frac{\xi_1}{\sqrt{3}} \left(\frac{\alpha\mathcal{Y}_5\mathcal{Y}_7}{\sqrt{3}\mathcal{Y}_4} + \sqrt{3} \frac{\mathcal{Y}_3 - \gamma}{\xi_1} - \sqrt{3} \frac{\mathcal{Y}_3 - \gamma}{\xi_1} \right) = \mathcal{Y}_3 - \frac{\xi_1\mathcal{Y}_9}{\sqrt{3}}$$

Therefore, on simplifying and solving for y we obtain the following.

$$y = - \frac{g^2|\alpha|^2 \mathcal{R} \left[\frac{8\mathcal{Y}_7}{\mathcal{Y}_4} - \frac{12\mathcal{Y}_{10}}{\mathcal{Y}_2} \right]}{3 \left(\gamma - \frac{2g^2|\alpha|^2}{\sqrt{3}} \mathcal{R} \left[\frac{\mathcal{Y}_9}{\mathcal{Y}_3} + \frac{4\mathcal{Y}_7}{\sqrt{3}\mathcal{Y}_4} + \frac{\sqrt{3}\mathcal{Y}_{10}}{\mathcal{Y}_2} \right] \right)} z - \frac{2\sqrt{3}g \mathcal{R} \left[\frac{\alpha\xi^* \left(\mathcal{Y}_3 - \frac{\xi_1\mathcal{Y}_9}{\sqrt{3}} \right)}{\mathcal{Y}_3} \right] + 2\sqrt{3}g^2|\alpha|^2 \mathcal{R} \left[\frac{\mathcal{Y}_9}{\mathcal{Y}_3} - \sqrt{3} \frac{\mathcal{Y}_{10}}{\mathcal{Y}_2} \right] x + \frac{3\gamma}{4}}{3 \left(\gamma - \frac{2g^2|\alpha|^2}{\sqrt{3}} \mathcal{R} \left[\frac{\mathcal{Y}_9}{\mathcal{Y}_3} + \frac{4\mathcal{Y}_7}{\sqrt{3}\mathcal{Y}_4} + \frac{\sqrt{3}\mathcal{Y}_{10}}{\mathcal{Y}_2} \right] \right)}$$

To aid in substituting the above into our other current variable expressions we make the following abstractions.

$$\mathcal{Y}_{10} \equiv \frac{2\alpha\mathcal{Y}_6\mathcal{Y}_7}{3\mathcal{Y}_4} + \frac{\gamma\mathcal{Y}_1}{\mathcal{Y}_3}, \mathcal{Y}_{11} \equiv \frac{\mathcal{Y}_9}{\mathcal{Y}_3} + \frac{4\mathcal{Y}_7}{\sqrt{3}\mathcal{Y}_4} + \frac{\sqrt{3}\mathcal{Y}_{10}}{\mathcal{Y}_2},$$

$$\mathcal{Y}_{12} \equiv \frac{\mathcal{Y}_6}{\mathcal{Y}_2} + \frac{\mathcal{Y}_5}{2\mathcal{Y}_3} + \frac{2}{\alpha}, \mathcal{Y}_{13} \equiv \mathcal{Y}_{12} \frac{\frac{\alpha}{3} - \frac{\xi_1\alpha^2}{\mathcal{Y}_2}}{\mathcal{Y}_4} + \frac{1 - \frac{\xi_1\mathcal{Y}_1}{\mathcal{Y}_2}}{2} = \left(\frac{\mathcal{Y}_6}{\mathcal{Y}_2} + \frac{\mathcal{Y}_5}{2\mathcal{Y}_3} + \frac{2}{\alpha} \right) \frac{\frac{\alpha}{3} - \frac{\xi_1\alpha^2}{\mathcal{Y}_2}}{\mathcal{Y}_4} + \frac{1 - \frac{\xi_1\mathcal{Y}_1}{\mathcal{Y}_2}}{2},$$

$$\text{and } \mathcal{Y}_{14} \equiv \left(\frac{2\alpha\mathcal{Y}_6}{\mathcal{Y}_2\mathcal{Y}_4} + \frac{\alpha\mathcal{Y}_5 + 4}{\mathcal{Y}_4} \right) \left(1 - \frac{\xi_4 \left(\frac{1}{3} - \frac{\xi_1\alpha}{\mathcal{Y}_2} \right)}{\mathcal{Y}_3} \right) + \frac{\mathcal{Y}_1}{\alpha} + \frac{\xi_4}{\mathcal{Y}_3} \left(\frac{\xi_1\mathcal{Y}_1}{\mathcal{Y}_2} - 1 \right).$$

With the above definitions, we obtain the following expressions, with the appropriate variable eliminations.

$$y = - \frac{g^2|\alpha|^2 \mathcal{R} \left[\frac{8\mathcal{Y}_7}{\mathcal{Y}_4} - \frac{12\mathcal{Y}_{10}}{\mathcal{Y}_2} \right]}{3 \left(\gamma - \frac{2g^2|\alpha|^2}{\sqrt{3}} \mathcal{R}[\mathcal{Y}_{11}] \right)} z - \frac{2\sqrt{3}g \mathcal{R} \left[\frac{\alpha\xi^* \left(\mathcal{Y}_3 - \frac{\xi_1\mathcal{Y}_9}{\sqrt{3}} \right)}{\mathcal{Y}_3} \right] + 2\sqrt{3}g^2|\alpha|^2 \mathcal{R} \left[\frac{\mathcal{Y}_9}{\mathcal{Y}_3} - \sqrt{3} \frac{\mathcal{Y}_{10}}{\mathcal{Y}_2} \right] x + \frac{3\gamma}{4}}{3 \left(\gamma - \frac{2g^2|\alpha|^2}{\sqrt{3}} \mathcal{R}[\mathcal{Y}_{11}] \right)}$$

$$p = \frac{\mathcal{Y}_3 - \frac{\xi_1\mathcal{Y}_9}{\sqrt{3}}}{\mathcal{Y}_3} \xi^* + \mathcal{Y}_7 \frac{4g\alpha^*}{\sqrt{3}\mathcal{Y}_4} z - \frac{\sqrt{3}g\alpha^*\mathcal{Y}_{10}}{\mathcal{Y}_2} (x + 2z) + \frac{g\alpha^*}{\mathcal{Y}_3} \mathcal{Y}_9 x \\ + \frac{g^3\alpha^*|\alpha|^2 \mathcal{R} \left[\frac{8\mathcal{Y}_7}{\mathcal{Y}_4} - \frac{12\mathcal{Y}_{10}}{\mathcal{Y}_2} \right] \left(\frac{\mathcal{Y}_9}{\mathcal{Y}_3} + \frac{4\mathcal{Y}_7}{\sqrt{3}\mathcal{Y}_4} + \frac{\sqrt{3}\mathcal{Y}_{10}}{\mathcal{Y}_2} \right)}{3 \left(\gamma - \frac{2g^2|\alpha|^2}{\sqrt{3}} \mathcal{R} \left[\frac{\mathcal{Y}_9}{\mathcal{Y}_3} + \frac{4\mathcal{Y}_7}{\sqrt{3}\mathcal{Y}_4} + \frac{\sqrt{3}\mathcal{Y}_{10}}{\mathcal{Y}_2} \right] \right)} z$$

$$\begin{aligned}
& + \alpha^* \left(\frac{\mathcal{r}_9}{\mathcal{r}_3} + \frac{4\mathcal{r}_7}{\sqrt{3}\mathcal{r}_4} + \frac{\sqrt{3}\mathcal{r}_{10}}{\mathcal{r}_2} \right) \frac{2\sqrt{3}g^2\mathcal{R} \left[\frac{\alpha^* \left(\mathcal{r}_3 - \frac{\xi_1\mathcal{r}_9}{\sqrt{3}} \right)}{\mathcal{r}_3} \right] + 2\sqrt{3}g^3|\alpha|^2\mathcal{R} \left[\frac{\mathcal{r}_9}{\mathcal{r}_3} - \sqrt{3}\frac{\mathcal{r}_{10}}{\mathcal{r}_2} \right] x + \frac{3g\gamma}{4}}{3 \left(\gamma - \frac{2g^2|\alpha|^2}{\sqrt{3}} \mathcal{R} \left[\frac{\mathcal{r}_9}{\mathcal{r}_3} + \frac{4\mathcal{r}_7}{\sqrt{3}\mathcal{r}_4} + \frac{\sqrt{3}\mathcal{r}_{10}}{\mathcal{r}_2} \right] \right)} \\
q = & \frac{\alpha^*}{\mathcal{r}_4} \left(\frac{\mathcal{r}_6}{\mathcal{r}_2} - \frac{\mathcal{r}_5}{2\mathcal{r}_3} - \frac{2g^2|\alpha|^2\mathcal{R} \left[\frac{\mathcal{r}_9}{\mathcal{r}_3} - \sqrt{3}\frac{\mathcal{r}_{10}}{\mathcal{r}_2} \right] \left(\frac{2}{\alpha} + \frac{\mathcal{r}_6}{\mathcal{r}_2} + \frac{\mathcal{r}_5}{2\mathcal{r}_3} \right)}{3 \left(\gamma - \frac{2g^2|\alpha|^2}{\sqrt{3}} \mathcal{R} \left[\frac{\mathcal{r}_9}{\mathcal{r}_3} + \frac{4\mathcal{r}_7}{\sqrt{3}\mathcal{r}_4} + \frac{\sqrt{3}\mathcal{r}_{10}}{\mathcal{r}_2} \right] \right)} \right) x + \frac{\zeta^*}{6} \frac{\xi_1\mathcal{r}_5}{g\mathcal{r}_3\mathcal{r}_4} \\
& + \frac{2\alpha^*}{\sqrt{3}\mathcal{r}_4} \left(\frac{\mathcal{r}_6}{\mathcal{r}_2} - \frac{1}{\alpha} - \frac{g^2|\alpha|^2 \left(\frac{2}{\alpha} + \frac{\mathcal{r}_6}{\mathcal{r}_2} + \frac{\mathcal{r}_5}{2\mathcal{r}_3} \right) \mathcal{R} \left[\frac{8\mathcal{r}_7}{\mathcal{r}_4} - \frac{12\mathcal{r}_{10}}{\mathcal{r}_2} \right]}{6 \left(\gamma - \frac{2g^2|\alpha|^2}{\sqrt{3}} \mathcal{R} \left[\frac{\mathcal{r}_9}{\mathcal{r}_3} + \frac{4\mathcal{r}_7}{\sqrt{3}\mathcal{r}_4} + \frac{\sqrt{3}\mathcal{r}_{10}}{\mathcal{r}_2} \right] \right)} \right) z \\
& - \frac{\alpha^* \left(\frac{2}{\alpha} + \frac{\mathcal{r}_6}{\mathcal{r}_2} + \frac{\mathcal{r}_5}{2\mathcal{r}_3} \right) \left(2g\mathcal{R} \left[\alpha^* \left(1 - \frac{\xi_1\mathcal{r}_9}{\sqrt{3}\mathcal{r}_3} \right) \right] + \frac{\sqrt{3}\gamma}{4} \right)}{3 \left(\gamma - \frac{2g^2|\alpha|^2}{\sqrt{3}} \mathcal{R} \left[\frac{\mathcal{r}_9}{\mathcal{r}_3} + \frac{4\mathcal{r}_7}{\sqrt{3}\mathcal{r}_4} + \frac{\sqrt{3}\mathcal{r}_{10}}{\mathcal{r}_2} \right] \right) \mathcal{r}_4} \\
r = & \frac{\alpha^*}{\mathcal{r}_3} \left(\mathcal{r}_{13} \frac{g^3|\alpha|^2\mathcal{R} \left[\frac{8\mathcal{r}_7}{\mathcal{r}_4} - \frac{12\mathcal{r}_{10}}{\mathcal{r}_2} \right]}{3 \left(\gamma - \frac{2g^2|\alpha|^2}{\sqrt{3}} \mathcal{R}[\mathcal{r}_{11}] \right)} + 2g \left(\left(1 - \frac{\alpha\mathcal{r}_6}{\mathcal{r}_2} \right) \frac{1 - \frac{3\xi_1\alpha}{\mathcal{r}_2}}{3\mathcal{r}_4} + \frac{\xi_1\mathcal{r}_1}{2\mathcal{r}_2} \right) \right) z \\
& + \frac{2\alpha^*\mathcal{r}_{13} \left(\mathcal{R} \left[\frac{\alpha^* \left(\mathcal{r}_3 - \frac{\xi_1\mathcal{r}_9}{\sqrt{3}} \right)}{\mathcal{r}_3} \right] + \frac{\sqrt{3}\gamma}{8g} \right)}{\sqrt{3} \left(\frac{\gamma}{g^2} - \frac{2|\alpha|^2}{\sqrt{3}} \mathcal{R}[\mathcal{r}_{11}] \right) \mathcal{r}_3} - \frac{\xi_1 \left(1 + \frac{\alpha}{3} \frac{1 - \frac{3\xi_1\alpha}{\mathcal{r}_2}}{\mathcal{r}_3} - \frac{\mathcal{r}_5}{\mathcal{r}_4} \right) \zeta^*}{2\sqrt{3}\mathcal{r}_3} \\
& + \frac{g\alpha^*}{\mathcal{r}_3} \left(\frac{1 + \frac{\xi_1\mathcal{r}_1}{2}}{2} + \left(\frac{\mathcal{r}_5}{2\mathcal{r}_3} - \frac{\mathcal{r}_6}{\mathcal{r}_2} \right) \frac{\alpha - \frac{3\xi_1\alpha^2}{\mathcal{r}_2}}{3\mathcal{r}_4} + \frac{2\mathcal{r}_{13}\mathcal{R} \left[\frac{\mathcal{r}_9}{\mathcal{r}_3} - \sqrt{3}\frac{\mathcal{r}_{10}}{\mathcal{r}_2} \right]}{\sqrt{3} \left(\frac{\gamma}{g^2|\alpha|^2} - \frac{2}{\sqrt{3}} \mathcal{R}[\mathcal{r}_{11}] \right)} \right) x \\
s = & \frac{g\alpha^{*2}}{\mathcal{r}_2} \left(6 \left(2 - \frac{\xi_1\xi_6\mathcal{r}_1}{2\mathcal{r}_3\mathcal{r}_2} \right) + \frac{\mathcal{r}_8\mathcal{r}_6}{\mathcal{r}_1\mathcal{r}_4} \right) z + \frac{\alpha^*\xi_1}{2\mathcal{r}_3} \left(\frac{\sqrt{3}\xi_6}{\mathcal{r}_2} + \frac{1}{\sqrt{3}} \frac{\mathcal{r}_8}{\mathcal{r}_1} \frac{\mathcal{r}_5}{\mathcal{r}_4} \right) \zeta^* \\
& - \frac{g\alpha^{*2}}{\mathcal{r}_1} \frac{2\mathcal{r}_8}{\alpha\mathcal{r}_4} z + g\alpha^{*2} \left(\frac{3 \left(2 - \frac{\xi_1\xi_6\mathcal{r}_1}{2\mathcal{r}_3\mathcal{r}_2} \right) + \frac{\mathcal{r}_8\mathcal{r}_6}{\mathcal{r}_1\mathcal{r}_4}}{\mathcal{r}_2} - \frac{3\xi_6 + \frac{\mathcal{r}_8\mathcal{r}_5}{\mathcal{r}_1\mathcal{r}_4}}{2\mathcal{r}_3} \right) x \\
& + g\alpha^{*2} \left(\frac{3\xi_6}{2\mathcal{r}_3} + \frac{\mathcal{r}_{12}\mathcal{r}_8}{\mathcal{r}_1\mathcal{r}_4} + \frac{3 \left(2 - \frac{\xi_1\xi_6\mathcal{r}_1}{2\mathcal{r}_3\mathcal{r}_2} \right)}{\mathcal{r}_2} \right) \left(- \frac{g^2|\alpha|^2\mathcal{R} \left[\frac{8\mathcal{r}_7}{\mathcal{r}_4} - \frac{12\mathcal{r}_{10}}{\mathcal{r}_2} \right]}{3 \left(\gamma - \frac{2g^2|\alpha|^2}{\sqrt{3}} \mathcal{R}[\mathcal{r}_{11}] \right)} z \right) \\
& - g\alpha^{*2} \left(\frac{3\xi_6}{2\mathcal{r}_3} + \frac{\mathcal{r}_{12}\mathcal{r}_8}{\mathcal{r}_1\mathcal{r}_4} + \frac{3 \left(2 - \frac{\xi_1\xi_6\mathcal{r}_1}{2\mathcal{r}_3\mathcal{r}_2} \right)}{\mathcal{r}_2} \right) \left(\frac{2\sqrt{3}g\mathcal{R} \left[\frac{\alpha^* \left(\mathcal{r}_3 - \frac{\xi_1\mathcal{r}_9}{\sqrt{3}} \right)}{\mathcal{r}_3} \right] + 2\sqrt{3}g^2|\alpha|^2\mathcal{R} \left[\frac{\mathcal{r}_9}{\mathcal{r}_3} - \sqrt{3}\frac{\mathcal{r}_{10}}{\mathcal{r}_2} \right] x + \frac{3\gamma}{4}}{3 \left(\gamma - \frac{2g^2|\alpha|^2}{\sqrt{3}} \mathcal{R}[\mathcal{r}_{11}] \right)} \right) \\
u = & - \frac{2\alpha^*}{\mathcal{r}_2} \left(\sqrt{3}\xi_4 \left(2 - \frac{\xi_6\mathcal{r}_1\xi_1}{2\mathcal{r}_3} \right) + \frac{\xi_6 \left(1 - \alpha \frac{\mathcal{r}_6}{\mathcal{r}_2} \right)}{\sqrt{3}\mathcal{r}_4} \left(3 - \xi_4 \frac{1 - \frac{3\xi_1\alpha}{\mathcal{r}_2}}{\mathcal{r}_3} \right) \right) z \\
& + \frac{\xi_6\xi_1}{2g\mathcal{r}_3\mathcal{r}_2} \left(\left(3 - \xi_4 \frac{1 - \frac{3\xi_1\alpha}{\mathcal{r}_2}}{\mathcal{r}_3} \right) \frac{\alpha}{3} \frac{\mathcal{r}_5}{\mathcal{r}_4} - \xi_4 \right) \zeta^* \\
& + \frac{\alpha^*}{\mathcal{r}_2} \left(\frac{\alpha\xi_6}{\sqrt{3}\mathcal{r}_4} \left(\frac{\mathcal{r}_6}{\mathcal{r}_2} - \frac{\mathcal{r}_5}{2\mathcal{r}_3} \right) \left(3 - \xi_4 \frac{1 - \frac{3\xi_1\alpha}{\mathcal{r}_2}}{\mathcal{r}_3} \right) + \sqrt{3}\xi_4 \left(\frac{\xi_6}{2\mathcal{r}_3} - \left(2 - \frac{\xi_6\mathcal{r}_1\xi_1}{2\mathcal{r}_3} \right) \right) \right) x \\
& - \frac{\alpha^*\xi_6}{\mathcal{r}_2} \left(\frac{\alpha\mathcal{r}_{12}}{\sqrt{3}\mathcal{r}_4} \left(3 - \xi_4 \frac{1 - \frac{3\xi_1\alpha}{\mathcal{r}_2}}{\mathcal{r}_3} \right) - \sqrt{3}\xi_4 \left(\frac{1}{2\mathcal{r}_3} + \frac{2 - \frac{\xi_6\mathcal{r}_1\xi_1}{2\mathcal{r}_3}}{\xi_6} \right) \right) \frac{g^2|\alpha|^2\mathcal{R} \left[\frac{8\mathcal{r}_7}{\mathcal{r}_4} - \frac{12\mathcal{r}_{10}}{\mathcal{r}_2} \right]}{3 \left(\gamma - \frac{2g^2|\alpha|^2}{\sqrt{3}} \mathcal{R}[\mathcal{r}_{11}] \right)} z \\
& - \frac{\alpha^*\xi_6}{\mathcal{r}_2} \left(\frac{\alpha\mathcal{r}_{12}}{\sqrt{3}\mathcal{r}_4} \left(3 - \xi_4 \frac{1 - \frac{3\xi_1\alpha}{\mathcal{r}_2}}{\mathcal{r}_3} \right) - \sqrt{3}\xi_4 \left(\frac{1}{2\mathcal{r}_3} + \frac{2 - \frac{\xi_6\mathcal{r}_1\xi_1}{2\mathcal{r}_3}}{\xi_6} \right) \right) \frac{2\sqrt{3}g^2|\alpha|^2\mathcal{R} \left[\frac{\mathcal{r}_9}{\mathcal{r}_3} - \sqrt{3}\frac{\mathcal{r}_{10}}{\mathcal{r}_2} \right] x}{3 \left(\gamma - \frac{2g^2|\alpha|^2}{\sqrt{3}} \mathcal{R}[\mathcal{r}_{11}] \right)} \\
& - \frac{\alpha^*\xi_6}{\mathcal{r}_2} \left(\frac{\alpha\mathcal{r}_{12}}{\sqrt{3}\mathcal{r}_4} \left(3 - \xi_4 \frac{1 - \frac{3\xi_1\alpha}{\mathcal{r}_2}}{\mathcal{r}_3} \right) - \sqrt{3}\xi_4 \left(\frac{1}{2\mathcal{r}_3} + \frac{2 - \frac{\xi_6\mathcal{r}_1\xi_1}{2\mathcal{r}_3}}{\xi_6} \right) \right) \frac{2\sqrt{3}g\mathcal{R} \left[\frac{\alpha^* \left(\mathcal{r}_3 - \frac{\xi_1\mathcal{r}_9}{\sqrt{3}} \right)}{\mathcal{r}_3} \right] + \frac{3\gamma}{4}}{3 \left(\gamma - \frac{2g^2|\alpha|^2}{\sqrt{3}} \mathcal{R}[\mathcal{r}_{11}] \right)}
\end{aligned}$$

$$\begin{aligned}
v = & \sqrt{3}g\alpha^* \left(\frac{\mathcal{r}_1}{\mathcal{r}_2} \left(1 + \frac{\alpha\xi_1\xi_4}{\mathcal{r}_2\mathcal{r}_3} \right) + \left(1 - \frac{\xi_4 \left(\frac{1}{3} - \frac{\xi_1\alpha}{\mathcal{r}_2} \right)}{\mathcal{r}_3} \right) \frac{2\alpha^2\mathcal{r}_6}{\mathcal{r}_2^2\mathcal{r}_4} \right) (x + 2z) \\
& + \frac{\xi_1}{\mathcal{r}_2} \left(\alpha^2 \left(1 - \frac{\xi_4 \left(\frac{1}{3} - \frac{\xi_1\alpha}{\mathcal{r}_2} \right)}{\mathcal{r}_3} \right) \frac{\mathcal{r}_5}{\mathcal{r}_3\mathcal{r}_4} - \frac{\alpha\xi_4}{\mathcal{r}_3} \right) \zeta^* - \left(1 - \frac{\xi_4 \left(\frac{1}{3} - \frac{\xi_1\alpha}{\mathcal{r}_2} \right)}{\mathcal{r}_3} \right) \frac{12\alpha^*}{\sqrt{3}\mathcal{r}_4} \frac{g\alpha}{\mathcal{r}_2} z \\
& - \left(\frac{6g\alpha^2}{\mathcal{r}_2} \left(1 - \frac{\xi_4 \left(\frac{1}{3} - \frac{\xi_1\alpha}{\mathcal{r}_2} \right)}{\mathcal{r}_3} \right) \frac{\alpha^*\mathcal{r}_5}{2\sqrt{3}\mathcal{r}_3\mathcal{r}_4} - \frac{g\alpha^* \sqrt{3}\alpha\xi_4}{\mathcal{r}_3} \right) x \\
& + \sqrt{3} \frac{g|\alpha|^2}{\mathcal{r}_2} \mathcal{r}_{14} \left(- \frac{g^2|\alpha|^2\mathcal{R} \left[\frac{8\mathcal{r}_7}{\mathcal{r}_4} - \frac{12\mathcal{r}_{10}}{\mathcal{r}_2} \right]}{3 \left(\gamma - \frac{2g^2|\alpha|^2}{\sqrt{3}} \mathcal{R}[\mathcal{r}_{11}] \right)} z \right) \\
& + \sqrt{3} \frac{g|\alpha|^2}{\mathcal{r}_2} \mathcal{r}_{14} \left(- \frac{2\sqrt{3}g\mathcal{R} \left[\frac{\alpha^* \left(\mathcal{r}_3 - \frac{\xi_1\mathcal{r}_9}{\sqrt{3}} \right)}{\mathcal{r}_3} \right] + 2\sqrt{3}g^2|\alpha|^2\mathcal{R} \left[\frac{\mathcal{r}_9}{\mathcal{r}_3} - \sqrt{3} \frac{\mathcal{r}_{10}}{\mathcal{r}_2} \right] x + \frac{3\gamma}{4}}{3 \left(\gamma - \frac{2g^2|\alpha|^2}{\sqrt{3}} \mathcal{R}[\mathcal{r}_{11}] \right)} \right)
\end{aligned}$$

C.7 Solve Eqn C.3 for x

$$0 = g(2\mathcal{R}[2r\alpha - \sqrt{3}p\alpha]) + \gamma(4z - 3y + \frac{1}{4})$$

It is useful to simplify the expression $2r - \sqrt{3}p$ before dealing with the whole thing

Recall that

$$\begin{aligned}
r = & \frac{\alpha^*}{\mathcal{r}_3} \left(\mathcal{r}_{13} \frac{g^3|\alpha|^2\mathcal{R} \left[\frac{8\mathcal{r}_7}{\mathcal{r}_4} - \frac{12\mathcal{r}_{10}}{\mathcal{r}_2} \right]}{3 \left(\gamma - \frac{2g^2|\alpha|^2}{\sqrt{3}} \mathcal{R}[\mathcal{r}_{11}] \right)} + 2g \left(\left(1 - \frac{\alpha\mathcal{r}_6}{\mathcal{r}_2} \right) \frac{1 - \frac{3\xi_1\alpha}{\mathcal{r}_2}}{3\mathcal{r}_4} + \frac{\xi_1\mathcal{r}_1}{2\mathcal{r}_2} \right) \right) z \\
& + \frac{2\alpha^*\mathcal{r}_{13} \left(\mathcal{R} \left[\frac{\alpha^* \left(\mathcal{r}_3 - \frac{\xi_1\mathcal{r}_9}{\sqrt{3}} \right)}{\mathcal{r}_3} \right] + \frac{\sqrt{3}\gamma}{8g} \right)}{\sqrt{3} \left(\frac{\gamma}{g^2} - \frac{2|\alpha|^2}{\sqrt{3}} \mathcal{R}[\mathcal{r}_{11}] \right) \mathcal{r}_3} - \frac{\xi_1 \left(1 + \frac{\alpha}{3} - \frac{1 - \frac{3\xi_1\alpha}{\mathcal{r}_2}}{\mathcal{r}_3} \frac{\mathcal{r}_5}{\mathcal{r}_4} \right) \zeta^*}{2\sqrt{3}\mathcal{r}_3} \\
& + \frac{g\alpha^*}{\mathcal{r}_3} \left(\frac{1 + \frac{\xi_1\mathcal{r}_1}{\mathcal{r}_2}}{2} + \left(\frac{\mathcal{r}_5}{2\mathcal{r}_3} - \frac{\mathcal{r}_6}{\mathcal{r}_2} \right) \frac{\alpha - \frac{3\xi_1\alpha^2}{\mathcal{r}_2}}{3\mathcal{r}_4} + \frac{2\mathcal{r}_{13}\mathcal{R} \left[\frac{\mathcal{r}_9}{\mathcal{r}_3} - \sqrt{3} \frac{\mathcal{r}_{10}}{\mathcal{r}_2} \right]}{\sqrt{3} \left(\frac{\gamma}{g^2|\alpha|^2} - \frac{2}{\sqrt{3}} \mathcal{R}[\mathcal{r}_{11}] \right)} \right) x
\end{aligned}$$

and

$$\begin{aligned}
p = & \frac{\mathcal{r}_3 - \frac{\xi_1\mathcal{r}_9}{\sqrt{3}}}{\mathcal{r}_3} \zeta^* + \mathcal{r}_7 \frac{4g\alpha^*}{\sqrt{3}\mathcal{r}_4} z - \frac{\sqrt{3}g\alpha^*\mathcal{r}_{10}}{\mathcal{r}_2} (x + 2z) + \frac{g\alpha^*}{\mathcal{r}_3} \mathcal{r}_9 x \\
& + \frac{g^3\alpha^*|\alpha|^2\mathcal{R} \left[\frac{8\mathcal{r}_7}{\mathcal{r}_4} - \frac{12\mathcal{r}_{10}}{\mathcal{r}_2} \right] \left(\frac{\mathcal{r}_9}{\mathcal{r}_3} + \frac{4\mathcal{r}_7}{\sqrt{3}\mathcal{r}_4} + \frac{\sqrt{3}\mathcal{r}_{10}}{\mathcal{r}_2} \right)}{3 \left(\gamma - \frac{2g^2|\alpha|^2}{\sqrt{3}} \mathcal{R} \left[\frac{\mathcal{r}_9}{\mathcal{r}_3} + \frac{4\mathcal{r}_7}{\sqrt{3}\mathcal{r}_4} + \frac{\sqrt{3}\mathcal{r}_{10}}{\mathcal{r}_2} \right] \right)} z \\
& + \alpha^* \left(\frac{\mathcal{r}_9}{\mathcal{r}_3} + \frac{4\mathcal{r}_7}{\sqrt{3}\mathcal{r}_4} + \frac{\sqrt{3}\mathcal{r}_{10}}{\mathcal{r}_2} \right) \frac{2\sqrt{3}g^2\mathcal{R} \left[\frac{\alpha^* \left(\mathcal{r}_3 - \frac{\xi_1\mathcal{r}_9}{\sqrt{3}} \right)}{\mathcal{r}_3} \right] + 2\sqrt{3}g^3|\alpha|^2\mathcal{R} \left[\frac{\mathcal{r}_9}{\mathcal{r}_3} - \sqrt{3} \frac{\mathcal{r}_{10}}{\mathcal{r}_2} \right] x + \frac{3g\gamma}{4}}{3 \left(\gamma - \frac{2g^2|\alpha|^2}{\sqrt{3}} \mathcal{R} \left[\frac{\mathcal{r}_9}{\mathcal{r}_3} + \frac{4\mathcal{r}_7}{\sqrt{3}\mathcal{r}_4} + \frac{\sqrt{3}\mathcal{r}_{10}}{\mathcal{r}_2} \right] \right)}
\end{aligned}$$

We then collect all x terms in the p expression and simplify

$$\begin{aligned}
p = & g\alpha^* \left(\frac{\mathcal{r}_9}{\mathcal{r}_3} - \frac{\sqrt{3}\mathcal{r}_{10}}{\mathcal{r}_2} + \mathcal{r}_{11} \frac{2g^2\mathcal{R} \left[\frac{\mathcal{r}_9}{\mathcal{r}_3} - \sqrt{3} \frac{\mathcal{r}_{10}}{\mathcal{r}_2} \right]}{\sqrt{3} \left(\frac{\gamma}{|\alpha|^2} - \frac{2g^2}{\sqrt{3}} \mathcal{R}[\mathcal{r}_{11}] \right)} \right) x \\
& + g\alpha^* \left(\frac{g^2\mathcal{R} \left[\frac{8\mathcal{r}_7}{\mathcal{r}_4} - \frac{12\mathcal{r}_{10}}{\mathcal{r}_2} \right] \mathcal{r}_{11}}{3 \left(\frac{\gamma}{|\alpha|^2} - \frac{2g^2}{\sqrt{3}} \mathcal{R}[\mathcal{r}_{11}] \right)} - \frac{2\sqrt{3}\mathcal{r}_{10}}{\mathcal{r}_2} + \mathcal{r}_7 \frac{4}{\sqrt{3}\mathcal{r}_4} \right) z
\end{aligned}$$

$$+g\alpha^*\mathcal{Y}_{11}\frac{2\sqrt{3}g\mathcal{R}\left[\frac{\alpha^*\left(r_3-\frac{\xi_1\mathcal{Y}_9}{\sqrt{3}}\right)}{r_3}\right]+\frac{3\gamma}{4}}{3\left(\frac{\gamma}{|\alpha|^2}-\frac{2g^2}{\sqrt{3}}\mathcal{R}[\mathcal{Y}_{11}]\right)}+\frac{r_3-\frac{\xi_1\mathcal{Y}_9}{\sqrt{3}}}{r_3}\zeta^*$$

Now let us consider $2\alpha(2r-\sqrt{3}p)$. Using the expressions we have for r and p , it can be

shown that

$$\begin{aligned} & 2\alpha(2r-\sqrt{3}p) \\ &= 2g|\alpha|^2\left(\frac{1+\frac{\xi_1\mathcal{Y}_1}{\mathcal{Y}_2}}{r_3}+\left(\frac{r_5}{r_3}-\frac{2r_6}{r_2}\right)\frac{\alpha-\frac{3\xi_1\alpha^2}{r_2}}{3r_3r_4}+\frac{2\left(\frac{2r_{13}}{r_3}-\sqrt{3}\mathcal{Y}_{11}\right)\mathcal{R}\left[\frac{r_9}{r_3}-\sqrt{3}\frac{r_{10}}{r_2}\right]}{\sqrt{3}\left(\frac{\gamma}{g^2|\alpha|^2}-\frac{2}{\sqrt{3}}\mathcal{R}[\mathcal{Y}_{11}]\right)}-\frac{\sqrt{3}r_9}{r_3}+\frac{3r_{10}}{r_2}\right)x \\ &+4|\alpha|^2\left(\frac{\left(\frac{r_{13}}{r_3}-\frac{\sqrt{3}}{2}\mathcal{Y}_{11}\right)g^3\mathcal{R}\left[\frac{8r_7}{r_4}-\frac{12r_{10}}{r_2}\right]}{3\left(\frac{\gamma}{|\alpha|^2}-\frac{2g^2}{\sqrt{3}}\mathcal{R}[\mathcal{Y}_{11}]\right)}+\left(\frac{2g}{r_3}\left(\left(1-\frac{\alpha r_6}{r_2}\right)\frac{1-\frac{3\xi_1\alpha}{r_2}}{3r_4}+\frac{\xi_1 r_1}{2r_2}\right)+g\left(\frac{3r_{10}}{r_2}-\frac{2r_7}{r_4}\right)\right)\right)z \\ &+g\left(\frac{2r_{13}}{r_3}-\sqrt{3}\mathcal{Y}_{11}\right)\frac{4\sqrt{3}g\mathcal{R}\left[\frac{\alpha^*\left(r_3-\frac{\xi_1\mathcal{Y}_9}{\sqrt{3}}\right)}{r_3}\right]+\frac{3\gamma}{2}}{3\left(\frac{\gamma}{|\alpha|^2}-\frac{2g^2}{\sqrt{3}}\mathcal{R}[\mathcal{Y}_{11}]\right)}-2\alpha\left(\frac{\xi_1\left(1+\frac{r_5}{3}-\frac{\alpha-\frac{3\xi_1\alpha^2}{r_2}}{r_3r_4}\right)}{\sqrt{3}r_3}+\sqrt{3}\frac{r_3-\frac{\xi_1\mathcal{Y}_9}{\sqrt{3}}}{r_3}\right)\zeta^* \end{aligned}$$

Recall that $0 = g(2\mathcal{R}[2r\alpha - \sqrt{3}p\alpha]) + \gamma(4z - 3y + \frac{1}{4})$. Note that both z and y are real

anyway, so we can just take the real part after we combine some terms in the expanded expression.

$$\begin{aligned} & 2\alpha(2r-\sqrt{3}p)+\frac{\gamma}{g}(4z-3y+\frac{1}{4})=\frac{\gamma}{g}(4z-3y+\frac{1}{4}) \\ &+2g|\alpha|^2\left(\frac{1+\frac{\xi_1\mathcal{Y}_1}{\mathcal{Y}_2}}{r_3}+\frac{\left(\frac{r_5}{r_3}-\frac{2r_6}{r_2}\right)\left(\alpha-\frac{3\xi_1\alpha^2}{r_2}\right)}{3r_3r_4}+\frac{2\left(\frac{2r_{13}}{r_3}-\sqrt{3}\mathcal{Y}_{11}\right)\mathcal{R}\left[\frac{r_9}{r_3}-\sqrt{3}\frac{r_{10}}{r_2}\right]}{\sqrt{3}\left(\frac{\gamma}{g^2|\alpha|^2}-\frac{2}{\sqrt{3}}\mathcal{R}[\mathcal{Y}_{11}]\right)}-\frac{\sqrt{3}r_9}{r_3}+\frac{3r_{10}}{r_2}\right)x \\ &+4|\alpha|^2\left(\frac{\left(\frac{r_{13}}{r_3}-\frac{\sqrt{3}}{2}\mathcal{Y}_{11}\right)g^3\mathcal{R}\left[\frac{8r_7}{r_4}-\frac{12r_{10}}{r_2}\right]}{3\left(\frac{\gamma}{|\alpha|^2}-\frac{2g^2}{\sqrt{3}}\mathcal{R}[\mathcal{Y}_{11}]\right)}+g\left(\frac{2\left(\left(1-\frac{\alpha r_6}{r_2}\right)\frac{1-\frac{3\xi_1\alpha}{r_2}}{3r_4}+\frac{\xi_1 r_1}{2r_2}\right)}{r_3}+\frac{3r_{10}}{r_2}-\frac{2r_7}{r_4}\right)\right)z \\ &+g\frac{\left(\frac{2r_{13}}{r_3}-\sqrt{3}\mathcal{Y}_{11}\right)\left(4\sqrt{3}g\mathcal{R}\left[\frac{\alpha^*\left(r_3-\frac{\xi_1\mathcal{Y}_9}{\sqrt{3}}\right)}{r_3}\right]+\frac{3\gamma}{2}\right)}{3\left(\frac{\gamma}{|\alpha|^2}-\frac{2g^2}{\sqrt{3}}\mathcal{R}[\mathcal{Y}_{11}]\right)}-2\alpha\left(\frac{\xi_1\left(1+\frac{r_5}{3}-\frac{\alpha-\frac{3\xi_1\alpha^2}{r_2}}{r_3r_4}\right)}{\sqrt{3}r_3}+\sqrt{3}\frac{r_3-\frac{\xi_1\mathcal{Y}_9}{\sqrt{3}}}{r_3}\right)\zeta^* \end{aligned}$$

Now we substitute the y expression into the above.

$$\begin{aligned} & 2\alpha(2r-\sqrt{3}p)+\frac{\gamma}{g}(4z-3y+\frac{1}{4}) \\ &= 2g|\alpha|^2\left(\frac{1+\frac{\xi_1\mathcal{Y}_1}{\mathcal{Y}_2}-\sqrt{3}r_9}{r_3}+\frac{\left(\frac{r_5}{r_3}-\frac{2r_6}{r_2}\right)\left(\alpha-\frac{3\xi_1\alpha^2}{r_2}\right)}{3r_3r_4}+\frac{2\left(\frac{2r_{13}}{r_3}-\sqrt{3}\mathcal{Y}_{11}\right)\mathcal{R}\left[\frac{r_9}{r_3}-\sqrt{3}\frac{r_{10}}{r_2}\right]}{\sqrt{3}\left(\frac{\gamma}{g^2|\alpha|^2}-\frac{2}{\sqrt{3}}\mathcal{R}[\mathcal{Y}_{11}]\right)}+\frac{3r_{10}}{r_2}\right)x \\ &+4|\alpha|^2\left(\frac{\left(\frac{r_{13}}{r_3}-\frac{\sqrt{3}}{2}\mathcal{Y}_{11}\right)g^3\mathcal{R}\left[\frac{8r_7}{r_4}-\frac{12r_{10}}{r_2}\right]}{3\left(\frac{\gamma}{|\alpha|^2}-\frac{2g^2}{\sqrt{3}}\mathcal{R}[\mathcal{Y}_{11}]\right)}+g\left(\frac{2\left(\left(1-\frac{\alpha r_6}{r_2}\right)\frac{1-\frac{3\xi_1\alpha}{r_2}}{3r_4}+\frac{\xi_1 r_1}{2r_2}\right)}{r_3}+\frac{3r_{10}}{r_2}-\frac{2r_7}{r_4}\right)\right)z \\ &+g\frac{\left(\frac{2r_{13}}{r_3}-\sqrt{3}\mathcal{Y}_{11}\right)\left(4\sqrt{3}g\mathcal{R}\left[\frac{\alpha^*\left(r_3-\frac{\xi_1\mathcal{Y}_9}{\sqrt{3}}\right)}{r_3}\right]+\frac{3\gamma}{2}\right)}{3\left(\frac{\gamma}{|\alpha|^2}-\frac{2g^2}{\sqrt{3}}\mathcal{R}[\mathcal{Y}_{11}]\right)}-2\alpha\left(\frac{\xi_1\left(1+\frac{r_5}{3}-\frac{\alpha-\frac{3\xi_1\alpha^2}{r_2}}{r_3r_4}\right)}{\sqrt{3}r_3}+\sqrt{3}\frac{r_3-\frac{\xi_1\mathcal{Y}_9}{\sqrt{3}}}{r_3}\right)\zeta^* \end{aligned}$$

$$+ \frac{\gamma \left(4z + 3 \left(\frac{g^2 |\alpha|^2 \mathcal{R} \left[\frac{8\mathcal{Y}_7}{\mathcal{Y}_4} - \frac{12\mathcal{Y}_{10}}{\mathcal{Y}_2} \right]}{3 \left(\gamma - \frac{2g^2 |\alpha|^2}{\sqrt{3}} \mathcal{R}[\mathcal{Y}_{11}] \right)} z + \frac{2\sqrt{3}g\mathcal{R} \left[\frac{\alpha \varsigma^* \left(\mathcal{Y}_3 - \frac{\xi_1 \mathcal{Y}_9}{\sqrt{3}} \right)}{\mathcal{Y}_3} \right] + 2\sqrt{3}g^2 |\alpha|^2 \mathcal{R} \left[\frac{\mathcal{Y}_9}{\mathcal{Y}_3} - \sqrt{3} \frac{\mathcal{Y}_{10}}{\mathcal{Y}_2} \right] x + \frac{3\gamma}{4} \right)}{3 \left(\gamma - \frac{2g^2 |\alpha|^2}{\sqrt{3}} \mathcal{R}[\mathcal{Y}_{11}] \right)} + \frac{1}{4} \right)}{g}$$

Let us define the following

$$\mathcal{Y}_{15} \equiv \frac{g^2 |\alpha|^2 \mathcal{R} \left[\frac{8\mathcal{Y}_7}{\mathcal{Y}_4} - \frac{12\mathcal{Y}_{10}}{\mathcal{Y}_2} \right]}{3 \left(\gamma - \frac{2g^2 |\alpha|^2}{\sqrt{3}} \mathcal{R}[\mathcal{Y}_{11}] \right)}, \mathcal{Y}_{16} \equiv \frac{\mathcal{R} \left[\frac{\mathcal{Y}_9}{\mathcal{Y}_3} - \sqrt{3} \frac{\mathcal{Y}_{10}}{\mathcal{Y}_2} \right]}{\sqrt{3} \left(\frac{\gamma}{g^2 |\alpha|^2} - \frac{2}{\sqrt{3}} \mathcal{R}[\mathcal{Y}_{11}] \right)}, \mathcal{Y}_{17} \equiv \frac{2\sqrt{3}g\mathcal{R} \left[\frac{\alpha \varsigma^* \left(\mathcal{Y}_3 - \frac{\xi_1 \mathcal{Y}_9}{\sqrt{3}} \right)}{\mathcal{Y}_3} \right] + \frac{3\gamma}{4}}{3 \left(\gamma - \frac{2g^2 |\alpha|^2}{\sqrt{3}} \mathcal{R}[\mathcal{Y}_{11}] \right)}, \text{ and}$$

$$\chi_1 \equiv \mathcal{R} \left[\frac{1 + \frac{\xi_1 \mathcal{Y}_1}{\mathcal{Y}_2}}{\mathcal{Y}_3} + \left(\frac{\mathcal{Y}_5}{\mathcal{Y}_3} - \frac{2\mathcal{Y}_6}{\mathcal{Y}_2} \right) \frac{\alpha - \frac{3\xi_1 \alpha^2}{\mathcal{Y}_2}}{3\mathcal{Y}_3 \mathcal{Y}_4} + 2 \left(\frac{2\mathcal{Y}_{13}}{\mathcal{Y}_3} - \sqrt{3}\mathcal{Y}_{11} \right) \mathcal{Y}_{16} + \frac{3\mathcal{Y}_{10}}{\mathcal{Y}_2} - \frac{\sqrt{3}\mathcal{Y}_9}{\mathcal{Y}_3} \right] + \frac{6\gamma\mathcal{Y}_{16}}{2g^2 |\alpha|^2}$$

Next we substitute the above abstractions into the equation of motion and solve for x

$$x = \frac{2\mathcal{R} \left[\left(\frac{\mathcal{Y}_{13}}{\mathcal{Y}_3} - \frac{\sqrt{3}}{2} \mathcal{Y}_{11} \right) \mathcal{Y}_{15} + \frac{2 \left(\left(1 - \frac{\alpha \mathcal{Y}_6}{\mathcal{Y}_2} \right) \frac{1 - \frac{3\xi_1 \alpha}{\mathcal{Y}_2}}{3\mathcal{Y}_4} + \frac{\xi_1 \mathcal{Y}_1}{2\mathcal{Y}_2} \right)}{\mathcal{Y}_3} + \frac{3\mathcal{Y}_{10}}{\mathcal{Y}_2} - \frac{2\mathcal{Y}_7}{\mathcal{Y}_4} \right]}{\chi_1} z - \frac{\gamma(4z + 3(\mathcal{Y}_{15}z + \mathcal{Y}_{17}) + \frac{1}{4})}{2g^2 |\alpha|^2 \chi_1}$$

$$- \frac{\mathcal{R} \left[\left(\frac{2\mathcal{Y}_{13}}{\mathcal{Y}_3} - \sqrt{3}\mathcal{Y}_{11} \right) \mathcal{Y}_{17} - \frac{\xi_1 \left(1 + \frac{\mathcal{Y}_5}{3} \frac{\alpha - \frac{3\xi_1 \alpha^2}{\mathcal{Y}_2}}{\mathcal{Y}_3 \mathcal{Y}_4} \right) + 3(\mathcal{Y}_3 - \xi_1 \mathcal{Y}_9 / \sqrt{3})}{\sqrt{3}g\alpha^* \mathcal{Y}_3} \varsigma^* \right]}{\chi_1}$$

We further define the following two abstractions prior to updating the rest of our variable expressions

$$\chi_2 \equiv \frac{\gamma(4 + 3\mathcal{Y}_{15})}{2g^2 |\alpha|^2} + 2\mathcal{R} \left[\left(\frac{\mathcal{Y}_{13}}{\mathcal{Y}_3} - \frac{\sqrt{3}}{2} \mathcal{Y}_{11} \right) \mathcal{Y}_{15} + \frac{2 \left(\left(1 - \frac{\alpha \mathcal{Y}_6}{\mathcal{Y}_2} \right) \frac{1 - \frac{3\xi_1 \alpha}{\mathcal{Y}_2}}{3\mathcal{Y}_4} + \frac{\xi_1 \mathcal{Y}_1}{2\mathcal{Y}_2} \right)}{\mathcal{Y}_3} + \frac{3\mathcal{Y}_{10}}{\mathcal{Y}_2} - \frac{2\mathcal{Y}_7}{\mathcal{Y}_4} \right]$$

$$\chi_3 \equiv \mathcal{R} \left[\left(\frac{2\mathcal{Y}_{13}}{\mathcal{Y}_3} - \sqrt{3}\mathcal{Y}_{11} \right) \mathcal{Y}_{17} - \frac{\xi_1 \left(1 + \frac{\mathcal{Y}_5}{3} \frac{\alpha - \frac{3\xi_1 \alpha^2}{\mathcal{Y}_2}}{\mathcal{Y}_3 \mathcal{Y}_4} \right) + 3(\mathcal{Y}_3 - \xi_1 \mathcal{Y}_9 / \sqrt{3})}{\sqrt{3}g\alpha^* \mathcal{Y}_3} \varsigma^* \right]$$

$$x = -\frac{\chi_2}{\chi_1} z - \frac{\gamma(3\mathcal{Y}_{17} + \frac{1}{4})}{2g^2 |\alpha|^2 \chi_1}$$

$$y = \frac{2\mathcal{R} \left[\left(\frac{2\mathcal{Y}_{13}}{\mathcal{Y}_3} - \sqrt{3}\mathcal{Y}_{11} \right) \mathcal{Y}_{17} - \frac{\xi_1 \left(1 + \frac{\mathcal{Y}_5}{3} \frac{\alpha - \frac{3\xi_1 \alpha^2}{\mathcal{Y}_2}}{\mathcal{Y}_3 \mathcal{Y}_4} \right) + 3(\mathcal{Y}_3 - \xi_1 \mathcal{Y}_9 / \sqrt{3})}{\sqrt{3}g\alpha^* \mathcal{Y}_3} \varsigma^* \right] + \frac{\gamma(4z + 3\mathcal{Y}_{17} + \frac{1}{4})}{g^2 |\alpha|^2}}{\chi_1 / \mathcal{Y}_{16}}$$

$$\begin{aligned}
& + \left(\frac{4\mathcal{R} \left[\left(\frac{r_{13}}{r_3} - \frac{\sqrt{3}}{2} r_{11} \right) r_{15} + \frac{2 \left(\left(1 - \frac{\alpha r_6}{r_2} \right)^{\frac{1-3\xi_1\alpha}{r_2}} - \frac{\xi_1 r_1}{3r_4} + \frac{\xi_1 r_1}{2r_2} \right)}{r_3} + \frac{3r_{10}}{r_2} - \frac{2r_7}{r_4} \right] + \frac{3\gamma r_{15}}{g^2 |\alpha|^2}}{\chi_1 / r_{16}} - \gamma_{15} \right) z - \gamma_{17} \\
p &= \frac{r_3 - \frac{\xi_1 r_9}{\sqrt{3}}}{r_3} \varsigma^* + g\alpha^* \left(\gamma_{15} \gamma_{11} + \frac{4r_7}{\sqrt{3}r_4} - 2\frac{\sqrt{3}r_{10}}{r_2} \right) z + g\alpha^* r_{11} r_{17} \\
& - g\alpha^* \left(\frac{r_9}{r_3} - \frac{\sqrt{3}r_{10}}{r_2} + 2\gamma_{11} r_{16} \right) \frac{\chi_2}{\chi_1} z \\
& - g\alpha^* \left(\frac{r_9}{r_3} - \frac{\sqrt{3}r_{10}}{r_2} + 2\gamma_{11} r_{16} \right) \frac{\chi_3 + \frac{\gamma(3r_{17} + \frac{1}{4})}{2g^2 |\alpha|^2}}{\chi_1} \\
q &= -\frac{\alpha^*}{r_4} \left(\frac{r_6 - \frac{r_5}{\sqrt{3}}}{\sqrt{3}} - \frac{2}{\sqrt{3}} r_{12} r_{16} \right) \left(\frac{\chi_2}{\chi_1} z + \frac{\chi_3 + \frac{\gamma(3r_{17} + \frac{1}{4})}{2g^2 |\alpha|^2}}{\chi_1} \right) + \frac{\varsigma^*}{6} \frac{\xi_1 r_5}{g r_3 r_4} \\
& + \frac{2\alpha^*}{\sqrt{3}r_4} \left(\frac{r_6}{r_2} - \frac{1}{\alpha} - \frac{r_{12}}{2} r_{15} \right) z - \alpha^* \frac{r_{12}}{\sqrt{3}r_4} r_{17} \\
r &= g\frac{\alpha^*}{r_3} \left(\gamma_{13} \gamma_{15} + 2 \left(1 - \frac{\alpha r_6}{r_2} \right)^{\frac{1-3\xi_1\alpha}{r_2}} - \frac{\xi_1 r_1}{r_2} \right) z + g\frac{\alpha^* r_{13}}{r_3} r_{17} - \frac{\xi_1 \left(1 + \frac{\alpha}{3} \frac{1-3\xi_1\alpha}{r_3} \frac{r_5}{r_4} \right) \varsigma^*}{2\sqrt{3}r_3} \\
& - \frac{g\alpha^*}{r_3} \left(\frac{1 + \frac{\xi_1 r_1}{r_2}}{2} + \left(\frac{r_5}{2r_3} - \frac{r_6}{r_2} \right)^{\frac{\alpha - 3\xi_1\alpha^2}{r_2}} + 2\gamma_{13} r_{16} \right) \left(\frac{\chi_2}{\chi_1} z + \frac{\chi_3 + \frac{\gamma(3r_{17} + \frac{1}{4})}{2g^2 |\alpha|^2}}{\chi_1} \right) \\
s &= \frac{g\alpha^{*2}}{r_2} \left(3 \left(2 - \frac{\xi_1 \xi_6 r_1}{2r_3 r_2} \right) + \frac{r_8 r_6}{r_1 r_4} \right) 2z + \frac{\alpha^* \xi_1}{2r_3} \left(\frac{\sqrt{3}\xi_6}{r_2} + \frac{1}{\sqrt{3}} \frac{r_8}{r_1} \frac{r_5}{r_4} \right) \varsigma^* \\
& - g\alpha^{*2} \left(\gamma_{18} \frac{\chi_3 + \frac{\gamma(3r_{17} + \frac{1}{4})}{2g^2 |\alpha|^2}}{\chi_1} + \left(\frac{3\xi_6}{r_2} + \frac{r_{12} r_8}{r_1 r_4} + 3 \frac{2 - \frac{\xi_1 \xi_6 r_1}{2r_3 r_2}}{r_2} \right) r_{17} \right) \\
& - g\alpha^{*2} \left(\gamma_{18} \frac{\chi_2}{\chi_1} + \left(\frac{3\xi_6}{2r_3} + \frac{r_{12} r_8}{r_1 r_4} + \frac{3 \left(2 - \frac{\xi_1 \xi_6 r_1}{2r_3 r_2} \right)}{r_2} \right) r_{15} + \frac{2r_8}{\alpha r_1 r_4} \right) z \\
u &= \frac{2\alpha^* \left(-\sqrt{3}\xi_4 \left(2 - \frac{\xi_6 r_1}{2r_3} \right) - \xi_6 \left(\frac{1 - \alpha r_6}{r_4} + \frac{1}{2} \frac{\alpha r_{12}}{r_4} r_{15} \right)^{\frac{1-3\xi_1\alpha}{r_2}} - \frac{3 - \xi_4}{\sqrt{3}} \frac{1 - \frac{3\xi_1\alpha}{r_2}}{r_3} + \frac{\sqrt{3}\xi_4 \xi_6}{2} \left(\frac{1}{2r_3} + \frac{2 - \frac{r_2}{2r_3}}{\xi_6} \right) r_{15} \right)}{r_2} z \\
& - \frac{\alpha \frac{r_6 - \frac{r_5}{\sqrt{3}} - 2r_{12} r_{16}}{r_4} \frac{3 - \xi_4}{\sqrt{3}} \frac{1 - \frac{3\xi_1\alpha}{r_2}}{r_3} + \sqrt{3}\xi_4 \left(\frac{1}{r_3} + (2r_{16} - 1) \left(\frac{1}{2r_3} + \frac{2 - \frac{r_2}{2r_3}}{\xi_6} \right) \right)}{r_2} \frac{\xi_6 r_1 \xi_1}{\xi_6}}{\chi_1} \frac{\chi_2 z + \chi_3 + \frac{\gamma(3r_{17} + \frac{1}{4})}{2g^2 |\alpha|^2}}{\chi_1} \\
& - \alpha^* \xi_6 \\
& + \frac{\xi_6 \xi_1 \left(\frac{3 - \xi_4}{\sqrt{3}} \frac{1 - \frac{3\xi_1\alpha}{r_2}}{r_3} - \frac{\alpha}{\sqrt{3}} \frac{r_5}{r_4} - \xi_4 \right) \varsigma^*}{2g r_3 r_2} - \frac{\alpha^* \xi_6}{r_2} \left(\frac{\alpha r_{12}}{r_4} \frac{3 - \xi_4}{\sqrt{3}} \frac{1 - \frac{3\xi_1\alpha}{r_2}}{r_3} - \sqrt{3}\xi_4 \left(\frac{1}{2r_3} + \frac{2 - \frac{r_2}{2r_3}}{\xi_6} \right) \right) r_{17} \\
v &= \frac{\xi_1 g |\alpha|^2}{r_2} \left(\frac{\alpha r_5 \frac{1 - \xi_4}{r_4} \frac{\frac{1}{3} - \frac{\xi_1 \alpha}{r_2}}{r_3} - \xi_4}{r_3} \frac{\varsigma^*}{g\alpha^*} - \frac{\sqrt{3} r_{14} r_{17}}{\xi_1} \right)
\end{aligned}$$

$$\begin{aligned}
& -\frac{\sqrt{3}g|\alpha|^2}{\mathcal{r}_2} \left(\mathcal{r}_1 \frac{1+\frac{\alpha\xi_1\xi_4}{\mathcal{r}_2\mathcal{r}_3}}{\alpha} + \frac{1-\xi_4}{\mathcal{r}_4} \frac{\frac{1}{3}-\frac{\xi_1\alpha}{\mathcal{r}_2}}{\mathcal{r}_3} \left(\frac{2\alpha\mathcal{r}_6}{\mathcal{r}_2} - \frac{\alpha\mathcal{r}_5}{\mathcal{r}_3} \right) + \frac{\xi_4}{\mathcal{r}_3} - 2\mathcal{r}_{14}\mathcal{r}_{16} \right) \frac{\chi_3 + \frac{\gamma(3\mathcal{r}_{17} + \frac{1}{4})}{2g^2|\alpha|^2}}{\chi_1} \\
& + \sqrt{3}g|\alpha|^2 \frac{\left(2 - \frac{\chi_2}{\chi_1} \right) \mathcal{r}_1 \frac{1+\frac{\alpha\xi_1\xi_4}{\mathcal{r}_2\mathcal{r}_3}}{\alpha} + \left(\frac{2\alpha\mathcal{r}_6(2-\frac{\chi_2}{\chi_1})}{\mathcal{r}_2} - 4 + \frac{\alpha\mathcal{r}_5\chi_2}{\mathcal{r}_3\chi_1} \right) \frac{1-\xi_4}{\mathcal{r}_4} \frac{\frac{1}{3}-\frac{\xi_1\alpha}{\mathcal{r}_2}}{\mathcal{r}_3} + \left(2\mathcal{r}_{16}\frac{\chi_2}{\chi_1} - \mathcal{r}_{15} \right) \mathcal{r}_{14} - \frac{\xi_4\chi_2}{\mathcal{r}_3\chi_1}}{\mathcal{r}_2} z
\end{aligned}$$

C.8 Solve Eqn C.4 for z

$$0 = 2g \left(\sqrt{3}\mathcal{R}[v\alpha] - 2\mathcal{R}[r\alpha] \right) + \gamma \left(3 \left(\frac{1}{4} - x - y \right) - 1 - 7z \right)$$

We can simplify our expanded expressions for x and y .

Using the abstraction functions χ_2 and χ_3 , we find the following expression for $x + y$

$$x + y = (2\mathcal{r}_{16} - 1) \frac{\chi_3 + \frac{\gamma(3\mathcal{r}_{17} + \frac{1}{4})}{2g^2|\alpha|^2}}{\chi_1} - \mathcal{r}_{17} + \left(\frac{2\chi_2}{\chi_1/\mathcal{r}_{16}} - \mathcal{r}_{15} - \frac{\chi_2}{\chi_1} \right) z$$

Now let us define the following.

$$\begin{aligned}
\chi_4 & \equiv Re \left[\frac{\frac{\alpha\mathcal{r}_5}{\mathcal{r}_3} \frac{1-\xi_4}{\mathcal{r}_4} \frac{\frac{1}{3}-\frac{\xi_1\alpha}{\mathcal{r}_2}}{\mathcal{r}_3} - \xi_4 \frac{\xi_1\varsigma^*}{g\alpha^*} - \sqrt{3}\mathcal{r}_{14}\mathcal{r}_{17} - \sqrt{3} \frac{\mathcal{r}_1 \frac{1+\alpha\xi_4}{\alpha} \frac{\frac{1}{3}-\frac{\xi_1\alpha}{\mathcal{r}_2}}{\mathcal{r}_3} + \frac{1-\xi_4}{\mathcal{r}_4} \frac{\frac{1}{3}-\frac{\xi_1\alpha}{\mathcal{r}_2}}{\mathcal{r}_3} \left(\frac{2\alpha\mathcal{r}_6}{\mathcal{r}_2} - \frac{\alpha\mathcal{r}_5}{\mathcal{r}_3} \right) - 2\mathcal{r}_{14}\mathcal{r}_{16}}{\chi_1}}{\chi_3 + \frac{\gamma(3\mathcal{r}_{17} + \frac{1}{4})}{2g^2|\alpha|^2}}}{\mathcal{r}_2/(2\sqrt{3}g^2\alpha|\alpha|^2)} \right] \\
& - Re \left[\frac{\mathcal{r}_{13}\mathcal{r}_{17} - \xi_1\varsigma^* \frac{1+\frac{\alpha\mathcal{r}_5}{3\mathcal{r}_4} \frac{1-\frac{3\xi_1\alpha}{\mathcal{r}_2}}{\mathcal{r}_3}}{2\sqrt{3}g\alpha^*} - \frac{1+\frac{\xi_1\mathcal{r}_1}{\mathcal{r}_2} + \left(\frac{\mathcal{r}_5}{2\mathcal{r}_3} - \frac{\mathcal{r}_6}{\mathcal{r}_2} \right) \frac{\alpha-3\xi_1\alpha^2}{3\mathcal{r}_4}}{\chi_1} + 2\mathcal{r}_{13}\mathcal{r}_{16} \left(\chi_3 + \frac{\gamma(3\mathcal{r}_{17} + \frac{1}{4})}{2g^2|\alpha|^2} \right)}{\mathcal{r}_3/(4g^2|\alpha|^2)} \right] \\
& + \gamma \left(\left(\frac{3}{4} - 3 \left((2\mathcal{r}_{16} - 1) \frac{\chi_3 + \frac{\gamma(3\mathcal{r}_{17} + \frac{1}{4})}{2g^2|\alpha|^2}}{\chi_1} - \mathcal{r}_{17} \right) \right) - 1 \right) \\
\chi_5 & \equiv Re \left[\frac{\left(2 - \frac{\chi_2}{\chi_1} \right) \mathcal{r}_1 \frac{1+\frac{\alpha\xi_1\xi_4}{\mathcal{r}_2\mathcal{r}_3}}{\alpha} + \left(2\alpha\mathcal{r}_6 \frac{2-\frac{\chi_2}{\chi_1}}{\mathcal{r}_2} + \frac{\alpha\mathcal{r}_5\chi_2}{\mathcal{r}_3\chi_1} - 4 \right) \frac{1-\xi_4}{\mathcal{r}_4} \frac{\frac{1}{3}-\frac{\xi_1\alpha}{\mathcal{r}_2}}{\mathcal{r}_3} + \left(\frac{2\mathcal{r}_{16}\chi_2}{\chi_1} - \mathcal{r}_{15} \right) \mathcal{r}_{14} - \frac{\xi_4\chi_2}{\mathcal{r}_3\chi_1}}{\mathcal{r}_2/(6g^2\alpha|\alpha|^2)} \right] \\
& - Re \left[\frac{\mathcal{r}_{13} \left(\mathcal{r}_{15} - \frac{2\mathcal{r}_{16}\chi_2}{\chi_1} \right) + \left(2 + \alpha \left(\frac{\chi_2-2}{\chi_1} \frac{\mathcal{r}_5}{\mathcal{r}_2} \mathcal{r}_6 - \frac{\chi_2\mathcal{r}_5}{2\mathcal{r}_3\chi_1} \right) \right) \frac{1-\frac{3\xi_1\alpha}{\mathcal{r}_2}}{3\mathcal{r}_4} + \xi_1\mathcal{r}_1 \frac{1-\frac{1}{2}\frac{\chi_2}{\chi_1} - \frac{\chi_2}{2\chi_1}}{\mathcal{r}_2}}{\mathcal{r}_3/(4g^2|\alpha|^2)} \right] \\
& - \gamma \left((2\mathcal{r}_{16} - 1) \frac{3\chi_2}{\chi_1} - 3\mathcal{r}_{15} + 7 \right)
\end{aligned}$$

With all the above abstractions and some simplification, we find the following expression for

z on solving.

$$z = -\frac{\chi_4}{\chi_5}$$

From here, we can eliminate z from all other expressions, creating a set of solutions for the dot variables solely as functions of α . The results are summarized below.

C.9 Cleanup prior to last equation

We can see readily that the expressions have gotten quite a bit messy. It is worth noting that prior to doing the real variables, the last variable we solved for was q , with this expression

$$q = -\frac{2\alpha^*}{\sqrt{3}\alpha\gamma_4} (z - y) + \frac{1}{6} \frac{\xi_1 \gamma_5}{g\gamma_3\gamma_4} \zeta^* - \frac{\alpha^* \gamma_6}{\sqrt{3}\gamma_2\gamma_4} (-x - y - 2z) + \frac{\alpha^*}{2\sqrt{3}\gamma_3\gamma_4} \gamma_5 (y - x)$$

This makes it quite tempting to put x, y, z into this and backtrack through the others to get simple expressions that bypass some of the layers of abstraction. In the process we introduce the following three functions, but in exchange are able to eliminate $\gamma_7, \gamma_8, \gamma_9, \gamma_{10}, \gamma_{11}, \gamma_{12}, \gamma_{13}$, and γ_{14} .

The three new functions we define are shown below.

$$\begin{aligned} \chi_6 &\equiv \frac{\chi_3 + \gamma \frac{3\gamma_{17} + \frac{1}{4}}{2g^2|\alpha|^2}}{\chi_1}, \quad \chi_7 \equiv \frac{\chi_2\chi_4}{\chi_1\chi_5} - \chi_6 \\ \varkappa &\equiv \sqrt{3}g\alpha^* \frac{\left(\frac{\xi_1\gamma_1}{\gamma_2} - 1\right) \left(2\chi_6\gamma_{16} - \gamma_{17} + \frac{\gamma_{15} - \gamma_{16} \frac{2\chi_2}{\chi_1}}{\chi_5/\chi_4}\right) + \left(1 + \frac{\xi_1\gamma_1}{\gamma_2}\right) \left(\frac{\chi_2\chi_4}{\chi_5\chi_1} - \chi_6\right) - \frac{2\chi_4\xi_1\gamma_1}{\chi_5\gamma_2} - \frac{\xi_1\zeta^*}{\sqrt{3}g\alpha^*}}{2\gamma_3} \\ &\quad + g|\alpha|^2 \frac{1 - \frac{3\xi_1\alpha}{\gamma_2}}{\xi_4 - \frac{\gamma_2}{\gamma_3}} \left(\frac{\gamma_6 - \frac{\gamma_5}{2\gamma_3}}{\sqrt{3}} \chi_7 - 2 \frac{\gamma_6 - \frac{1}{\alpha} \chi_4}{\sqrt{3}} \frac{\chi_4}{\chi_5} + \frac{\xi_1\gamma_5\zeta^*}{6\alpha^*g\gamma_3} + \frac{\left(\frac{\chi_4\gamma_{15} - 2\chi_7\gamma_{16} - \gamma_{17}}{\chi_5} - \frac{\gamma_6 + \frac{2}{\alpha} + \frac{\gamma_5}{2\gamma_3}\right)}{\sqrt{3}} \right) \end{aligned}$$

It can then readily be shown that the dot parameter expressions are as follows.

$$\begin{aligned} x &= \chi_7, \quad y = \frac{\chi_4\gamma_{15}}{\chi_5} - 2\chi_7\gamma_{16} - \gamma_{17}, \quad z = -\frac{\chi_4}{\chi_5} \\ p &= \zeta^* - \frac{2g\alpha^*}{\sqrt{3}} \left(\frac{\xi_1 + 3\gamma_3}{\gamma_2} - 1 \right) \left((1 - 2\gamma_{16})\chi_7 - \gamma_{17} + \frac{\gamma_{15} - 2}{\chi_5/\chi_4} \right) + 2\chi_7 - \frac{2\chi_4}{\chi_5} - \frac{\xi_1\zeta^*}{\sqrt{3}g\alpha^*} - \frac{2\alpha\xi_4\varkappa}{\gamma_2} \\ &\quad + \frac{2g|\alpha|^2}{3\sqrt{3}} \frac{1 - \frac{3\xi_1\alpha}{\gamma_2}}{\gamma_3} \frac{\frac{\xi_1\zeta^*}{\sqrt{3}\alpha^*g} - \chi_7 + \frac{\chi_7 - 2\chi_4}{\gamma_2/\gamma_6} + \frac{2}{\alpha} \frac{\chi_4}{\chi_5} + \left(\frac{\chi_4\gamma_{15} - 2\chi_7\gamma_{16} - \gamma_{17}}{\chi_5}\right) \left(\frac{\gamma_6 + \frac{2}{\alpha} + \frac{\gamma_5}{2\gamma_3}\right)}{\gamma_4} \\ q &= \alpha^* \left(\frac{\gamma_6 - \frac{\gamma_5}{2\gamma_3}}{\sqrt{3}\gamma_4} \chi_7 - 2 \frac{\gamma_6 - \frac{1}{\alpha} \chi_4}{\sqrt{3}\gamma_4} \frac{\chi_4}{\chi_5} + \frac{\xi_1\gamma_5\zeta^*}{6\alpha^*g\gamma_3\gamma_4} + \frac{\frac{\chi_4\gamma_{15} - 2\chi_7\gamma_{16} - \gamma_{17}}{\chi_5}}{\sqrt{3}\gamma_4} \left(\frac{\gamma_6}{\gamma_2} + \frac{2}{\alpha} + \frac{\gamma_5}{2\gamma_3} \right) \right) \\ r &= g\alpha^* \frac{\left(\frac{\xi_1\gamma_1}{\gamma_2} - 1\right) \left(-2\gamma_{16}\chi_7 - \gamma_{17} + \frac{\gamma_{15} - 2}{\chi_5/\chi_4} + \chi_7\right) + 2\chi_7 - \frac{2\chi_4}{\chi_5}}{2\gamma_3} - \frac{\xi_1\zeta^*}{\sqrt{3}2\gamma_3} \\ &\quad - \frac{g|\alpha|^2}{3} \frac{1 - \frac{3\xi_1\alpha}{\gamma_2}}{\gamma_3} \frac{\frac{\xi_1\zeta^*}{\sqrt{3}\alpha^*g} - \chi_7 + \frac{\chi_7 - 2\chi_4}{\gamma_2/\gamma_6} + \frac{2}{\alpha} \frac{\chi_4}{\chi_5} + \left(\frac{\chi_4\gamma_{15} - 2\chi_7\gamma_{16} - \gamma_{17}}{\chi_5}\right) \left(\frac{\gamma_6 + \frac{2}{\alpha} + \frac{\gamma_5}{2\gamma_3}\right)}{\gamma_4} \\ s &= \frac{\sqrt{3}g\alpha^*}{\xi_4} \frac{\left(\frac{\gamma_6 - \frac{\gamma_5}{2\gamma_3}}{\gamma_2} - 1\right) \chi_7 - \frac{2\gamma_6 - \frac{2}{\alpha}}{\chi_5/\chi_4} + \left(\frac{\chi_4\gamma_{15} - 2\chi_7\gamma_{16} - \gamma_{17}}{\chi_5}\right) \left(\frac{\gamma_6}{\gamma_2} + \frac{2}{\alpha} + \frac{\gamma_5}{2\gamma_3}\right)}{\sqrt{3}\gamma_4} \end{aligned}$$

$$\begin{aligned}
& + \frac{\sqrt{3}g\alpha^*}{\xi_4} \frac{\chi_7(1-2\mathcal{Y}_{16}) + \frac{\mathcal{Y}_{15}-2}{\chi_5} \chi_4 - \mathcal{Y}_{17}}{\frac{\mathcal{Y}_1 \mathcal{Y}_2}{2\xi_4 \sqrt{3\alpha^*} \mathcal{Y}_1}} + \alpha^* \frac{\frac{\xi_1 \mathcal{Y}_5 \varsigma^*}{2\sqrt{3}\mathcal{Y}_3 \mathcal{Y}_4} - \sqrt{3} \frac{\xi_4 - \frac{4\alpha\xi_4^2}{\mathcal{Y}_2}}{\mathcal{Y}_1}}{\xi_4} \\
u &= \frac{\xi_4}{g} \frac{1 - \frac{4\alpha\xi_4}{\mathcal{Y}_2}}{\mathcal{Y}_1} \mathcal{X} - \frac{\chi_7(1-2\mathcal{Y}_{16}) + \frac{\mathcal{Y}_{15}-2}{\chi_5} \chi_4 - \mathcal{Y}_{17}}{\frac{\mathcal{Y}_1 \mathcal{Y}_2}{2\xi_4 \sqrt{3\alpha^*} \mathcal{Y}_1}} \\
v &= \frac{\sqrt{3}g\alpha^* \mathcal{Y}_1 \left(\chi_7(1-2\mathcal{Y}_{16}) + \frac{\mathcal{Y}_{15}-2}{\chi_5} \chi_4 - \mathcal{Y}_{17} \right)}{\mathcal{Y}_2} + \frac{2\alpha\xi_4}{\mathcal{Y}_2} \mathcal{X}
\end{aligned}$$

C.10 Summary of abstractions:

$$\begin{aligned}
\mathcal{Y}_1 &\equiv 3\alpha + \frac{\xi_4 \xi_5}{g^2 \alpha^*} \mathcal{Y}_2 \equiv \xi_6 \mathcal{Y}_1 + 4\alpha \xi_4 \mathcal{Y}_3 \equiv \gamma - \xi_1 \left(\frac{1}{3} + \frac{\alpha \xi_4}{\mathcal{Y}_2} \right) \\
\mathcal{Y}_4 &\equiv \frac{\left(3 - \frac{12\alpha \xi_4}{\mathcal{Y}_2} \right) \alpha}{\mathcal{Y}_1} - \left(\alpha \xi_4 \left(\frac{1 - \frac{4\alpha \xi_4}{\mathcal{Y}_2}}{\mathcal{Y}_1} + \frac{4\gamma}{\mathcal{Y}_2} \right) + \frac{\xi_3}{3} \right) \frac{1 - \frac{3\xi_1 \alpha}{\mathcal{Y}_2}}{\mathcal{Y}_3} + \gamma \frac{12\alpha}{\mathcal{Y}_2} - 1 \\
\mathcal{Y}_5 &\equiv \frac{3\xi_4}{\mathcal{Y}_1} \left(1 - \frac{4\alpha \xi_4}{\mathcal{Y}_2} \right) + \frac{12\gamma \xi_4}{\mathcal{Y}_2} + \frac{\xi_3}{\alpha}, \mathcal{Y}_6 \equiv \xi_4 \left(6 - \frac{\left(3 - \frac{12\alpha \xi_4}{\mathcal{Y}_2} \right) \xi_1}{2\mathcal{Y}_3} \right) - 6\gamma \mathcal{Y}_1 \left(\frac{1}{\alpha} + \frac{\xi_4 \xi_1}{\mathcal{Y}_2 \mathcal{Y}_3} \right) - \frac{\xi_1 \mathcal{Y}_1 \xi_3}{2\mathcal{Y}_3 \alpha} \\
\mathcal{Y}_{15} &= \frac{4g^2 |\alpha|^2 \mathcal{R} \left[2 \frac{\frac{3\alpha}{\mathcal{Y}_2} + \frac{\mathcal{Y}_3 - \gamma}{\xi_1} \frac{1 - \frac{3\xi_1 \alpha}{\mathcal{Y}_2}}{\mathcal{Y}_3}}{3\mathcal{Y}_4} \left(1 - \frac{\alpha \mathcal{Y}_6}{\mathcal{Y}_2} \right) - \frac{\gamma}{\mathcal{Y}_3} \frac{\mathcal{Y}_1}{\mathcal{Y}_2} \right]}{\gamma - \frac{2g^2 |\alpha|^2}{\sqrt{3}} \mathcal{R} \left[2\alpha \frac{\frac{3\alpha}{\mathcal{Y}_2} + \frac{\mathcal{Y}_3 - \gamma}{\xi_1} \frac{1 - \frac{3\xi_1 \alpha}{\mathcal{Y}_2}}{\mathcal{Y}_3}}{\sqrt{3}\mathcal{Y}_4} \left(\frac{\mathcal{Y}_5}{2\mathcal{Y}_3} + \frac{\mathcal{Y}_6}{\mathcal{Y}_2} + \frac{2}{\alpha} \right) + \frac{\mathcal{Y}_3 - \gamma + \frac{\gamma \mathcal{Y}_1}{\mathcal{Y}_2}}{\mathcal{Y}_3 / \sqrt{3}} \right]} \\
\mathcal{Y}_{16} &= \frac{\mathcal{R} \left[\alpha \frac{\frac{3\alpha}{\mathcal{Y}_2} + \frac{\mathcal{Y}_3 - \gamma}{\xi_1} \frac{1 - \frac{3\xi_1 \alpha}{\mathcal{Y}_2}}{\mathcal{Y}_3}}{\sqrt{3}\mathcal{Y}_4} \left(\frac{\mathcal{Y}_5}{\mathcal{Y}_3} - \frac{2\mathcal{Y}_6}{\mathcal{Y}_2} \right) + \frac{\mathcal{Y}_3 - \gamma - \frac{\gamma \mathcal{Y}_1}{\mathcal{Y}_2}}{\mathcal{Y}_3 / \sqrt{3}} \right]}{\frac{\sqrt{3}\gamma}{g^2 |\alpha|^2} - 2\mathcal{R} \left[2\alpha \frac{\frac{3\alpha}{\mathcal{Y}_2} + \frac{\mathcal{Y}_3 - \gamma}{\xi_1} \frac{1 - \frac{3\xi_1 \alpha}{\mathcal{Y}_2}}{\mathcal{Y}_3}}{\sqrt{3}\mathcal{Y}_4} \left(\frac{\mathcal{Y}_5}{2\mathcal{Y}_3} + \frac{\mathcal{Y}_6}{\mathcal{Y}_2} + \frac{2}{\alpha} \right) + \frac{\mathcal{Y}_3 - \gamma + \frac{\gamma \mathcal{Y}_1}{\mathcal{Y}_2}}{\mathcal{Y}_3 / \sqrt{3}} \right]} \\
\mathcal{Y}_{17} &\equiv \frac{2\sqrt{3}g\mathcal{R} \left[\alpha \varsigma^* \frac{\frac{\frac{3\alpha^2}{\mathcal{Y}_2} \frac{\mathcal{Y}_5}{\sqrt{3}\mathcal{Y}_4} + \frac{\alpha \mathcal{Y}_5 - \frac{1 - \frac{3\xi_1 \alpha}{\mathcal{Y}_2}}{\mathcal{Y}_3} + 3\mathcal{Y}_4}{\sqrt{3}\mathcal{Y}_4} \frac{\mathcal{Y}_3 - \gamma}{\xi_1}}{\mathcal{Y}_3}}{\sqrt{3}} \right] + \frac{3\gamma}{4}}{3 \left(\gamma - \frac{2g^2 |\alpha|^2}{\sqrt{3}} \mathcal{R} \left[2\alpha \frac{\frac{3\alpha}{\mathcal{Y}_2} + \frac{\mathcal{Y}_3 - \gamma}{\xi_1} \frac{1 - \frac{3\xi_1 \alpha}{\mathcal{Y}_2}}{\mathcal{Y}_3}}{\sqrt{3}\mathcal{Y}_4} \left(\frac{\mathcal{Y}_5}{2\mathcal{Y}_3} + \frac{\mathcal{Y}_6}{\mathcal{Y}_2} + \frac{2}{\alpha} \right) + \frac{\mathcal{Y}_3 - \gamma + \frac{\gamma \mathcal{Y}_1}{\mathcal{Y}_2}}{\mathcal{Y}_3 / \sqrt{3}} \right] \right)} \\
\chi_1 &\equiv \mathcal{R} \left[\frac{4 + \frac{3\gamma \mathcal{Y}_3}{g^2 |\alpha|^2}}{\mathcal{Y}_3 / \mathcal{Y}_{16}} + \frac{1 + \frac{\xi_1 + 3\gamma}{\mathcal{Y}_2 / \mathcal{Y}_1}}{\mathcal{Y}_3 / (1 - 2\mathcal{Y}_{16})} - \frac{3}{\mathcal{Y}_3 / (1 + 2\mathcal{Y}_{16})} \frac{\mathcal{Y}_3 - \gamma}{\xi_1} + \left(\frac{4\mathcal{Y}_6}{\mathcal{Y}_2} + \frac{2\mathcal{Y}_5}{\mathcal{Y}_3} + \frac{8}{\alpha} + \frac{\mathcal{Y}_5 - 2\mathcal{Y}_6}{\mathcal{Y}_3 - \mathcal{Y}_2} \right) \frac{\frac{\mathcal{Y}_2 - 3\xi_1}{\alpha} \left(\frac{1}{3} - \frac{\mathcal{Y}_3 - \gamma}{\xi_1} \right) - 3}{\mathcal{Y}_2 / \alpha^2} \right] \\
\chi_2 &\equiv \gamma \frac{4 + 3\mathcal{Y}_{15}}{2g^2 |\alpha|^2} + 2\mathcal{R} \left[\frac{\left(\frac{\mathcal{Y}_2}{3} - \xi_1 \alpha \right) \frac{\xi_1 - \mathcal{Y}_3 + \gamma}{\xi_1 / 3} - 3\alpha \mathcal{Y}_3 \frac{\frac{\mathcal{Y}_5}{2\mathcal{Y}_3} + \frac{\mathcal{Y}_6}{\mathcal{Y}_2} + \frac{2}{\alpha} + \frac{2 - 2\alpha \mathcal{Y}_6}{\mathcal{Y}_3}}{\mathcal{Y}_3 / \alpha \mathcal{Y}_{15}} + \frac{1 - \frac{\mathcal{Y}_3 - \gamma}{\xi_1 / 3}}{2\mathcal{Y}_3 / \mathcal{Y}_{15}} + \frac{\xi_1 + 3\gamma}{\mathcal{Y}_3 / \mathcal{Y}_1} \frac{1 - \frac{\mathcal{Y}_{15}}{\mathcal{Y}_2}}{\mathcal{Y}_2} \right] \\
\chi_3 &\equiv \mathcal{R} \left[\frac{\left(1 - \frac{\mathcal{Y}_3 - \gamma}{\xi_1 / 3} \right) \left(\frac{\alpha - \xi_1 \alpha^2}{3} - \frac{3\alpha^2 \mathcal{Y}_3}{\mathcal{Y}_2} \right)}{\mathcal{Y}_4} \left(\frac{2\mathcal{Y}_6}{\mathcal{Y}_2} + \frac{\mathcal{Y}_5}{\mathcal{Y}_3} + \frac{4}{\alpha} - \frac{\xi_1 \mathcal{Y}_5 \varsigma^*}{\sqrt{3}g\alpha^* \mathcal{Y}_3^2} \right) + \frac{1 - \frac{\xi_1 + 3\gamma}{\mathcal{Y}_2 / \mathcal{Y}_1} - \frac{\mathcal{Y}_3 - \gamma}{\xi_1 / 3}}{\mathcal{Y}_3 / \mathcal{Y}_{17}} - \frac{\varsigma^* (\xi_1 + 3\gamma)}{\sqrt{3}g\alpha^* \mathcal{Y}_3} \right]
\end{aligned}$$

$$\begin{aligned}
\chi_4 &\equiv \mathcal{R} \left[\frac{\frac{r_2 - \xi_4 \alpha}{3} \frac{1}{3} - \frac{\xi_1 \alpha}{r_2} + \frac{\alpha}{r_2}}{r_4 / (2\sqrt{3}g^2 \alpha |\alpha|^2)} \left(\frac{\xi_1 s^* + \sqrt{3}\chi_6}{r_3 / r_5} - \frac{2\sqrt{3}r_6}{r_2 / \chi_6} \right) - \frac{\frac{\xi_1 s^*}{2g\alpha^*} + \frac{1 + \xi_1 r_1}{2/\sqrt{3}\chi_6} + \frac{r_1 \chi_6}{2/3}}{r_2 / (4g^2 |\alpha|^2)} + \frac{12(\chi_6 + r_{17} - 2r_{16}\chi_6) - 1}{4/\gamma} \right] \\
&- (r_{17} - 2r_{16}\chi_6) 2g^2 |\alpha|^2 \mathcal{R} \left[\frac{1 - \frac{\xi_1 r_1}{r_2} (r_2 - 3\alpha\xi_4) + 3r_1}{r_2} + \left(\frac{r_6}{r_2} + \frac{r_5}{2r_3} + \frac{2}{\alpha} \right) \frac{\left(\frac{2}{\alpha} - \frac{6\xi_4}{r_2} \right) \frac{\alpha}{3} - \frac{\xi_1 \alpha^2}{r_2} + \frac{6\alpha}{r_2}}{r_4 / \alpha} \right] \\
\chi_5 &\equiv g^2 |\alpha|^2 \operatorname{Re} \left[\frac{2\alpha r_6 \frac{2 - \chi_2}{r_2} + \frac{\alpha r_5 \chi_2}{r_3 \chi_1} - 4}{r_4 / 2} \frac{3\alpha + (r_2 - 3\alpha\xi_4) \frac{1 - \frac{3\xi_1 \alpha}{r_2}}{3r_3}}{r_2} + \frac{2 - \frac{3\alpha\xi_4 \chi_2}{\chi_1 r_2} + \left(2 - \frac{\chi_2}{\chi_1} \right) \frac{r_3 + \xi_1 \frac{\alpha\xi_4 - \frac{r_2}{3}}{r_2} - \frac{r_2}{3r_1}}{3r_1}}{r_3 / 2} \right] \\
&- \gamma \frac{r_{17} - 3\chi_2}{\chi_1} + \frac{\operatorname{Re} \left[\frac{1 - \frac{\xi_1 r_1}{r_2} (r_2 - 3\alpha\xi_4) + 3r_1}{r_2} + \left(\frac{r_6}{r_2} + \frac{r_5}{2r_3} + \frac{2}{\alpha} \right) \frac{\left(\frac{2}{\alpha} - \frac{6\xi_4}{r_2} \right) \frac{\alpha}{3} - \frac{\xi_1 \alpha^2}{r_2} + \frac{6\alpha}{r_2}}{r_4 / \alpha} \right] - \frac{3\gamma}{g^2 |\alpha|^2}}{\chi_1 / (2g^2 |\alpha|^2 (2r_{16}\chi_2 - r_{15}\chi_1))} \\
\chi_6 &\equiv \frac{\chi_3 + \gamma \frac{3r_{17} + \frac{1}{4}}{2g^2 |\alpha|^2}}{\chi_1}, \quad \chi_7 \equiv \frac{\chi_2 \chi_4}{\chi_1 \chi_5} - \chi_6 \\
\mathcal{Z} &\equiv \sqrt{3} g \alpha^* \frac{\left(\frac{\xi_1 r_1}{r_2} - 1 \right) \left(2\chi_6 r_{16} - r_{17} + \frac{r_{15} - r_{16} \frac{2\chi_2}{\chi_1}}{\chi_5 / \chi_4} \right) + \left(1 + \frac{\xi_1 r_1}{r_2} \right) \left(\frac{\chi_2 \chi_4}{\chi_5 \chi_1} - \chi_6 \right) - \frac{2\chi_4 \xi_1 r_1}{\chi_5 r_2} - \frac{\xi_1 s^*}{\sqrt{3} g \alpha^*}}{2r_3} \\
&+ \frac{g |\alpha|^2 \left(\frac{3}{\xi_4} - \frac{1 - \frac{3\xi_1 \alpha}{r_2}}{r_3} \right)}{r_4} \left(\left(\frac{r_6}{r_2} - \frac{r_5}{2r_3} \right) \chi_7 - \frac{r_6 - \frac{1}{\alpha}}{\sqrt{3}/2} \frac{\chi_4}{\chi_5} + \frac{\xi_1 r_5 s^*}{6\alpha^* g r_3} + \frac{\left(\frac{\chi_4 r_{15}}{\chi_5} - 2\chi_7 r_{16} - r_{17} \right) \left(\frac{r_6}{r_2} + \frac{2}{\alpha} + \frac{r_5}{2r_3} \right)}{\sqrt{3}} \right)
\end{aligned}$$

D Equations of Motion for Four Quantum Dots

In this appendix we develop the equations of motion for a system of four identical coupled quantum dots that form a regular tetrahedron inside a driven cavity with dissipation and detuning. These equations of motion can either be used in the time dependent regime, via a Runge-Kutta technique of appropriate accuracy, or in the steady state regime by reducing the parameter space to simply α , creating a two-dimensional parameter space, greatly reducing the numerical complexity of the problem but at the expense of making the function less well-behaved in the remaining parameter space, with more local extrema to contend with, much as was the case with the three dot system.

Following the pattern of the parametrization first developed by Mitra et al [1] for two quantum dots and the extension we created for three dots in Chapter 4, the density matrix of a system of four identical equidistant coupled quantum dots in a driven cavity with dissipation can be parameterized as shown below, which in this case creates a twenty-six-dimensional problem.

$$\Lambda = \begin{pmatrix} \frac{1}{5} + x & p & q & s & \Gamma \\ p^* & \frac{1}{5} + y & r & u & \Theta \\ q^* & r^* & \frac{1}{5} + z & v & \varpi \\ s^* & u^* & v^* & \frac{1}{5} + \Omega & \vartheta \\ \Gamma^* & \Theta^* & \varpi^* & \vartheta^* & \frac{1}{5} - x - y - z - \Omega \end{pmatrix}$$

We can find operators corresponding to each parameter, which are shown below.

$$\begin{aligned} a \rightarrow \alpha, |0\rangle\langle 0| \rightarrow x + \frac{1}{5} \rightarrow \dot{x}, |1\rangle\langle 0| \rightarrow p, |2\rangle\langle 0| \rightarrow q, |3\rangle\langle 0| \rightarrow s, |1\rangle\langle 1| \rightarrow \frac{1}{5} + y \rightarrow \dot{y} \\ |2\rangle\langle 1| \rightarrow r, |2\rangle\langle 2| \rightarrow \frac{1}{5} + z \rightarrow \dot{z}, |3\rangle\langle 1| \rightarrow u, |3\rangle\langle 2| \rightarrow v, |3\rangle\langle 3| \rightarrow \frac{1}{5} + \Omega \\ |4\rangle\langle 0| \rightarrow \Gamma, |4\rangle\langle 1| \rightarrow \Theta, |4\rangle\langle 2| \rightarrow \varpi, |4\rangle\langle 3| \rightarrow \vartheta, |4\rangle\langle 4| \rightarrow \frac{1}{5} - x - y - z - \Omega \end{aligned}$$

This implies that fifteen equations of motion are needed to work with these parameters. To find the equations of motion we use $\langle \dot{A} \rangle = Tr \rho \dot{A}$ and the master equation shown in Chapters 2 and 4.

D.1 Summary of Operator Effects and Repeatable Simplifications

Define the following states:

$$|0\rangle \equiv |0000\rangle, |1\rangle \equiv \frac{|1000\rangle + |0100\rangle + |0010\rangle + |0001\rangle}{2}, |2\rangle \equiv \frac{|1100\rangle + |1010\rangle + |1001\rangle + |0110\rangle + |0101\rangle + |0011\rangle}{\sqrt{6}},$$

$$|3\rangle \equiv \frac{|0111\rangle + |1011\rangle + |1101\rangle + |1110\rangle}{2}, |4\rangle \equiv |1111\rangle$$

Now consider the following expression.

$$J_+ |1\rangle = (J_{1+} + J_{2+} + J_{3+} + J_{4+}) |1\rangle = |1100\rangle + |1010\rangle + |1001\rangle + |0110\rangle + |0101\rangle + |0011\rangle$$

$$= \sqrt{6} |2\rangle$$

We can similarly show that

$$J_+ |0\rangle = 2 |1\rangle, J_+ |2\rangle = \sqrt{6} |3\rangle, J_+ |3\rangle = 2 |4\rangle, J_+ |4\rangle = 0$$

$$J_- |4\rangle = 2 |3\rangle, J_- |3\rangle = \sqrt{6} |2\rangle, J_- |2\rangle = \sqrt{6} |1\rangle, \text{ and } J_- |1\rangle = 2 |0\rangle.$$

The T operator for four dots is as follows.

$$T = I + j_{1+}j_{2-} + j_{1+}j_{3-} + j_{1+}j_{4-} + j_{1-}j_{2+} + j_{1-}j_{3+} + j_{1-}j_{4+}$$

$$+ j_{2+}j_{3-} + j_{2+}j_{4-} + j_{2-}j_{3+} + j_{2-}j_{4+} + j_{3+}j_{4-} + j_{3-}j_{4+}$$

$$T |1\rangle = T \frac{|1000\rangle + |0100\rangle + |0010\rangle + |0001\rangle}{2} = \frac{3|0100\rangle + 3|0010\rangle + 3|0001\rangle + 3|1000\rangle}{2} = 3 |1\rangle$$

Similarly, then $T |2\rangle = 4 |2\rangle$, $T |3\rangle = 3 |3\rangle$, and $T |4\rangle = |4\rangle$. This means also that the operator T will commute with any diagonal element.

Any term in the master equation lacking dot operators will go to zero (by both the fact that it's an independent space, and the cyclic property of the trace allowing you to rewrite $B\rho A = AB\rho$). Therefore, the only relevant terms for the equations of motion regarding the dot parameters will be Δ_d, g, γ, w . Further terms can be eliminated in the case of diagonal elements. Since the diagonal elements commute with J_z , the diagonals will have no Δ_d term. Likewise, they commute with the T operator. So there will be no w term.

D.2 Field Parameter α Equation

$$\Delta_c \text{ term: } \text{Tr } a (-i\Delta_c[a^\dagger a, \rho]) = -i\Delta_c (\text{Tr } aa^\dagger a\rho - \text{Tr } a\rho a^\dagger a) = -i\Delta_c \text{Tr } a\rho$$

$$g \text{ term: } \text{Tr } a (g[aJ_- - aJ_+, \rho]) = g \text{Tr } J_- \rho$$

$$\varepsilon \text{ term: } \text{Tr } a (\varepsilon[a^\dagger - a, \rho]) = \varepsilon (\text{Tr } aa^\dagger \rho - \text{Tr } aa\rho - \text{Tr } a\rho a^\dagger + \text{Tr } a\rho a) = \varepsilon$$

$$\kappa \text{ term: } \text{Tr } a (\kappa[2a\rho a^\dagger - a^\dagger a\rho - \rho a^\dagger a]) = \kappa[2\text{Tr } aa\rho a^\dagger - \text{Tr } aa^\dagger a\rho - \text{Tr } a\rho a^\dagger a] - \kappa \langle \alpha \rangle$$

The overall equation of motion, then, is as follows.

$$\langle \alpha \rangle = -(\kappa + i\Delta_c) \langle \alpha \rangle + \varepsilon + 2(\langle \vartheta^* \rangle + \langle p^* \rangle) + \sqrt{6}(\langle v^* \rangle + \langle r^* \rangle)$$

D.3 $x, y, z,$ and Ω Equations

For the x equation of motion, we must take $Tr |0\rangle \langle 0| \dot{\rho}$. Let us break this trace down by terms.

$$g \text{ term: } Tr |0\rangle \langle 0| (g[a^\dagger J_- - a J_+, \rho]) = 2g (\langle p^* \alpha^* \rangle + \langle p \alpha \rangle)$$

$$\gamma \text{ term: } Tr |0\rangle \langle 0| \left(\frac{\gamma}{2} [2J_- \rho J_+ - J_+ J_- \rho - \rho J_+ J_-] \right) = 4\gamma \left(\frac{1}{5} + \langle y \rangle \right)$$

The overall equation of motion, then, is as follows.

$$\dot{x} = 2g (\langle p^* \alpha^* \rangle + \langle p \alpha \rangle) + 4\gamma \left(\frac{1}{5} + \langle y \rangle \right)$$

Now we break $Tr |1\rangle \langle 1| \dot{\rho}$ down by terms to obtain the equation of motion for y .

$$g \text{ term: } Tr |1\rangle \langle 1| (g[a^\dagger J_- - a J_+, \rho]) = g (\sqrt{6} (\langle \alpha^* r^* \rangle + \langle \alpha r \rangle) - 2 (\langle \alpha p \rangle + \langle \alpha^* p^* \rangle))$$

$$\gamma \text{ term: } Tr |1\rangle \langle 1| \left(\frac{\gamma}{2} [2J_- \rho J_+ - J_+ J_- \rho - \rho J_+ J_-] \right) = \gamma \left(6 \left(\frac{1}{5} + \langle z \rangle \right) - 4 \left(\frac{1}{5} + \langle y \rangle \right) \right)$$

The overall equation of motion, then, is as follows.

$$\dot{y} = g (\sqrt{6} (\langle \alpha^* r^* \rangle + \langle \alpha r \rangle) - 2 (\langle \alpha p \rangle + \langle \alpha^* p^* \rangle)) + \gamma \left(6 \left(\frac{1}{5} + \langle z \rangle \right) - 4 \left(\frac{1}{5} + \langle y \rangle \right) \right)$$

Let us now break $Tr |2\rangle \langle 2| \dot{\rho}$ down by terms to obtain the equation for z .

$$g \text{ term: } Tr |2\rangle \langle 2| (g[a^\dagger J_- - a J_+, \rho]) = \sqrt{6}g ((\langle \alpha^* v^* \rangle + \langle \alpha v \rangle) - (\langle r \alpha \rangle + \langle r^* \alpha^* \rangle))$$

$$\gamma \text{ term: } Tr |2\rangle \langle 2| \left(\frac{\gamma}{2} [2J_- \rho J_+ - J_+ J_- \rho - \rho J_+ J_-] \right) = 6\gamma (\langle \Omega \rangle - \langle z \rangle)$$

We then find the following overall equation of motion for z .

$$\dot{z} = \sqrt{6}g ((\langle \alpha^* v^* \rangle + \langle \alpha v \rangle) - (\langle r \alpha \rangle + \langle r^* \alpha^* \rangle)) + 6\gamma (\langle \Omega \rangle - \langle z \rangle)$$

Let us break $Tr |3\rangle \langle 3| \dot{\rho}$ down by terms to find the equation of motion of Ω .

$$g \text{ term: } Tr |3\rangle \langle 3| (g[a^\dagger J_- - a J_+, \rho]) = g (2 (\langle \vartheta^* \alpha^* \rangle + \langle \vartheta \alpha \rangle) - \sqrt{6} (\langle \alpha \Omega \rangle + \langle \alpha^* \Omega \rangle))$$

γ term:

$$Tr |3\rangle \langle 3| \left(\frac{\gamma}{2} [2J_- \rho J_+ - J_+ J_- \rho - \rho J_+ J_-] \right) = 2\gamma (2 (-\langle x \rangle - \langle y \rangle - \langle z \rangle - \langle \Omega \rangle) - 3 (\langle \Omega \rangle - \frac{1}{5}))$$

The overall equation of motion for Ω then is as follows.

$$\dot{\Omega} = g (2 (\langle \vartheta^* \alpha^* \rangle + \langle \vartheta \alpha \rangle) - \sqrt{6} (\langle \alpha \Omega \rangle + \langle \alpha^* \Omega \rangle)) + 2\gamma (2 (-\langle x \rangle - \langle y \rangle - \langle z \rangle) - 5 \langle \Omega \rangle - \frac{3}{5})$$

D.4 p , q , and r Equations

Now we must find the p equation through $Tr |1\rangle \langle 0| \dot{\rho}$.

$$g \text{ term: } Tr |1\rangle \langle 0| (g[a^\dagger J_- - a J_+, \rho]) = g (2 (\langle y\alpha^* \rangle - \langle x\alpha^* \rangle) + \sqrt{6} \langle q\alpha \rangle)$$

$$\gamma \text{ term: } Tr |1\rangle \langle 0| \left(\frac{\gamma}{2}[2J_- \rho J_+ - J_+ J_- \rho - \rho J_+ J_-]\right) = \gamma (2\sqrt{6} \langle r \rangle - 2 \langle p \rangle)$$

$$w \text{ term: } -Tr |1\rangle \langle 0| (iw[T, \rho]) = 2iw \langle p \rangle$$

$$\Delta_d \text{ term: } Tr |1\rangle \langle 0| (-i\Delta_d[J_z, \rho]) = i\Delta_d \langle p \rangle$$

The overall equation of motion, then, is as follows.

$$\dot{p} = g (2 (\langle y\alpha^* \rangle - \langle x\alpha^* \rangle) + \sqrt{6} \langle q\alpha \rangle) + \gamma (2\sqrt{6} \langle r \rangle - 2 \langle p \rangle) + 2iw \langle p \rangle + i\Delta_d \langle p \rangle$$

And now let us find the expression for $Tr |2\rangle \langle 0| \dot{\rho}$ to find the equation for q .

$$g \text{ term: } Tr |2\rangle \langle 0| (g[a^\dagger J_- - a J_+, \rho]) = g (2 \langle r\alpha^* \rangle - \sqrt{6} \langle p\alpha^* \rangle + \sqrt{6} \langle s\alpha \rangle)$$

$$\gamma \text{ term: } Tr |2\rangle \langle 0| \left(\frac{\gamma}{2}[2J_- \rho J_+ - J_+ J_- \rho - \rho J_+ J_-]\right) = \gamma (2\sqrt{6} \langle u \rangle - 3 \langle q \rangle)$$

$$w \text{ term: } -Tr |2\rangle \langle 0| (iw[T, \rho]) = 3iw \langle q \rangle$$

$$\Delta_d \text{ term: } Tr |2\rangle \langle 0| (-i\Delta_d[J_z, \rho]) = 2i\Delta_d \langle q \rangle$$

The overall equation of motion, then, is as follows

$$\dot{q} = g (2 \langle r\alpha^* \rangle - \sqrt{6} \langle p\alpha^* \rangle + \sqrt{6} \langle s\alpha \rangle) + \gamma (2\sqrt{6} \langle u \rangle - 3 \langle q \rangle) + 3iw \langle q \rangle + 2i\Delta_d \langle q \rangle$$

Now let us find the expression for $Tr |2\rangle \langle 1| \dot{\rho}$ and use it to obtain the equation of motion for r .

$$g \text{ term: } Tr |2\rangle \langle 1| (g[a^\dagger J_- - a J_+, \rho]) = g (\sqrt{6} \langle z\alpha^* \rangle - 2 \langle q\alpha \rangle - \sqrt{6} \langle y\alpha^* \rangle + \sqrt{6} \langle u\alpha \rangle)$$

$$\gamma \text{ term: } Tr |2\rangle \langle 1| \left(\frac{\gamma}{2}[2J_- \rho J_+ - J_+ J_- \rho - \rho J_+ J_-]\right) = \gamma (6 \langle v \rangle - 5 \langle r \rangle)$$

$$w \text{ term: } -Tr |2\rangle \langle 1| (iw[T, \rho]) = iw \langle r \rangle$$

$$\Delta_d \text{ term: } Tr |2\rangle \langle 1| (-i\Delta_d[J_z, \rho]) = i\Delta_d \langle r \rangle$$

The overall equation of motion, then, is as follows.

$$\dot{r} = g (\sqrt{6} \langle z\alpha^* \rangle - 2 \langle q\alpha \rangle - \sqrt{6} \langle y\alpha^* \rangle + \sqrt{6} \langle u\alpha \rangle) + \gamma (6 \langle v \rangle - 5 \langle r \rangle) + i(\Delta_d + w) \langle r \rangle$$

D.5 s , u , and v Equations

To find the equation of motion for s we must break $Tr |3\rangle \langle 0| \dot{\rho}$ down by terms.

$$g \text{ term: } Tr |3\rangle \langle 0| (g[a^\dagger J_- - a J_+, \rho]) = g (2 \langle u \alpha^* \rangle - \sqrt{6} \langle q \alpha^* \rangle + 2 \langle \Gamma \alpha \rangle)$$

$$\gamma \text{ term: } Tr |3\rangle \langle 0| \left(\frac{\gamma}{2} [2J_- \rho J_+ - J_+ J_- \rho - \rho J_+ J_-] \right) = \gamma (4 \langle \Theta \rangle - 3 \langle s \rangle)$$

$$w \text{ term: } -Tr |3\rangle \langle 0| (iw[T, \rho]) = 2iw \langle s \rangle$$

$$\Delta_d \text{ term: } Tr |3\rangle \langle 0| (-i\Delta_d[J_z, \rho]) = 3i\Delta_d \langle s \rangle$$

The overall equation of motion is as follows.

$$\dot{s} = g (2 \langle u \alpha^* \rangle - \sqrt{6} \langle q \alpha^* \rangle + 2 \langle \Gamma \alpha \rangle) + \gamma (4 \langle \Theta \rangle - 3 \langle s \rangle) + 2iw \langle s \rangle + 3i\Delta_d \langle s \rangle$$

Now, to find u , consider the expression $Tr |3\rangle \langle 1| \dot{\rho}$.

$$g \text{ term: } Tr |3\rangle \langle 1| (g[a^\dagger J_- - a J_+, \rho]) = g (\sqrt{6} (\langle v \alpha^* \rangle - \langle r \alpha^* \rangle) + 2 (\langle \Theta \alpha \rangle - \langle s \alpha \rangle))$$

$$\gamma \text{ term: } Tr |3\rangle \langle 1| \left(\frac{\gamma}{2} [2J_- \rho J_+ - J_+ J_- \rho - \rho J_+ J_-] \right) = \gamma (2\sqrt{6} \langle \varpi \rangle - 5 \langle u \rangle)$$

$$w \text{ term: } Tr |3\rangle \langle 1| (iw[T, \rho]) = iw (Tr |3\rangle \langle 1| T \rho - Tr |3\rangle \langle 1| \rho T) = 0$$

$$\Delta_d \text{ term: } Tr |3\rangle \langle 1| (-i\Delta_d[J_z, \rho]) = -i\Delta_d (Tr |3\rangle \langle 1| J_z \rho - Tr |3\rangle \langle 1| \rho J_z) = 2i\Delta_d \langle u \rangle$$

The overall equation of motion, then, is as follows.

$$\dot{u} = g (\sqrt{6} (\langle v \alpha^* \rangle - \langle r \alpha^* \rangle) + 2 (\langle \Theta \alpha \rangle - \langle s \alpha \rangle)) + \gamma (2\sqrt{6} \langle \varpi \rangle - 5 \langle u \rangle) + 2i\Delta_d \langle u \rangle$$

Let us now consider $Tr |3\rangle \langle 2| \dot{\rho}$ to find v .

$$g \text{ term: } Tr |3\rangle \langle 2| (g[a^\dagger J_- - a J_+, \rho]) = g (\sqrt{6} (\langle \Omega \alpha^* \rangle - \langle z \alpha^* \rangle - \langle \alpha u \rangle) + 2 \langle \alpha \varpi \rangle)$$

$$\gamma \text{ term: } Tr |3\rangle \langle 2| \left(\frac{\gamma}{2} [2J_- \rho J_+ - J_+ J_- \rho - \rho J_+ J_-] \right) = 2\gamma (\sqrt{6} \langle \vartheta \rangle - 3 \langle v \rangle)$$

$$w \text{ term: } -Tr |3\rangle \langle 2| (iw[T, \rho]) = -iw (Tr |3\rangle \langle 2| T \rho - Tr |3\rangle \langle 2| \rho T) = -iw \langle v \rangle$$

$$\Delta_d \text{ term: } Tr |3\rangle \langle 2| (-i\Delta_d[J_z, \rho]) = -i\Delta_d (Tr |3\rangle \langle 2| J_z \rho - Tr |3\rangle \langle 2| \rho J_z) = i\Delta_d \langle v \rangle$$

The overall equation of motion found is given below.

$$\dot{v} = g (\sqrt{6} (\langle \Omega \alpha^* \rangle - \langle z \alpha^* \rangle - \langle \alpha u \rangle) + 2 \langle \alpha \varpi \rangle) + 2\gamma (\sqrt{6} \langle \vartheta \rangle - 3 \langle v \rangle) + i(\Delta_d - w) \langle v \rangle$$

D.6 Γ , Θ , ϖ , and ϑ Equations

We now evaluate the expression $Tr |4\rangle \langle 0| \dot{\rho}$ to obtain the equation of motion for the dot variable Γ .

$$g \text{ term: } Tr |4\rangle \langle 0| (g[a^\dagger J_- - aJ_+, \rho]) = 2g (\langle \alpha^* \Theta \rangle - \langle \alpha^* s \rangle)$$

$$\gamma \text{ term: } Tr |4\rangle \langle 0| \left(\frac{\gamma}{2} [2J_- \rho J_+ - J_+ J_- \rho - \rho J_+ J_-] \right) = -2\gamma \langle \Gamma \rangle$$

$$w \text{ term: } Tr |4\rangle \langle 0| (iw[T, \rho]) = iw (Tr |4\rangle \langle 0| T\rho - Tr |4\rangle \langle 0| \rho T) = 0$$

$$\Delta_d \text{ term: } Tr |4\rangle \langle 0| (-i\Delta_d[J_z, \rho]) = -i\Delta_d (Tr |4\rangle \langle 0| J_z \rho - Tr |4\rangle \langle 0| \rho J_z) = 4i\Delta_d \langle \Gamma \rangle$$

We can then find the overall equation of motion.

$$\dot{\Gamma} = 2g (\langle \alpha^* \Theta \rangle - \langle \alpha^* s \rangle) - 2\gamma \langle \Gamma \rangle + 4i\Delta_d \langle \Gamma \rangle$$

Breaking down the expression $Tr |4\rangle \langle 1| \dot{\rho}$ by terms, we see the following in the case of Θ .

$$g \text{ term: } Tr |4\rangle \langle 1| (g[a^\dagger J_- - aJ_+, \rho]) = g (\sqrt{6} \langle \alpha^* \varpi \rangle - 2(\langle \alpha \Gamma \rangle + \langle u\alpha^* \rangle))$$

$$\gamma \text{ term: } Tr |4\rangle \langle 1| \left(\frac{\gamma}{2} [2J_- \rho J_+ - J_+ J_- \rho - \rho J_+ J_-] \right) = -4\gamma \langle \Theta \rangle$$

$$w \text{ term: } -Tr |4\rangle \langle 1| (iw[T, \rho]) = -iw (Tr |4\rangle \langle 1| T\rho - Tr |4\rangle \langle 1| \rho T) = -2iw \langle \Theta \rangle$$

$$\Delta_d \text{ term: } Tr |4\rangle \langle 1| (-i\Delta_d[J_z, \rho]) = -i\Delta_d (Tr |4\rangle \langle 1| J_z \rho - Tr |4\rangle \langle 1| \rho J_z) = 3i\Delta_d \langle \Theta \rangle$$

The overall equation of motion, then, is as follows.

$$\dot{\Theta} = g (\sqrt{6} \langle \alpha^* \varpi \rangle - 2(\langle \alpha \Gamma \rangle + \langle u\alpha^* \rangle)) - 4\gamma \langle \Theta \rangle + i(3\Delta_d - w) \langle \Theta \rangle$$

The expression we must consider this time is $Tr |4\rangle \langle 2| \dot{\rho}$. This will allow us to find the equation of motion for the dot variable ϖ .

$$g \text{ term: } Tr |4\rangle \langle 2| (g[a^\dagger J_- - aJ_+, \rho]) = g (\sqrt{6} (\langle \vartheta \alpha^* \rangle - \langle \Theta \alpha \rangle) - 2 \langle \alpha^* v \rangle)$$

$$\gamma \text{ term: } Tr |4\rangle \langle 2| \left(\frac{\gamma}{2} [2J_- \rho J_+ - J_+ J_- \rho - \rho J_+ J_-] \right) = -5\gamma \langle \varpi \rangle$$

$$w \text{ term: } -Tr |4\rangle \langle 2| (iw[T, \rho]) = -iw (Tr |4\rangle \langle 2| T\rho - Tr |4\rangle \langle 2| \rho T) = -3iw \langle \varpi \rangle$$

$$\Delta_d \text{ term: } Tr |4\rangle \langle 2| (-i\Delta_d[J_z, \rho]) = -i\Delta_d (Tr |4\rangle \langle 2| J_z \rho - Tr |4\rangle \langle 2| \rho J_z) = 2i\Delta_d \langle \varpi \rangle$$

We then can see that the overall equation of motion is as follows below.

$$\dot{\varpi} = g (\sqrt{6} (\langle \vartheta \alpha^* \rangle - \langle \Theta \alpha \rangle) - 2 \langle \alpha^* v \rangle) - 5\gamma \langle \varpi \rangle + i(2\Delta_d - 3w) \langle \varpi \rangle$$

Finally, we must consider $Tr |4\rangle \langle 3| \dot{\rho}$, in order to find the equation for ϑ .

g term:

$$Tr |4\rangle \langle 3| (g[a^\dagger J_- - a J_+, \rho]) = -g (2(\langle x\alpha^* \rangle + \langle y\alpha^* \rangle + \langle z\alpha^* \rangle) + \sqrt{6} \langle \alpha\varpi \rangle + 4 \langle \alpha^*\Omega \rangle)$$

$$\gamma \text{ term: } Tr |4\rangle \langle 3| \left(\frac{\gamma}{2} [2J_- \rho J_+ - J_+ J_- \rho - \rho J_+ J_-] \right) = -5\gamma \langle \vartheta \rangle$$

$$w \text{ term: } -Tr |4\rangle \langle 3| (iw[T, \rho]) = -iw (Tr |4\rangle \langle 3| T\rho - Tr |4\rangle \langle 3| \rho T) = -2iw \langle \vartheta \rangle$$

$$\Delta_d \text{ term: } Tr |4\rangle \langle 3| (-i\Delta_d [J_z, \rho]) = -i\Delta_d (Tr |4\rangle \langle 3| J_z \rho - Tr |4\rangle \langle 3| \rho J_z) = i\Delta_d \langle \vartheta \rangle$$

The overall equation of motion, then, is as follows.

$$\dot{\vartheta} = -g (2(\langle x\alpha^* \rangle + \langle y\alpha^* \rangle + \langle z\alpha^* \rangle) + \sqrt{6} \langle \alpha\varpi \rangle + 4 \langle \alpha^*\Omega \rangle) - 5\gamma \langle \vartheta \rangle + i(\Delta_d - 2w) \langle \vartheta \rangle$$

D.7 Summary of all equations

$$\langle \dot{\alpha} \rangle = -(\kappa + i\Delta_c) \langle \alpha \rangle + \varepsilon + 2(\langle \vartheta^* \rangle + \langle p^* \rangle) + \sqrt{6}(\langle v^* \rangle + \langle r^* \rangle)$$

$$\langle \dot{x} \rangle = 2g(\langle p^* \alpha^* \rangle + \langle p\alpha \rangle) + 4\gamma \left(\frac{1}{5} + \langle y \rangle \right)$$

$$\langle \dot{y} \rangle = g(\sqrt{6}(\langle \alpha^* r^* \rangle + \langle \alpha r \rangle) - 2(\langle \alpha p \rangle + \langle \alpha^* p^* \rangle)) + \gamma \left(6 \left(\frac{1}{5} + \langle z \rangle \right) - 4 \left(\frac{1}{5} + \langle y \rangle \right) \right)$$

$$\langle \dot{z} \rangle = \sqrt{6}g(\langle \alpha^* v^* \rangle + \langle \alpha v \rangle) - (\langle r\alpha \rangle + \langle r^* \alpha^* \rangle) + 6\gamma(\langle \Omega \rangle - \langle z \rangle)$$

$$\langle \dot{\Omega} \rangle =$$

$$g(2(\langle \vartheta^* \alpha^* \rangle + \langle \vartheta \alpha \rangle) - \sqrt{6}(\langle \alpha \Omega \rangle + \langle \alpha^* \Omega \rangle)) + 2\gamma(2(-\langle x \rangle - \langle y \rangle - \langle z \rangle) - 5\langle \Omega \rangle - \frac{3}{5})$$

$$\langle \dot{p} \rangle = g(2(\langle y\alpha^* \rangle - \langle x\alpha^* \rangle) + \sqrt{6}\langle q\alpha \rangle) + \gamma(2\sqrt{6}\langle r \rangle - 2\langle p \rangle) + 2iw\langle p \rangle + i\Delta_d\langle p \rangle$$

$$\langle \dot{q} \rangle = g(2\langle r\alpha^* \rangle - \sqrt{6}\langle p\alpha^* \rangle + \sqrt{6}\langle s\alpha \rangle) + \gamma(2\sqrt{6}\langle u \rangle - 3\langle q \rangle) + 3iw\langle q \rangle + 2i\Delta_d\langle q \rangle$$

$$\langle \dot{r} \rangle = g(\sqrt{6}\langle z\alpha^* \rangle - 2\langle q\alpha \rangle - \sqrt{6}\langle y\alpha^* \rangle + \sqrt{6}\langle u\alpha \rangle) + \gamma(6\langle v \rangle - 5\langle r \rangle) + i(\Delta_d + w)\langle r \rangle$$

$$\langle \dot{s} \rangle = g(2\langle u\alpha^* \rangle - \sqrt{6}\langle q\alpha^* \rangle + 2\langle \Gamma\alpha \rangle) + \gamma(4\langle \Theta \rangle - 3\langle s \rangle) + 2iw\langle s \rangle + 3i\Delta_d\langle s \rangle$$

$$\langle \dot{u} \rangle = g(\sqrt{6}(\langle v\alpha^* \rangle - \langle r\alpha^* \rangle) + 2(\langle \Theta\alpha \rangle - \langle s\alpha \rangle)) + \gamma(2\sqrt{6}\langle \varpi \rangle - 5\langle u \rangle) + 2i\Delta_d\langle u \rangle$$

$$\langle \dot{v} \rangle = g(\sqrt{6}(\langle \Omega\alpha^* \rangle - \langle z\alpha^* \rangle - \langle \alpha u \rangle) + 2\langle \alpha\varpi \rangle) + 2\gamma(\sqrt{6}\langle \vartheta \rangle - 3\langle v \rangle) + i(\Delta_d - w)\langle v \rangle$$

$$\langle \dot{\Gamma} \rangle = 2g(\langle \alpha^* \Theta \rangle - \langle \alpha^* s \rangle) - 2\gamma\langle \Gamma \rangle + 4i\Delta_d\langle \Gamma \rangle$$

$$\langle \dot{\Theta} \rangle = g(\sqrt{6}\langle \alpha^* \varpi \rangle - 2(\langle \alpha\Gamma \rangle + \langle u\alpha^* \rangle)) - 4\gamma\langle \Theta \rangle + i(3\Delta_d - w)\langle \Theta \rangle$$

$$\langle \dot{\varpi} \rangle = g(\sqrt{6}(\langle \vartheta\alpha^* \rangle - \langle \Theta\alpha \rangle) - 2\langle \alpha^* v \rangle) - 5\gamma\langle \varpi \rangle + i(2\Delta_d - 3w)\langle \varpi \rangle$$

$$\langle \dot{\vartheta} \rangle = -g(2(\langle x\alpha^* \rangle + \langle y\alpha^* \rangle + \langle z\alpha^* \rangle) + \sqrt{6}\langle \alpha\varpi \rangle + 4\langle \alpha^*\Omega \rangle) - 5\gamma\langle \vartheta \rangle + i(\Delta_d - 2w)\langle \vartheta \rangle$$